

Regulation of Podocyte Survival and Endoplasmic Reticulum Stress by Fatty Acids and its Modification by Stearoyl-CoA Desaturases and Cyclic AMP

Inauguraldissertation

zur
Erlangung der Würde eines Doktors der Philosophie vorgelegt
der Philosophisch-Naturwissenschaftlichen Fakultät der
Universität Basel

von

Jonas Sieber

aus Widnau, St. Gallen

Basel, Dezember 2011

Originaldokument gespeichert auf dem Dokumentenserver der Universität Basel
edoc.unibas.ch



Dieses Werk ist unter dem Vertrag „Creative Commons Namensnennung-Keine
kommerzielle Nutzung-Keine Bearbeitung 2.5 Schweiz“ lizenziert. Die vollständige

Lizenz kann unter

creativecommons.org/licences/by-nc-nd/2.5/ch eingesehen werden.

Genehmigt von der Philosophisch-Naturwissenschaftlichen
Fakultät auf Antrag von

Prof. Dr. Ed Palmer

Prof. Dr. Marc Donath

PD Dr. Andreas Jehle

Basel, den 13. Dezember 2011

Prof. Dr. Martin Spiess

Dekan der Philosophisch-
Naturwissenschaftlichen
Fakultät



Namensnennung-Keine kommerzielle Nutzung-Keine Bearbeitung 2.5 Schweiz

Sie dürfen:



das Werk vervielfältigen, verbreiten und öffentlich zugänglich machen

Zu den folgenden Bedingungen:



Namensnennung. Sie müssen den Namen des Autors/Rechteinhabers in der von ihm festgelegten Weise nennen (wodurch aber nicht der Eindruck entstehen darf, Sie oder die Nutzung des Werkes durch Sie würden entlohnt).



Keine kommerzielle Nutzung. Dieses Werk darf nicht für kommerzielle Zwecke verwendet werden.



Keine Bearbeitung. Dieses Werk darf nicht bearbeitet oder in anderer Weise verändert werden.

- Im Falle einer Verbreitung müssen Sie anderen die Lizenzbedingungen, unter welche dieses Werk fällt, mitteilen. Am Einfachsten ist es, einen Link auf diese Seite einzubinden.
- Jede der vorgenannten Bedingungen kann aufgehoben werden, sofern Sie die Einwilligung des Rechteinhabers dazu erhalten.
- Diese Lizenz lässt die Urheberpersönlichkeitsrechte unberührt.

Die gesetzlichen Schranken des Urheberrechts bleiben hiervon unberührt.

Die Commons Deed ist eine Zusammenfassung des Lizenzvertrags in allgemeinverständlicher Sprache: <http://creativecommons.org/licenses/by-nc-nd/2.5/ch/legalcode.de>

Haftungsausschluss:

Die Commons Deed ist kein Lizenzvertrag. Sie ist lediglich ein Referenztext, der den zugrundeliegenden Lizenzvertrag übersichtlich und in allgemeinverständlicher Sprache wiedergibt. Die Deed selbst entfaltet keine juristische Wirkung und erscheint im eigentlichen Lizenzvertrag nicht. Creative Commons ist keine Rechtsanwaltsgesellschaft und leistet keine Rechtsberatung. Die Weitergabe und Verlinkung des Commons Deeds führt zu keinem Mandatsverhältnis.

ABSTRACT

Podocyte apoptosis is a hallmark in the development and progression of diabetic nephropathy (DN). Several factors of the diabetic milieu are known to induce podocyte apoptosis. Currently, the role of free fatty acids (FFAs) for podocytopathy and podocyte cell death is unknown, although FFAs are considered to be crucially involved in the development of diabetes mellitus type II. It is well known that FFAs are toxic to several cell types including pancreatic β cells and they may contribute to the development of insulin resistance. The aims of this study were to elucidate the role of the saturated palmitic acid and the monounsaturated palmitoleic and oleic acid on podocyte cell death and endoplasmic reticulum (ER)-stress, to investigate more specifically the impact of ER-stress on podocyte survival as well as to elaborate strategies to protect podocytes from lipotoxicity.

The present study uncovered that palmitic acid induces podocyte apoptosis and necrosis and leads to ER-stress as reflected by induction of the unfolded protein response (UPR), i.e. upregulation of the ER chaperone immunoglobulin heavy chain binding protein (BiP), X-box protein 1 (XBP-1) mRNA splicing, and a strong upregulation of the proapoptotic transcription factor C/EBP homologous protein (CHOP). Gene silencing experiments of CHOP support a crucial involvement of CHOP and ER-stress in mediating the proapoptotic effect of palmitic acid in podocytes. Contrariwise, monounsaturated FFAs (MUFAs) such as palmitoleic and oleic acid prevent palmitic acid-induced podocyte death and attenuate ER-stress.

This study further revealed that the liver X receptor (LXR) agonist TO901317 (TO) ameliorates survival of palmitic acid-treated podocytes. Mechanistically, this beneficial effect can be explained mainly by the induction of stearoyl-CoA desaturase (SCD-) 1 and 2 as shown by gene silencing experiments and further supported from overexpression studies of SCD-1. Moreover, palmitic acid tracing experiments revealed a higher incorporation of palmitic acid into the triglyceride (TG) fraction in podocytes treated with TO or oleic acid, which is at least compatible with a benefit of increased fatty acid storage, by TO, i.e. SCDs, and MUFAs, respectively.

In addition, this study provides some preliminary data that adenylate cyclases (AC) may be an interesting target to protect podocytes from ER-stress in general and in

particular from palmitic acid-induced podocytopathy and cell death. Experiments with forskolin, a specific AC agonist, and cyclic AMP (cAMP) analogs protect from palmitic acid-induced podocyte lipotoxicity. The effect cannot be explained by an involvement of PKA-CREB signaling as overexpression of a dominant negative CREB mutant could not abrogate the protective effect of forskolin. Furthermore, the beneficial impact of forskolin is not influencing the intrinsic (mitochondrial) apoptotic pathway. However, in addition to the protection from palmitic acid-induced cell death, forskolin is suppressing podocyte death caused by other independent ER-stressors such as tunicamycin and thapsigargin. These findings suggest a direct role of forskolin and increased cAMP levels for a protection from ER-stress in podocytes.

In summary, this study unveiled antagonistic effects of palmitic acid versus monounsaturated FFAs for podocyte survival, ER-stress and the UPR. They support an important role of CHOP in the regulation of podocyte death by FFAs. Similarly to exogenous MUFAs, induction of SCDs partially protects podocytes from palmitic acid-induced ER-stress and podocyte death. The protective effect of MUFAs may be related to increased incorporation of palmitic acid into TGs. Additionally, preliminary data indicate that AC agonists such as forskolin may be interesting compounds to protect podocytes from ER-stress and from the toxic effects of FFAs. The results of this study offer a rationale for interventional studies aimed at testing whether dietary shifting of the FFA balance toward MUFAs, or tissue- (podocyte-) specific stimulation or overexpression of SCDs can delay the progression of DN. Similarly, the results of this study should encourage more studies to evaluate the therapeutic potential of AC agonists or phosphodiesterase inhibitors for the prevention and treatment of DN.

TABLE OF CONTENT

ABSTRACT	I
TABLE OF CONTENT	III
LIST OF FIGURES AND TABLES.....	VII
List of Figures	VII
List of Tables	IX
LIST OF ABBREVIATIONS	X
1. INTRODUCTION	1
1.1 Diabetic nephropathy (DN): prevalence, pathogenesis and the role of podocyte injury	1
1.1.1 Prevalence of diabetic nephropathy (DN): The most common cause of end-stage renal disease	1
1.1.2 Pathogenesis of DN.....	1
1.1.3 The role of podocytes in the pathogenesis of DN.....	2
Factors contributing to apoptosis of podocytes in DN.....	3
1.2 Pathophysiology of dyslipidemia in obesity and type II diabetes: causes and consequences of lipotoxicity	4
1.2.1 Disturbed lipid metabolism in obesity and type II diabetes	5
1.2.2 FFA lipotoxicity: opposing effects of saturated – and monounsaturated fatty acids.....	5
1.2.2.1 ER-stress and the unfolded proteins response (UPR).....	7
1.2.2.2 FFA-mediated ER-stress.....	9
1.3 Aim of the study.....	10
2. MATERIALS AND METHODS	11
2.1 Cell culture.....	11
2.2 Agonists, inhibitors, analogons and cytokines.....	11

2.3	Fatty acid preparation	12
2.4	Apoptosis assay.....	12
2.5	Cytochrome c release.....	12
2.6	Vectors and lentivirus production.....	13
2.6.1	Knockdown	13
2.6.2	Overexpression.....	13
2.6.2.1	SCD-1	13
2.6.2.2	ACREB	14
2.6.3	Lentivirus production.....	14
2.7	Western blot.....	14
2.8	Quantitative Reverse Transcription PCR (XBP-1 splicing)	15
2.9	Quantitative real-time PCR (SCD expression)	16
2.10	Quantitative real-time PCR of renal biopsies	17
2.11	Incorporation of palmitic acid into diglycerides (DAGs) and triglycerides (TGs) and β -oxidation [108]	17
2.11.1	DAG and TG analysis	17
2.11.2	β -oxidation determination	18
2.12	Statistical analysis.....	18
3.	RESULTS	19
3.1	Regulation of podocyte survival and endoplasmic reticulum stress by fatty acids [109].....	19
3.1.1	Palmitic acid induces apoptosis in podocytes	19
3.1.2	Palmitic acid induces ER-stress	22
3.1.3	CHOP silencing attenuates palmitic acid-induced podocyte death.....	23
3.1.4	Chemical chaperones do not protect podocytes from palmitic acid-mediated death	26
3.1.5	Monounsaturated fatty acids prevent the induction of ER-stress and block palmitic acid-induced podocyte death.....	27

3.1.6	Glomerular mRNA levels of BiP are induced in patients with DN	28
3.2	Role of Steroly-CoA Desaturases in palmitic acid-induced ER-stress and cell death in podocytes (Manuscript in preparation).....	29
3.2.1	TO901317 (TO) ameliorates survival of palmitic acid-treated podocytes.....	29
3.2.2	In podocytes SCD-2 is the predominant SCD isoform and TO strongly induces SCD-1 and SCD-2.....	30
3.2.3	Gene-silencing of SCD-2 and SCD-1 reverts the protective effect of TO on palmitic acid-induced podocyte death.....	31
3.2.4	Genetic overexpression of SCD-1 partially protects from palmitic acid-induced apoptosis	33
3.2.5	MUFAs and TO shift palmitic acid into triglycerides (TGs) and MUFAs induce fatty acid β -oxidation.....	35
3.3	The role of cAMP levels on palmitic acid-induced apoptosis in podocytes	37
3.3.1	Forskolin protects podocytes from palmitic acid-induced ER-stress and death by increasing cAMP levels.....	38
3.3.2	8-CPT-2Me-cAMP is less potent than 8-Br-cAMP in preventing palmitic acid-induced podocyte death.....	39
3.3.3	H89 partially reverts the protective effect of forskolin on palmitic acid-induced apoptosis but is itself enhancing the effect of palmitic acid.....	40
3.3.4	Forskolin is activating the transcription factor CREB	41
3.3.5	Forskolin is obviously acting not directly on the intrinsic apoptotic pathway	43
3.3.6	Forskolin generally protects podocytes from ER-stress-induced apoptosis and necrosis.....	44
4.	DISCUSSION	46
4.1	Palmitic acid induces podocytes death; involvement of ER-stress and CHOP	46
4.2	Palmitoleic and oleic acid attenuate palmitic acid-induced ER-stress and prevent palmitic acid-induced podocyte death	47

4.3	Stearoyl-CoA desaturases protect from palmitic acid-induced cell death ..	48
4.4	The protective effect of increased cAMP levels on palmitic acid-induced podocyte death	50
5.	CONCLUSION	53
6.	REFERENCES.....	54
7.	ACKNOWLEDGEMENT.....	68
APPENDIX	A-I	
	Regulation of podocyte survival and endoplasmic reticulum stress by free fatty acids. Am J Physiol Renal Physiol. 2010 Oct;299(4):F821-9.	A-I
7.1.1	- Am J Physiol Renal Physiol Article	A-I
7.1.2	- Supplemental material	A-XI
	Curriculum vitae	A-XV

LIST OF FIGURES AND TABLES

List of Figures

Figure 1:	Structure of the glomerular filtration barrier.....	2
Figure 2:	The unfolded protein response (UPR), adapted from [75].....	8
Figure 3:	Time-dependent induction of apoptosis and necrosis by palmitic acid.	19
Figure 4:	Palmitic acid induces apoptosis and necrosis in a dose-dependent manner.....	20
Figure 5:	Palmitic acid activates caspase 3 and induces mitochondrial cytochrome c release.	21
Figure 6:	Palmitic acid induces ER-stress: the chaperone BiP, the proapoptotic transcription factor CHOP and splicing of XBP-1 mRNA.....	23
Figure 7:	CHOP-silencing protects against palmitic acid-induced cell death.	24
Figure 8:	Gene-silencing of CHOP with a second shRNA sequence.....	26
Figure 9:	The chemical chaperone TUDCA has no protective effect on palmitic acid-induced cell death.....	27
Figure 10:	Palmitoleic and oleic acid prevent podocytes from palmitic acid-induced cell death and attenuate CHOP induction.	28
Figure 11:	In DN patients mRNA expression levels of BiP are increased and CHOP levels are downregulated.....	29
Figure 12:	TO induces SCD-1 and ameliorates survival of palmitic acid-treated podocytes.....	30

Figure 13: The expression pattern of SCD isoforms in the whole kidney differs from podocytes and TO strongly upregulates SCD-1 and SCD-2 in podocytes.....	31
Figure 14: SCD-2 silencing does not affect the protective effect of TO on palmitic acid-induced podocyte death.	32
Figure 15: Combined silencing of SCD-1 and SCD-2 partially reverses the protective effect of TO on palmitic acid-induced apoptosis.	33
Figure 16: Overexpressing SCD-1 moderately protects from palmitic acid-induced apoptosis and necrosis.	34
Figure 17: Oleic acid and TO increase palmitic acid incorporation into the TG fraction but only oleic acid reduces palmitic acid containing DAG levels in palmitic acid-treated podocytes.....	35
Figure 18: Cotreatment with oleic acid but not TO increases palmitic acid β -oxidation.	37
Figure 19: Forskolin protects from palmitic acid-induced apoptosis and reduces the induction of ER-stress.	39
Figure 20: The positive effect of forskolin on palmitic acid-induced apoptosis is caused by elevating levels of cAMP.	40
Figure 21: H89 is partially reverting the beneficial effect of forskolin on palmitic acid-induced apoptosis and necrosis but is enhancing itself the effect of palmitic acid.	41
Figure 22: Forskolin activates CREB in podocytes and induces its downstream target Bcl-2 at an early time point.	42

Figure 23: A dominant negative CREB does not impair the effect of forskolin on palmitic acid-induced cell death.....43

Figure 24: Forskolin ameliorates survival of thapsigargin- and tunicamycin-treated podocytes.....45

List of Tables

Table 1: Agonists, inhibitors and compounds with their applied concentrations11

Table 2: shRNA sequences and the particular vectors.....13

Table 3: The specific antibodies and the applied concentrations.....15

Table 4: Specific primer sequences.16

LIST OF ABBREVIATIONS

4-PBA	4-phenylbutyric acid
AC	Adenylate cyclase
ACC	Acetyl-CoA carboxylase
AGE	Advanced glycated end product
Aicar	5-aminoimidazole-4-carboxamide ribonucleoside
AMPK	AMP-activated protein kinase
ATF	Activating transcription factor
ATP	Adenosine triphosphate
Bcl-2	B-cell lymphoma 2
BiP	Immunoglobulin heavy chain binding protein
BSA	Bovine serum albumin
cAMP	3',5'-cyclic adenosine monophosphate
CHOP	C/EBP homologous protein
CMV	Cytomegalovirus
CPT-1	Carnitine palmitoyl transferase 1
CREB	cAMP response element binding protein
DAG	Diglyceride
DGAT1	DAG acyltransferase 1
DMEM	Dulbecco's modified eagle medium
DMSO	Dimethyl sulfoxide
DN	Diabetic nephropathy
DNA	Desoxyribonucleic acid
dNTP	Deoxyribonucleoside triphosphate
DPM	Disintegrations per minute
EDTA	Ethylenediaminetetraacetic acid
EGTA	Ethylene glycol-bis(2-aminoethylether)-N,N,N',N'-tetraacetic acid
Epac	Exchange protein directly activated by cAMP
ER	Endoplasmic reticulum
ERAD	ER associated protein degradation

ESRD	End-stage renal disease
FBS	Fetal bovine serum
FFA	Free fatty acid
FOXO4	Forkhead box protein O4
GAPDH	Glyceraldehyde 3-phosphate dehydrogenase
GBM	Glomerular basement membrane
GFP	Green fluorescent protein
GlcNAc	N-acetylglucosamine
GLP-1	Glucagon-like peptide-1
HEK	Human embryonic kidney
HYOU1	Hypoxia-upregulated protein 1
IRE-1	Inositol-requiring enzyme 1
IRS	Insulin receptor substrate
JNK	c-Jun NH ₂ -terminal kinase
LXR	Liver X receptor
MAP	Mitogen-activated protein
MCD	Minimal change disease
MPT	Mitochondrial membrane permeability transition
MUFA	Monounsaturated fatty acid
PBS	Phosphate-buffered saline
PCR	Polymerase chain reaction
PERK	Double-stranded DNA-dependent protein kinase (PKR)-like ER kinase
PI	Propidium iodide
PKA	Protein Kinase A
PPAR α	Peroxisome proliferator-activated receptor α
RAAS	Renin-angiotensin-aldosterone system
RIPA	Radioimmunoprecipitation assay
ROS	Reactive oxygen species
RPM	Revolutions per minutes
RPMI	Roswell Park Memorial Institute
SCD	Stearoyl-CoA desaturase
SD	Standard deviation

SDS-PAGE	Sodium dodecyl sulfate polyacrylamid gel electrophoresis
SERCA	Sarcoplasmic/endoplasmic reticulum calcium ATPase
SFA	Saturated fatty acid
SNP	Single nucleotide polymorphism
SREBP1c	Stearoyl regulatory-element binding protein 1c
TBS	Tris-buffered saline
TG	Triglyceride
TGF- β	Transforming growth factor β
TO	TO901317
TUDCA	Tauroursodeoxycholic acid
UPR	Unfolded protein response
VEGF	Vascular endothelial growth factor
VSV	Vesicular stomatitis virus
XBP-1	X-box binding protein 1

1. INTRODUCTION

In the following I will highlight the relevance of diabetic nephropathy (DN) and I will give an introduction into its pathogenesis. Thereby, the main focus will lie on podocytes which are highly specialized epithelial cells of the glomerular filtration barrier and which are considered to play an important role in the pathogenesis of DN. In a second part I will outline causes and the pathophysiology of dyslipidemia, which is a hallmark of diabetes mellitus. Also, the distinct effects of saturated and unsaturated fatty acids on cell function and cell survival will be described in more detail.

1.1 Diabetic nephropathy (DN): prevalence, pathogenesis and the role of podocyte injury

1.1.1 Prevalence of diabetic nephropathy (DN): The most common cause of end-stage renal disease

Diabetic nephropathy (DN) is the most common cause of end-stage renal disease (ESRD) in industrialized countries, e.g. 44% in the US [1]. Although the progression to ESRD is less likely in patients with type II than with type I diabetes, the majority of diabetic patients starting renal replacement therapy today have type II diabetes as the prevalence of type II diabetes is much higher [1]. Of the patients with type II diabetes 20-40% develop ESRD [2]. The five-year survival rate of patients with DN and renal replacement therapy is significantly worse than in patients with other renal diseases mainly as a result of an increased cardiovascular mortality [1, 3]. Therefore, it is important to better understand the pathogenesis of DN, to identify new strategies and additional therapeutic targets for the prevention and treatment of DN.

1.1.2 Pathogenesis of DN

Dating back to the first description by Kimmelstiel and Wilson [4] histological analysis has focused on the increase in mesangial matrix as the main lesion of DN. In addition, glomerular basement membrane (GBM) thickening, and mesangial cell hypertrophy have been considered important pathophysiological events in the disease. However, the genesis of proteinuria in diabetes is not readily explained by the

associated mesangial expansion. Rather, consideration should be given to alterations of the glomerular filtration barrier. The glomerular filter consists of three layers: a fenestrated endothelium, the GBM, and the glomerular visceral epithelium cell or podocyte (Fig. 1). Podocytes are highly specialized cells forming primary processes, which are branching into secondary foot processes. Foot processes of neighboring podocytes interdigitate, leaving between them filtration slits that are connected by an extracellular structure, the slit diaphragm [5]

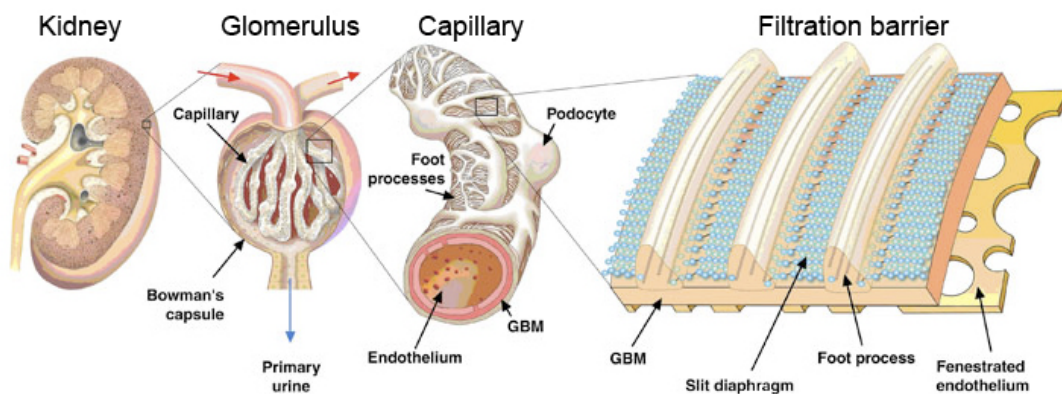


Figure 1: Structure of the glomerular filtration barrier. The glomerular filter consists of three layers: a fenestrated endothelium, the glomerular basement membrane (GBM) and the podocyte with their interdigitating foot process, the slit diaphragm. Picture adapted from website of Karolinska Institute, Stockholm, Sweden.

1.1.3 The role of podocytes in the pathogenesis of DN

Over the past two decades by elucidating the genetic origin of a number of single human gene defects that result in congenital or early onset nephrotic syndrome, it has become apparent that the final barrier restricting plasma proteins to the vasculature is the podocyte [6, 7]. Also, damage to podocytes has been linked to many renal diseases that often progress to ESRD [8]. However, little research has been conducted on podocyte biology in diabetes until recently.

Podocytopathy in DN is characterized by foot process widening which was shown to correlate in microalbuminuric type I diabetic subjects with the urinary albumin excretion rate [9]. In addition to foot process widening, the number and density of podocytes have been reported to be decreased in patients with type I or type II diabetes [10-14]. This podocyte loss clearly relates to elevated proteinuria [15]. The mechanism underlying proteinuria can be explained by the lack of charge and size selectivity in areas of podocyte loss. In Pima Indians with type II diabetes the reduced

number of podocytes per glomerulus was the strongest predictor of progressive kidney disease [16].

As podocytes have no or very limited ability to replicate [17] two mechanisms remain for the loss of podocytes in diabetes: apoptosis and/or cell detachment. The later scenario does not exclude a role of apoptosis, since cells may first detach and then undergo apoptosis or vice versa (anoikis = apoptosis caused by loss of attachment of cells to their basement membrane). Alternatively, detached cells can be shed in the urine as viable podocytes [18, 19]. In patients with type II diabetes podocyturia worsens with the progression from normoalbuminuria to microalbuminuria and to overt proteinuria [20].

Viable podocytes have also been isolated in the urine of DN-induced rats [18]. Podocytes are connected on the basolateral membrane to the GBM via integrins (α and β subunits) [21] and dystroglycans [22]. Decreased levels of $\alpha 3\beta 1$ integrins have been found in patients with DN and streptozotocin-induced diabetic rats [23], and altered expression of dystroglycan 1 has been observed in early DN of db/db mice, a type II diabetes model [24].

The second cause leading to a reduction in podocyte number is apoptosis. The decision whether a cell undergoes apoptosis can be seen as an imbalance between proapoptotic and survival factors. Data are increasing with the focus on factors that are altered in the diabetic milieu and shifting the cell fate towards apoptosis.

Factors contributing to apoptosis of podocytes in DN

In diabetes various factors are altered and contribute to the diabetic milieu. Several of these factors have been shown to damage the glomerulus and to influence directly podocyte survival. Among these factors are hyperglycemia, advanced glycated end products (AGEs), insulin resistance, TGF- β and angiotensin II.

Susztak and coworkers demonstrated that podocyte apoptosis is coinciding with the onset of diabetes in a type I diabetes (Akita mice) and a type II diabetes model (db/db mice) [25]. Furthermore they could show that hyperglycemia itself induces apoptosis in cultured podocytes via accumulation of reactive oxygen species (ROS).

Accordingly apocynin, a NADH oxidase inhibitor, could partially block podocyte depletion and proteinuria in diabetic mice [25].

In addition prolonged exposure of proteins to glucose leads to the formation of AGEs. In diabetes, tissue levels of AGEs are elevated [26]. In podocytes, AGEs result in increased expression of transforming growth factor β (TGF- β) and vascular endothelial growth factor (VEGF) [27]. Finally, AGEs lead to apoptosis involving the nuclear transcription factor FOXO4 [28] and endoplasmic reticulum (ER)-stress [29]. A recent study examined defective podocyte insulin signaling *in vivo* and it has been observed that insulin signaling itself is crucial for proper glomerular function. Podocyte-specific insulin receptor knockout mice are albuminuric at week 8 and show morphological changes of the glomerulus with loss of podocyte foot processes and increased apoptosis of podocytes [30].

The renin-angiotensin-aldosterone system (RAAS) is also critically involved in the pathogenesis of DN. Angiotensin II acts directly on the glomerulus by inhibiting mesangial matrix degradation [31]. Furthermore, angiotensin II is inducing podocyte apoptosis, potentially mainly through increased production of TGF- β [32]. TGF- β , a cytokine involved in tissue repair is known to be elevated in DN [33], leading to extracellular matrix expansion and consequently contributing to progressive glomerulosclerosis [34, 35]. Transgenic mice overexpressing TGF- β show glomerular abnormalities at three weeks of age and mice with the highest levels of TGF- β developed proteinuria after five weeks [35]. In the same mouse model podocyte number gradually decreased within five weeks. *In vitro* TGF- β induces apoptosis in podocytes via activation of the proapoptotic mitogen-activated protein (MAP) kinase p38 [36].

1.2 Pathophysiology of dyslipidemia in obesity and type II diabetes: causes and consequences of lipotoxicity

Apart from hyperglycemia and insulin resistance type II diabetes is characterized by altered blood lipid levels or dyslipidemia. In type II diabetes dyslipidemia is mainly manifested by increased lipid content (hyperlipidemia) such as hypertriglyceridemia and elevated plasma free fatty acids (FFAs). Contrariwise, increased plasma FFAs are critically involved in the pathogenesis of type II diabetes. Obesity is associated with

markedly increased plasma FFA, which is considered a major contributor to the development of type II diabetes [37, 38].

1.2.1 Disturbed lipid metabolism in obesity and type II diabetes

Under healthy conditions energy substrate metabolism is tightly controlled by endocrine and paracrine factors, e.g. insulin and catecholamines, to adjust energy availability to the particular needs. In general, availability of glucose is inhibiting lipolysis in fat cells (adipocytes) and fatty acid oxidation in tissue. In the fasted state, lipolysis is activated and provides fatty acids, or ketone bodies, which are produced by the liver. Both, fatty acids and ketone bodies are delivered as energy substrates to tissues [39, 40].

Obesity is caused by an imbalance of energy intake and expenditure leading to enlarged adipocytes (hypertrophy) and/or an increased adipocyte number (hyperplasia). Hypertrophy results from augmented storage of triglycerides (TGs) in lipid droplets. Enlarged, “saturated” adipocytes show decreased sensitivity towards the action of insulin, they release an increased amount of fatty acids, and they secrete inflammatory cytokines (adipokines) [41-43]. Adipokines are recruiting macrophages, which further amplify the inflammatory response [44]. The increased release of fatty acids from adipocytes elevates plasma FFA concentrations further, finally resulting in enhanced overspilling of fatty acids to non-adipose tissue [45, 46]. Constant exposure of non-adipose tissue to high levels of FFAs leads to accumulation of toxic metabolites such as diglycerides (DAGs) and ceramides. The associated cellular dysfunctions are referred to as lipotoxicity. Lipotoxicity aggravates insulin resistance, disrupts pancreatic β cell function (insulin secretion), and ultimately leads to programmed cell-death (lipoapoptosis) [46]. Once the compensatory hyperinsulinemia characteristic of obese, insulin-resistant individuals cannot be maintained as a result of pancreatic β cell failure, hyperglycemia i.e. type II diabetes manifests [45, 47, 48].

1.2.2 FFA lipotoxicity: opposing effects of saturated – and monounsaturated fatty acids

Up to 80% of the plasma FFAs consist of the saturated palmitic (C16:0) and stearic acid (C18:0), and the monounsaturated oleic acid (C18:1) [49]. Lipotoxicity has been

attributed mainly to saturated long chain fatty acids (SFAs) whereas monounsaturated fatty acids (MUFAs) exert beneficial and cytoprotective effects [50].

Adipocytes are naturally not susceptible to apoptosis induced by SFAs but they become insulin resistant and they express inflammatory cytokines [51]. However, preadipocytes with its little capacity to synthesize and store lipids undergo apoptosis when treated with palmitic acid [52]. Furthermore, exposure to palmitic acid is initiating insulin resistance and/or apoptosis in pancreatic β cells [48, 53-56], skeletal muscle cells [57, 58], cardiomyocytes [59, 60], hepatocytes [61-63], endothelial cells [64] and some breast cancer cells [65].

Palmitic acid-induced insulin resistance in hepatocytes has been attributed to increased reactive oxygen species (ROS) resulting from β -oxidation. ROS lead to phosphorylation and activation of c-Jun NH₂-terminal kinase (JNK) that is inhibiting insulin-stimulated tyrosine phosphorylation of insulin receptor substrate 2 (IRS-2) and subsequent serine phosphorylation of Akt via alternate threonine phosphorylation of IRS-2 [63, 66]. Alternatively, studies in skeletal muscle cells have shown that activation of protein kinase C isoforms by lipid metabolites such as DAGs and ceramide, inhibit insulin signaling by either serine phosphorylation of IRS-1 or by threonine phosphorylation of Akt [67]. In a recent study, JNK activation and insulin resistance have been causatively linked to the membrane-anchored tyrosine kinase c-Src. SFAs are leading to c-Src partitioning into membrane microdomains where c-Src likely becomes phosphorylated, which leads to phosphorylation and thereby activation of JNK [68]. Long-term exposure of cells to SFAs is generally causing apoptosis. Apoptosis has been linked, at least in part, to accumulation of ceramides and ROS that eventually induce the activation of the apoptotic machinery [53, 69].

In contrast, MUFAs are in general non-toxic and prevent from SFA-induced cell damage. The cytoprotective actions of MUFAs and their underlying mechanisms are not completely understood [50]. However, on one side MUFAs are more potent ligands of the peroxisome proliferator-activated receptor α (PPAR α), a transcription factor regulating lipid metabolism [70]. PPAR α is inducing transcription of genes involved in peroxisomal and mitochondrial β -oxidation [71]. Hence, MUFAs are thought to detoxify cells from SFAs by increasing β -oxidation. On the other side, coinubation of MUFAs and SFAs has been shown to restore TG synthesis as SFA-derived long chain acyl-CoAs are not incorporated into TGs very efficiently [65, 72].

It is thought that storage of SFAs in TGs prevent from the accumulation of toxic metabolites. Furthermore cotreatment restores levels of cardiolipin that, if reduced, results in increased cytochrome c release from mitochondria [65].

Associated with the distinct effects of SFAs and MUFAs is the initiation of endoplasmic reticulum (ER)-stress and the resulting activation of several signaling pathways, collectively known as unfolded protein response (UPR) [73].

1.2.2.1 ER-stress and the unfolded proteins response (UPR)

The ER is the organelle where secreted, membrane-bound and some organelle-targeted proteins are synthesized and folded. Optimal folding conditions require Ca^{2+} , ATP and an oxidizing environment to enable disulfide bond formation. As a consequence, the ER is highly sensitive to changes in Ca^{2+} and energy levels as well as in redox state [74, 75]. Such changes are reducing the folding capacity of the ER and thereby leading to an accumulation of unfolded and/or misfolded proteins, a condition that has been termed ER-stress. Cells have evolved strategies to counteract the detrimental effects of ER-stress, referred to as the UPR (Fig. 2). The UPR cascade is involving three signaling branches that are mediated by ER transmembrane receptors: double-stranded DNA-dependent protein kinase (PKR)-like ER kinase (PERK), inositol-requiring enzyme 1 (IRE-1), and activating transcription factor 6 (ATF6).

In the resting state the receptors are bound by the ER chaperone immunoglobulin heavy chain binding protein (BiP, also termed GRP78 or HSPA5) that keeps them silenced. Accumulation of unfolded and/or misfolded proteins is leading to dissociation of BiP and therefore to the activation of PERK, IRE-1 and ATF6.

PERK is dimerizing and autophosphorylation results in phosphorylation of eukaryotic initiation factor 2 that is inhibiting protein translation [76]. One of the genes not affected by this process is ATF4, a transcription factor which upregulates genes involved in stress response, redox reactions and amino acid metabolism [75, 77].

IRE-1 activation is occurring by oligomerization and its endoribonuclease domain is removing a 26 nucleotide long intron of X-box binding protein 1 (XBP-1) mRNA [78]. The spliced form of XBP-1 is an active transcription factor and binds to promoter elements to activate transcription of ER chaperones, ER associated protein

degradation (ERAD) factors and factors involved in ER membrane biogenesis [79-82].

Finally, dissociation of BiP leads to the transport of ATF6 to the Golgi where cleavage and release of the cytosolic domain takes place [79, 83, 84]. ATF6 translocates to the nucleus to activate transcription of target genes as chaperones and XBP-1.

If normal ER function cannot be restored apoptosis is initiated mainly by the transcription factor C/EBP homologous protein (CHOP). The promoter of CHOP contains binding sites for all three branches of the UPR: ATF4, ATF6 and XBP-1 [85]. However, the molecular mechanisms of CHOP-mediated apoptosis are not completely understood. Nevertheless CHOP has been linked to reduced expression of antiapoptotic Bcl-2, hyperoxidized ER lumen and calcium-related apoptotic signaling [86].

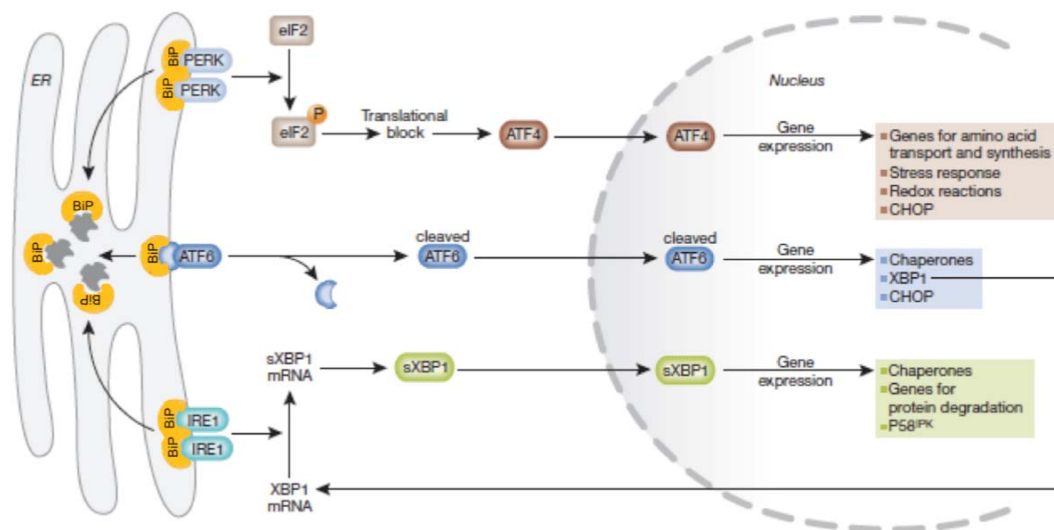


Figure 2: The unfolded protein response (UPR), adapted from [75]. After accumulation of un- and misfolded proteins, the ER chaperone BiP is dissociating from the three ER transmembrane receptors, PERK, IRE-1 and ATF-6, which are transmitting the ER-stress response. The UPR is leading to translational block, increased protein degradation and to expression of ER chaperones (e.g BiP). If ER-stress is persistent apoptosis is initiated, which is mainly executed by the transcription factor CHOP. PERK, PKR-like ER kinase; IRE-1, inositol-requiring enzyme-1; ATF6, activating factor 6; BiP, immunoglobulin heavy chain binding protein; CHOP, C/EBP homologous protein.

1.2.2.2 FFA-mediated ER-stress

Exposure to FFA is inducing ER-stress and initiating the UPR in several cell types. SFAs and MUFAs show quantitatively and qualitatively distinct or even opposite effects, i.e. MUFAs are protecting cells from the proapoptotic actions of SFA-induced ER-stress. Palmitic and oleic acid are rapidly incorporated into the ER membrane but only palmitic acid is leading to changes in ER structure and integrity [87]. Palmitic acid increases the saturated lipid content and compromises ER integrity, which is thought to trigger ER-stress. Of interest, overexpression and induction of ER-located stearoyl-CoA desaturases (SCDs), which catalyze the $\Delta 9$ -desaturation and thus the conversion of SFAs to MUFAs, have been shown to attenuate palmitic acid-induced ER-stress and apoptosis [88-90].

In pancreatic β cells, SFAs such as palmitic acid are activating all three branches of the UPR, PERK, IRE-1 and ATF-6. PERK and IRE-1 signaling are mainly responsible for the upregulation of the proapoptotic transcription factor CHOP [91]. In addition IRE-1 is activating JNK [91]. Both, CHOP and JNK, have been shown to be partially responsible for palmitic acid-induced pancreatic β cell apoptosis [91]. In contrast, MUFAs such as oleic acid are exclusively triggering ATF-6 signaling, which is inducing the ER chaperone BiP [91]. Moreover, oleic acid is preventing pancreatic β cells from palmitic acid-induced CHOP induction and JNK activation [91, 92]. These differences might explain the distinct actions of SFAs and MUFAs on cell lipotoxicity [93].

A similar picture has been observed in hepatocytes. Palmitic acid leads to an induction of CHOP and to JNK activation. CHOP-silencing revealed that CHOP can delay palmitic acid-induced hepatocyte apoptosis whereas inhibition of JNK signaling could suppress apoptosis [94]. Oleic acid is not inducing ER-stress but, consistently, prevented hepatocytes from palmitic acid-induced ER-stress [61].

In skeletal muscle cells, palmitic acid-induced ER-stress has been linked to impaired insulin signaling and oleic acid has been shown to block this effect by preventing from palmitic acid-induced abnormal cellular lipid composition and distribution [95]. Overall, ER-stress is thought to be crucially involved in FFA-mediated and in particular SFA-mediated lipotoxicity.

1.3 Aim of the study

As outlined before, podocytopathy is an early feature in the pathogenesis of DN and a decreased number of podocytes per glomerulus predicts progressive renal disease in type II diabetes patients [16]. Several factors of the diabetic milieu have been associated with podocyte dysfunction and/or apoptosis but very little is known about the role of dyslipidemia and FFAs on podocyte function and survival.

In vitro, SFAs in contrast to MUFAs are causing insulin resistance and/or apoptosis in several cell types and SFA-mediated lipotoxicity involves ER-stress. Importantly, ER-stress has been associated not only with the development of diabetes [86, 96, 97], but also with renal dysfunction [98].

The objectives of this study were to investigate the regulation of podocyte survival and ER-stress by fatty acids. More specifically, I explored the impact of the saturated palmitic acid and MUFAs, such as oleic and palmitoleic acid, on podocyte death and the involvement of ER-stress herein. Moreover, I investigated the role of cell autonomous conversion of SFAs into MUFAs by studying the impact of stearoyl-CoA desaturases, which catalyze the $\Delta 9$ -desaturation of SFA and thereby convert them to MUFAs. In addition, I examined the potential of elevated cAMP levels in preventing palmitic acid-induced podocyte death.

2. MATERIALS AND METHODS

2.1 Cell culture

Podocytes were cultured as described before by Mundel et al. [99, 100]. Briefly, conditionally immortalized podocytes were cultured under permissive conditions (33°C) in RPMI-1640 (#21875, Invitrogen) supplemented with 10% FBS (#10270, Invitrogen), 100 U/ml penicillin and 100 µg/ml streptomycin (#15140, Invitrogen) and interferon- γ (Cell Sciences) on type I collagen (BD Biosciences). Induction of differentiation is mediated by a thermo shift to 37°C without interferon- γ in 6-well plates (apoptosis assays, mRNA isolation, and lipid and β -oxidation analysis) and 10cm dishes (protein isolation). Experiments were performed at least at day 11 of differentiation.

HEK293 cells were cultured in DMEM (#41965, Invitrogen) supplemented with 10% FBS and penicillin/streptomycin.

2.2 Agonists, inhibitors, analogons and cytokines

The following agonists, inhibitors and compounds were used at the indicated concentrations (Table 1).

Substance	Product number #	Supplier	Action	Concentration
4-PBA	567615	Calbiochem	Chemical chaperone	0.5 mM
8-Br-cAMP	B7880	Sigma	cAMP analogon	100-200 µM
8-CPT-2Me-cAMP	116833	Calbiochem	cAMP analogon	200 µM
Forskolin	F6886	Sigma	AC agonist	1 µM
H89	371963	Calbiochem	PKA inhibitor	2-10 µM
Staurosporine	1048	BioVision	General kinase inhibitor	0.25 µM
TGF- β	100-21C	PeptoTech		5 ng/ml
Thapsigargin	586005	Calbiochem	SERCA inhibitor	1 µM
TO901317	71810	Cayman Chemical	LXR agonist	1 µM
TUDCA	580549	Calbiochem	Chemical chaperone	0.25-5 mM
Tunicamycin	T7765	Sigma	GlcNAc phosphotransferase inhibitor	2-5 µg/ml

Table 1: Agonists, inhibitors and compounds with their applied concentrations

2.3 Fatty acid preparation

Fatty acid preparation was applied by two different methods as described in Listenberger et al. (2001) and Maedler et al. (2001) [53, 69].

First, a 20 mM solution of palmitic or palmitoleic acid in 0.01 M NaOH (vehicle) was incubated at 70°C for 30 min and complexed to 10% BSA in a molar ratio of 6.6:1, shaken overnight at 37°C under N₂-atmosphere, sonicated for 10 min, sterile filtrated and stored at -20°C; the complexes were heated at 60°C for 15 min before use followed by dilution in culture medium.

Second, sodium palmitate, palmitoleic or oleic acid (all from Sigma) were dissolved overnight at 10 mM in glucose-free RPMI-1640 medium (#11879) containing 11% essential fatty-acid free BSA (Sigma) under N₂-atmosphere at 55°C, sonicated for 10 min and sterile filtered (stock solution). The molar ratio of fatty acid to BSA was 6:1. The effective free fatty acid concentrations were measured with a commercially available kit (Wako).

Both applications revealed comparable results but the second approach became the method of choice.

2.4 Apoptosis assay

The cells were trypsinized, washed once with PBS, and resuspended in 120 µl annexin V binding buffer (10 mM HEPES, 140 mM NaCl, 2.5 mM CaCl₂, pH 7.4). 100 µl of the cell suspension was used for the staining procedure. Alexa-647 annexin V (Invitrogen) staining was applied for 15 min at room temperature at a dilution of 1:100 (see producer protocol) and before analyzing an additional 400 µl of annexin V binding buffer and 0.5 µg propidium iodide (Invitrogen) were added. 20'000 – 25'000 cells were analyzed by flow cytometry (Beckman Coulter) [101]. Annexin V single positive cells were counted as apoptotic cells and annexin V and PI double positive cells were counted as (late apoptotic) necrotic cells.

2.5 Cytochrome c release

The cells were washed twice with ice cold PBS and incubated for 10 min on ice in digitonin lysis buffer (75 mM KCl, 1 mM NaH₂PO₄, 8 mM Na₂HPO₄, 250 mM sucrose and 190 µg/ml digitonin) in the presence of EDTA-free protease inhibitors

(Roche). The cytosolic fraction was collected and spun down at 500xg for 5 min at 4°C to remove cell debris. The supernatant was further analyzed by Western blotting.

2.6 Vectors and lentivirus production

2.6.1 Knockdown

A) Specific 21-nt CHOP oligonucleotides (see table 2) were cloned into a CMV vector (BbsI/BstBI) under an ubiquitin (U6) promoter. In a second step the U6-21-nt-oligonucleotides were cloned into a FUGW vector (BstBI/NheI) coexpressing GFP. A 21-nt scrambled sequence with no significant mammalian homology was applied as a control [101].

B) Specific SCD1 and SCD2 shRNAs in a PLKO.1 puro vector were obtained from Sigma.

Gene	shRNA sequence	Vector	GeneBank number
CHOP	GGAAACGAAGAGGAAGAATCA	FUGW	NM_007837
CHOP (2)	GGCGGGCTCTGATCGACCGCA	FUGW	NM_007837
Scrambled	GACCGCGACTCGCCGTCTGCG	FUGW	
Scrambled (2)	GACCGCATAGATACTAGACCC	FUGW	
SCD1	GCCTTTAATCAACCCAAGAAA	PLKO.1 puro	NM_009127
SCD1	CCTACGACAAGAACATTCAAT	PLKO.1 puro	NM_009127
SCD1	AGTTTCTAAGGCTACTGTCTT	PLKO.1 puro	NM_009127
SCD2	GAACATTAGCTCTCGGGAGAA	PLKO.1 puro	NM_009128
SCD2	CGCGTATTTGTACTATGTAAT	PLKO.1 puro	NM_009128

Table 2: shRNA sequences and the particular vectors.

2.6.2 Overexpression

2.6.2.1 SCD-1

The whole murine SCD1 sequence under a CMV promoter in an EZ-Lv153 vector was purchased from GeneCopoeia. GFP in a pLVX-puro vector, as well under a CMV promoter, was used as a control. It was kindly provided by Dr. Dennis Pfaff (University Hospital Basel, Switzerland).

2.6.2.2 ACREB

ACREB [102] was kindly provided by Prof. Handschin (University of Basel, Switzerland). The sequence was amplified with two primers (5'-ATAATTTTCGAACGGTGGGAGGT-3', 5'-AGAAGGCACAGTCGAGGCTG-3') and cloned into the vector pLVX-puro using the restriction sites BstBI and XbaI.

2.6.3 Lentivirus production

Lentivirus production was performed as previously reported by Dittgen et al. 2004 [103]. In brief, HEK293 cells (30-40% confluency in a T175 cm² flask (BD falcon)) were transfected using Fugene (Roche) with the expression (1 µg) and two helper plasmids, vesicular stomatitis virus (VSV) G protein (5 µg) and Δ8.9 (7.5 µg). The particular plasmids were added to a mixture of 45 µl Fugene and 500 µl Opti-MEM (Invitrogen), incubated for 15 min at room temperature and subsequently added to HEK293 cells in 20 ml culture medium (see part 2.1). 12 hours after transfection medium was exchanged and after 72 hours the supernatant was spun down at 780xg, filtered at 0.45 µm pore size and stored at -80°C.

Podocytes were transduced by adding virus-containing medium after five minutes pretreatment with 10 µg/ml Polybrene (Sigma). 8-24 hours after transduction medium was exchanged. Experiments were performed three to five days after viral transduction.

2.7 Western blot

Podocytes were washed with ice cold PBS and scraped in 200 µl RIPA lysis buffer (50mM Tris-HCl, pH 7.5, 200 mM NaCl, 1% Triton, 0.25% deoxycholic acid, 1 mM EDTA, 1mM EGTA) containing EDTA-free protease inhibitors (Roche) and phosphatase inhibitors (Pierce). To include the floating and detached cells, the culture medium and PBS (the cells were washed with) were collected, centrifuged (530xg) and resuspended in 20 µl lysis buffer. The pooled cells were lysed mechanically and rotated for 1 h at 4°C. To remove nuclei, the samples were spun down (10'000 rpm, 10 min) and the protein concentration of the supernatant was determined by D_C Protein Assay (Bio-Rad). 20 - 80 µg of protein was complemented with 6x sample buffer (200 mM Tris-HCl pH 6.8, 26% glycerol, 10% SDS, 0.01% bromphenol blue) and DTT (final concentration of 100 mM) and heated for 10 min at 95°C. Protein samples were loaded on 12-15% gels and SDS-PAGE was performed at 200 V.

Transfer to nitrocellulose membranes (Protran BA83, Whatman Schleicher und Schuell) was applied at 100 V in the coldroom for 1 hour and the blots were blocked for 2 hours with 5% milk powder in TBS-Tween (50 mM Tris HCl pH 7.4, 150 mM NaCl, 0.02% Tween). Primary antibodies were applied overnight and the secondary antibodies for 1 hour at the indicated dilutions in 5% milk in TBS-Tween (Table 3). The immunoblots were detected by enhanced chemiluminescence (Pierce) on Kodak BioMax light films (Sigma).

Antigen	Species	Conjugate	Supplier	Application	Dilution
Akt	Rabbit	Purified	Cell signaling	WB	1:1000
Bcl-2	Rabbit	Purified	Cell Signaling	WB	1:1000
BiP	Rabbit	Purified	Cell signaling	WB	1:500
Caspase 3	Rabbit	Purified	Cell signaling	WB	1:100
CHOP	Mouse	Purified	Santa Cruz	WB	1:200
CREB	Rabbit	Purified	Cell Signaling	WB	1:1000
Cytochrome c	Mouse	Purified	BD Bioscience	WB	1:3000
Flag	Mouse	Purified	Sigma	WB	1:2000
Mouse IgG	Goat antiserum	HRP	Jackson	WB	1:2000
P-Akt	Rabbit	Purified	Cell Signaling	WB	1:500
P-CREB	Rabbit	Purified	Cell Signaling	WB	1:500
Rabbit IgG	Goat antiserum	HRP	Dako	WB	1:1600
β -actin	Mouse	Purified	Sigma	WB	1:50'000

Table 3: The specific antibodies and the applied concentrations.

2.8 Quantitative Reverse Transcription PCR (XBP-1 splicing)

Total RNA was extracted with a Nucleospin kit (Macherey-Nagel GmbH) and first-strand cDNA was synthesized using oligo(dT) primers (Fermentas). The mRNA (0.5-2 μ g) and oligo(dT) (0.5 μ g) mix ($V_{\text{tot}} = 12.5 \mu\text{l}$) was heated at 70°C for 5 min and put on ice for 4 min. After addition of 5x RevertAid™ reaction buffer, dH₂O, RNase inhibitor (20 U), dNTPs (1 mM) and RevertAid™ Reverse Transcriptase (50 U; all from Fermentas) reverse transcription ($V_{\text{tot}} = 20 \mu\text{l}$) was performed at 42°C for 60 min and a final step at 72°C for 10 min.

cDNA (1 μ l) was amplified in a total volume of 10 μ l: 1 μ l dNTP mix (10 mM each, Sigma) 1 μ l of each primer (20 mM, see table 4), 1 μ l 25 mM MgCl₂ (Promega), 2 μ l Promega 5x Buffer, 3 μ l dH₂O and 0.2 μ l Taq Polymerase (Promega). Amplification

was performed with an initial denaturation at 94°C for 1 min, 30 cycles of PCR at 94°C for 30 s, 58°C for 30 s and 72°C for 1 min, and a final extension at 72°C for 10 min. β -actin was applied as a control. PCR products were separated by electrophoresis on 2.5% agarose gels in TAE running buffer (40 mM Tris acetate pH 8, 1 mM EDTA), stained for 10 min in 2 μ g/ml ethidium bromide (Sigma) and visualized by UV light.

2.9 Quantitative real-time PCR (SCD expression)

After cDNA synthesis (see part 2.7), real-time PCR was performed in a total volume of 20 μ l using 2x GoTaq® qPCR Master Mix (Promega) and 0.75 μ M of the particular primers (see table 4). GAPDH and β -actin were used as internal controls. The experiments were carried out in a 7500 Fast Real Time PCR System (Applied Biosystems) with an initial denaturation at 95°C for 10 min and 40 cycles of amplification (95°C for 15 sec and 60°C for 1 min).

Gene	Primer Sequence (5'-3')	Product Length (bp)	GeneBank number	Reference
XBP-1	Fw- TGAGAACCAGGAGTTAAGAACACGC Rv- TTCTGGGTAGACCTCTGGGAGTTCC	u* : 330 s* : 304	AF027963	[104]
SCD-1	Fw-TCTTGTCCCTATAGCCCAATCCAG Rv-AGCTCAGAGCGCGTGTTC	130	NM_009127	[105]
SCD-2	Fw-AGTGTTGCTCGTGAGCCTGTG Rv-CCTGCAGATCCATGTCCAGCTA	140	NM_009128	[105]
SCD-3	Fw-TCACACCGTGAACCCTGAGATTGT Rv-TGCTTGCTCTGCCTCTTGACCTAT	160	NM_024450	[105]
SCD-4	Fw-ACCTTGCTCTCTCTGCCTTCACAA Rv-TGCTGGAGATCTCTTGTGGCAAGT	84	NM_183216	[105]
β -actin	Fw-GAAATCGTGCGTGACATCAAA Rv-GTGCACCGCAAGTGCTTCTAG	510	NM_007393	
GAPDH	Fw-CTGCACCACCAACTGCTTAGC Rv-GGCATGGACTGTGGTCATGAG	88	NM_008084	

Table 4: Specific primer sequences.

2.10 Quantitative real-time PCR of renal biopsies

Experiments were performed by the group of Prof. Cohen at the University of Zurich. Human renal biopsy specimens were procured in an international multicenter study, the European Renal cDNA Bank-Kroener-Fresenius Biopsy bank (ERCB-KFB). Biopsies were obtained from patients after informed consent and with approval of the local ethnics committees. Following renal biopsy, the tissue was transferred to RNase inhibitor and microdissected into glomerular and tubular fragments. Total mRNA isolation from microdissected glomeruli and reverse transcription real-time PCR were performed as reported previously by Cohen and coworkers [106]. Pre-developed TaqMan reagents were used for human BiP (NM_005347.2), HYOU (NM_006389.2) CHOP (NM_004083.4), as well as reference genes (Applied Biosystems). The expression of BiP, HYOU1 and CHOP was normalized to the mean of three reference genes: GAPDH, 18 rRNA and synaptopodin. The mRNA expression was analyzed by standard curve quantification [107].

2.11 Incorporation of palmitic acid into diglycerides (DAGs) and triglycerides (TGs) and β -oxidation [108]

Pretreatment was carried out in complete medium for 14 hours. The experiment was performed in serum-free medium supplemented with 0.5% FFA-free BSA containing 200 μ M palmitic acid or the combination of palmitic and oleic acid (100 μ M each) in the presence of 0.5 μ Ci/ml [3 H]-palmitic acid.

2.11.1 DAG and TG analysis

At the particular time points the cells were washed three times with cold PBS and scraped in a volume of 120 μ l PBS. To extract total lipids the lysates were transferred to 500 μ l chloroform/methanol/5N HCl (2:1:0.05, v/v), rotated for 5 min and centrifuged at 350xg for 5 min. The organic phase was dried under N₂ and redissolved in 30 μ l of chloroform. 5 μ l were applied to measure radioactivity of the total lipid fraction and 20 μ l were loaded onto silica plates (20x20 cm; Sigma). Lipid fractions were separated by unidimensional thin layer chromatography in n-Hexane/diethyl ether/methanol (45:10:1, v/v). The lipid standards (Sigma) were visualized by spraying with KMnO₄ and subsequent drying and heating with a Bunsen burner. The spots corresponding to the adequate markers were scraped into scintillation vials and

after addition of 150 μ l methanol and 2 ml of scintillation buffer radioactivity was measured. Values of DAGs and TGs were normalized to total lipid.

2.11.2 β -oxidation determination

At the particular time points the supernatant (1 ml) was transferred to 5 ml of chloroform/methanol/5N HCl (2:1:0.05, v/v), rotated for 5 min and spun down at 350xg for 5 min. 500 μ l of the aqueous phase was added to 2 ml of scintillation buffer before measuring radioactivity. Values of β -oxidation were normalized either to total protein or total lipid.

2.12 Statistical analysis

Data are expressed as means and SD. Significance of differences was calculated with a two-sided, unpaired t-test. For the real-time RT-PCR data of mRNA expression in renal biopsies statistical analysis was performed using Kruskal-Wallis and Mann-Whitney U tests.

3. RESULTS

3.1 Regulation of podocyte survival and endoplasmic reticulum stress by fatty acids [109]

3.1.1 Palmitic acid induces apoptosis in podocytes

The saturated palmitic acid is inducing cell death in several cell types [53, 57, 110]. In a first experiment podocytes were exposed to 500 μ M palmitic acid complexed to BSA for 10, 24, 34 and 48 hours and stained with annexin V and PI (Fig. 3a).

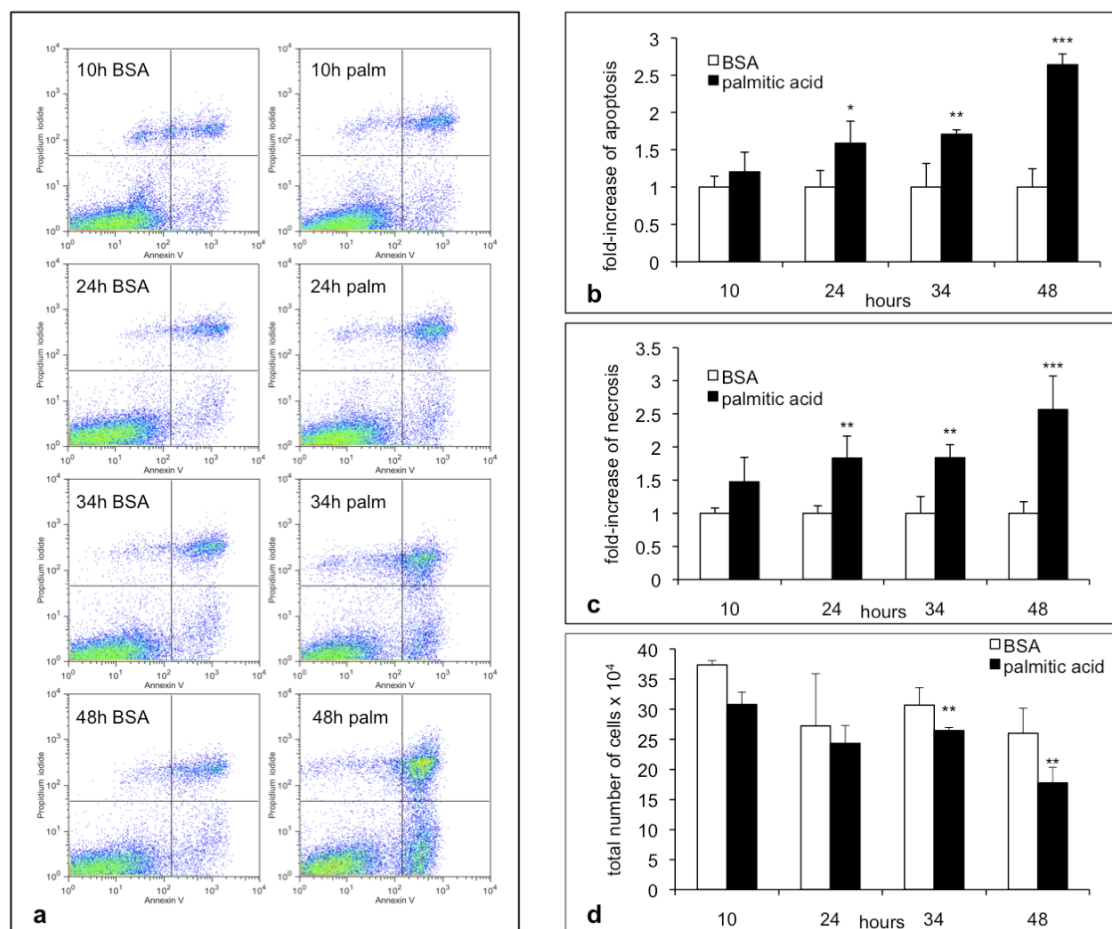


Figure 3: Time-dependent induction of apoptosis and necrosis by palmitic acid. a) Representative flow cytometry results for podocytes treated with 500 μ M palmitic acid or BSA for 10, 24, 34 and 48 hours and stained for annexin V and PI. b,c) Bar graphs represent mean fold-increase \pm SD of apoptotic (annexin V-positive/PI-negative) and necrotic (annexin V-positive/PI-positive) podocytes, respectively. BSA controls were set to 1. d) Bar graph represent the number of cells recovered from culture dishes to analyze by flow cytometry.

Decreasing number of cells reflect the accumulation of necrotic cell debris that could not be recovered for flow cytometry. (n = 3, * p = 0.05, ** p < 0.05, *** p < 0.01).

Fatty acid free BSA was used as a control. Annexin V single positive cells were considered as (early) apoptotic and annexin V and PI double positive cells as (late apoptotic and) necrotic cells. Cell death of podocytes, both apoptosis and necrosis, increased over time and became apparent after 24 hours. After 48 hours, a 2.5 to 3-fold increase of apoptotic and necrotic podocytes was observed (p < 0.01, Figs. 3b, c). Of note, the increase of annexin V/PI double positive late apoptotic/necrotic was underestimated by flow cytometry as more floating cellular debris was formed in the supernatants of cell pellets used for flow experiments over time. This was reflected in a decreased total number of cells recovered in cell pellets after 34 and 48 hours (p < 0.05; Fig. 3d).

500 μ M of palmitic acid is a high free fatty acid concentration even under diabetic conditions. Therefore, apoptosis and necrosis was additionally examined at lower concentrations (125, 250 μ M) of palmitic acid (Fig. 4).

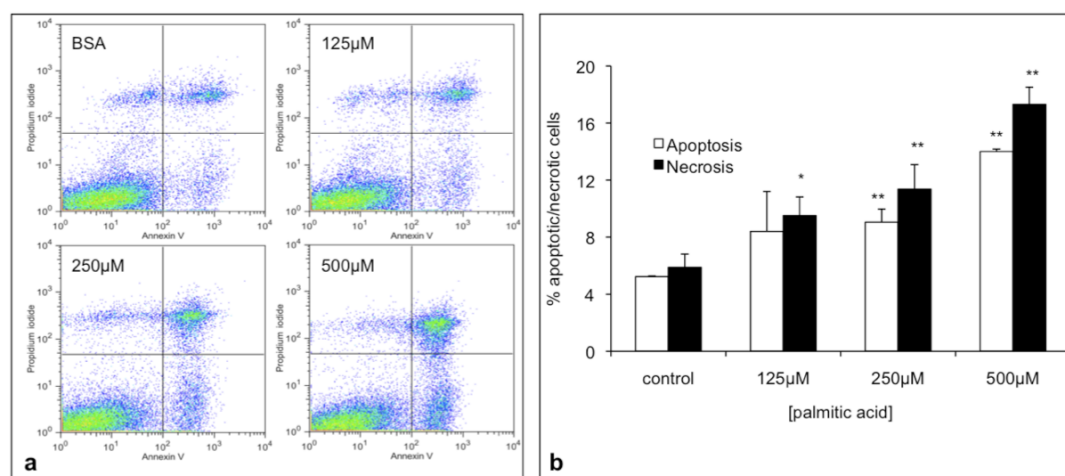


Figure 4: Palmitic acid induces apoptosis and necrosis in a dose-dependent manner. a) Representative flow cytometry results for podocytes exposed to 125, 250 and 500 μ M palmitic acid or BSA (at concentration equivalent to cells treated with 500 μ M palmitic acid complexed to BSA) for 38 hours. The abscissa and ordinate represent the fluorescence intensity of annexin V and PI, respectively. b) Quantitative analysis of palmitic acid-induced cell death. Bar graph represents the mean percentages \pm SD apoptotic and necrotic podocytes (n = 3; * p < 0.05, ** p < 0.01).

After 24 hours of treatment no toxic effect was visible at 125 and 250 μM (data not shown). Palmitic acid-induced cell death was dose-dependently increased after 38 hours. In BSA control, $5.2 \pm 0.1\%$ of podocytes were apoptotic and $5.9 \pm 0.9\%$ were necrotic. Palmitic acid significantly increased apoptosis at 250 ($9.1 \pm 0.9\%$, $p < 0.01$; Fig. 4b) and 500 μM ($14.0 \pm 0.2\%$, $p < 0.01$; Fig. 4b). Similar findings were observed for necrosis (at 500 μM , 17.3 ± 1.2 , $p < 0.01$; Fig. 4b). Furthermore necrotic cells were already increased at 125 μM (Fig. 4b).

To confirm the effect of palmitic acid on apoptosis and necrosis with a second independent approach caspase 3 cleavage and mitochondrial cytochrome c release were examined by Western blotting. As caspase 3 activation occurs before externalization [111] of phosphatidylserine podocytes were treated with palmitic acid for 1 and 16 hours. Staurosporine, a general kinase inhibitor and a strong inducer of apoptosis, was used as a positive control. Cleaved caspase 3 was detected in staurosporine-treated podocytes after 1 hour. In palmitic acid-treated podocytes the effect was visible after 16 hours (Fig. 5a). Consistent with the flow cytometry data activation of caspase 3 was also observed at lower concentrations of palmitic acid (Fig. 5b). In addition, mitochondrial cytochrome c was released into the cytosol after exposure to palmitic acid (Fig. 5c).

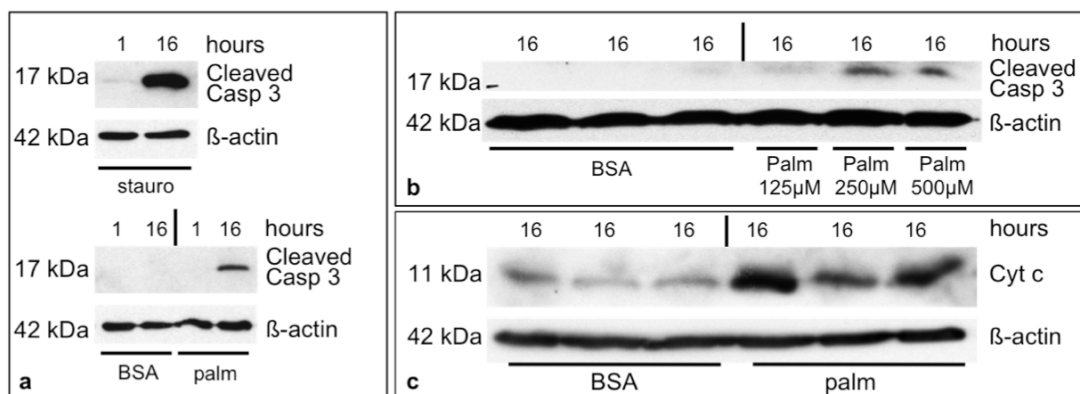


Figure 5: Palmitic acid activates caspase 3 and induces mitochondrial cytochrome c release. Western blot of activated, cleaved caspase 3 of podocytes exposed to staurosporine (0.25 μM), BSA or palmitic acid. β -actin was used as a control. a) Staurosporine and palmitic acid (500 μM) caused strong activation of caspase 3 at 16 hours. No signal was detected after 1 hour-treatment of palmitic acid. b) Dose-dependent cleavage of caspase 3 in podocytes exposed to 125, 250 or 500 μM palmitic acid for 16 hours. c) Western blot of cytosolic cytochrome c of podocytes exposed to palmitic acid (250 μM) for 16 hours. β -actin served as a loading control.

3.1.2 Palmitic acid induces ER-stress

The toxicity of palmitic acid has been attributed to involve the induction of ER-stress [52, 54, 56, 61, 62]. Therefore, the effect of palmitic acid on protein levels of BiP, an ER chaperone that is upregulated during ER-stress, and CHOP, a proapoptotic transcription factor that is typically upregulated in severe and prolonged ER-stress was studied [112]. 500 μ M palmitic acid led to a 6-fold ($p < 0.01$) upregulation of BiP at 24 hours (Fig. 6a). Analogous to apoptosis and necrosis BiP was also induced at lower concentrations (data not shown). Similarly, CHOP levels were increased 9 times ($p < 0.01$) in podocytes treated for 24 hours with 500 μ M palmitic acid (Fig. 6b). In addition, CHOP induction was dose- and time-dependent and it occurred as early as 6 hours (Fig. 6c). Other known apoptotic stimuli as high glucose [25], TGF- β [36] and staurosporine did not induce CHOP (Fig. 6e). However, high glucose might enhance the effect of palmitic acid. Interestingly, TGF- β (5 ng/ml) alone or in combination with high glucose induced BiP.

XBP-1 is involved in the transcriptional activation of CHOP in ER-stress, but only the spliced form of XBP-1 (sXBP-1) has transcriptional activity [113]. Therefore, RT-PCR had been used to amplify fragments of XBP-1 representing both the unspliced (uXBP-1) and the spliced (sXBP-1) forms of XBP-1 mRNA. Palmitic acid and tunicamycin (Tn), an established inducer of ER-stress, strongly induced sXBP-1 and an additional slower migrating band (Fig. 6d). The slowly migrating band represents a hybrid form of uXBP-1 and sXBP-1 (hXBP-1), which can form during annealing in the last PCR step [114]. XBP-1 splicing was increased as early as 4 hours after exposure to palmitic acid (data not shown), implying a potential role of XBP-1 splicing in transcriptional activation of CHOP [112].

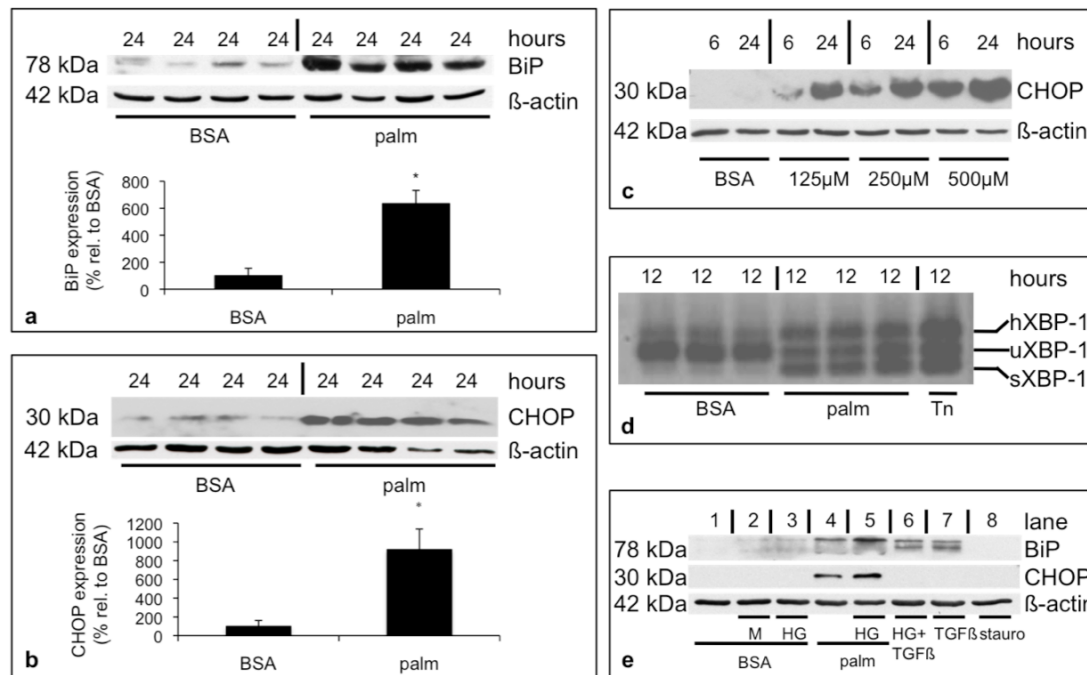


Figure 6: Palmitic acid induces ER-stress: the chaperone BiP, the proapoptotic transcription factor CHOP and splicing of XBP-1 mRNA. a) Palmitic acid-induced upregulation of BiP (top) and quantitative analysis of BiP levels normalized to β -actin. BSA control was set to 100% (n = 4; * p < 0.01). b) Palmitic acid-induced upregulation of CHOP (top) and quantitative analysis of CHOP levels normalized to β -actin. BSA control was set to 100% (n = 4; * p < 0.01). c) Time- and dose-dependent induction of CHOP in podocytes exposed to 125, 250 or 500 μ M palmitic acid for either 6 or 24 hours. d) RT-PCR of XBP-1 after exposure of 500 μ M palmitic acid for 12 hours. In BSA-treated controls the unspliced fragment (u) was predominant whereas treatment with palmitic acid and tunicamycin (5 μ g/ml) augmented the spliced (s) and the hybrid (h) form. e) BiP and CHOP expression after 24 hours of exposure. Lane 1, control BSA and 5 mM glucose (LG); lane 2, BSA control, LG and 17 mM Mannitol (M); lane 3, BSA control and 22 mM glucose (HG); lane 4, 500 μ M palmitic acid and LG; lane 5, 500 μ M palmitic acid and HG; lane 6, TGF- β (5 ng/ml) and HG; lane 7, TGF- β and LG; lane 8, 0.25 μ M staurosporine (stauro). β -actin was used as a control.

3.1.3 CHOP silencing attenuates palmitic acid-induced podocyte death

As shown before, the proapoptotic transcription factor CHOP is markedly induced by palmitic acid treatment and levels are already elevated at early time points. To test whether CHOP is mechanistically involved in palmitic acid-induced cell death CHOP knockdown podocytes were generated. CHOP silencing was performed by lentivirus transduction using CHOP-specific shRNA and a scrambled sequence was used as a

control. Knockdown efficiency was examined by Western immunoblotting of whole cell lysates of podocytes treated with tunicamycin for 24 hours. CHOP levels were reduced by $88 \pm 10\%$ ($p < 0.001$; Fig. 7a, b). Surprisingly, BiP levels were also significantly decreased ($44 \pm 1\%$, $p < 0.01$; Fig. 7a, b). A similar picture was observed in podocytes treated with $500 \mu\text{M}$ palmitic acid (Fig. 7c).

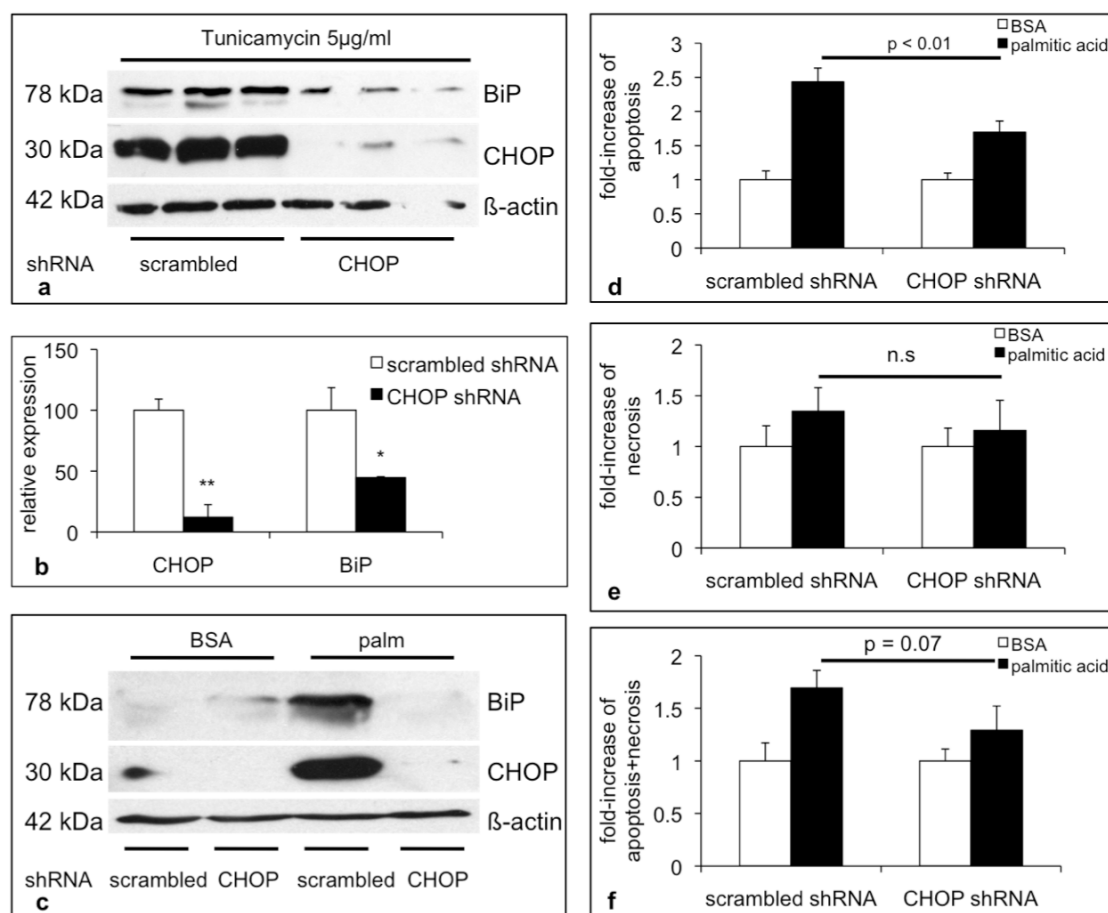


Figure 7: CHOP-silencing protects against palmitic acid-induced cell death. a,b) Gene-silencing of CHOP suppresses tunicamycin-induced upregulation of CHOP and BiP. Bar graphs (b) show the relative expression of CHOP \pm SD. A scrambled shRNA was used as a control and set to 100%. β -actin was used to normalize ($n = 3$, * $p < 0.01$, ** $p < 0.001$). c) CHOP shRNA suppresses palmitic acid-induced upregulation of CHOP and BiP. d-f) Gene-silencing of CHOP blocks palmitic acid-induced apoptosis ($200 \mu\text{M}$) after 38 hours but not necrosis. Bar graphs represent mean fold-increase \pm SD of apoptotic (d), necrotic (e), and apoptotic + necrotic (f) cells. BSA controls were set to 1 ($n = 3$).

In a next step, the effect of CHOP silencing on palmitic acid-induced apoptosis and necrosis was examined. As $500 \mu\text{M}$ is a high concentration and a protective effect of CHOP knockdown might not become visible the experiments were performed with

200 μ M palmitic acid for 48 hours. Podocytes either transduced with CHOP-shRNA or scrambled-shRNA were treated with palmitic acid or BSA and stained with annexin V and PI. Absolute numbers of apoptotic and necrotic cells were slightly increased in CHOP-silenced podocytes compared to control (data not shown). Although, the relative fold-increase of apoptosis (the ratio palmitic acid to BSA control) was significantly reduced in CHOP-silenced cells (1.7 ± 0.2 -fold) compared to control (2.4 ± 0.2 -fold; Fig. 7d). No significant reduction was observed for necrosis (Fig. 7e).

To verify the essential role of CHOP in inducing palmitic acid-induced podocyte death the experiments have been repeated with a second set of shRNA sequences (in Methods signed with (2)). Knockdown of CHOP was again efficient in podocytes treated with palmitic acid and tunicamycin but BiP levels remained unaffected (Fig. 8a). Absolute numbers of apoptosis and necrosis were lower in CHOP-silenced cells treated with BSA ($5.1 \pm 1.0\%$ and $5.8 \pm 1.1\%$) compared to controls ($8.8 \pm 0.7\%$ and $8.5 \pm 0.3\%$; Fig. 8b). Furthermore, apoptosis and necrosis were strongly prevented in palmitic acid-treated CHOP-silenced cells: $7.7 \pm 0.6\%$ vs. $21.8 \pm 3.2\%$ apoptotic cells and $7.6 \pm 1.0\%$ vs. $13.8 \pm 0.8\%$ necrotic cells (Fig. 8b). The effect is also highlighted in the significant reduction of the relative fold-increase in CHOP-silenced podocytes (Fig. 8c, d). Overall, the results of both CHOP-shRNA sequences indicate a crucial involvement of CHOP in mediating palmitic acid-induced cell death.

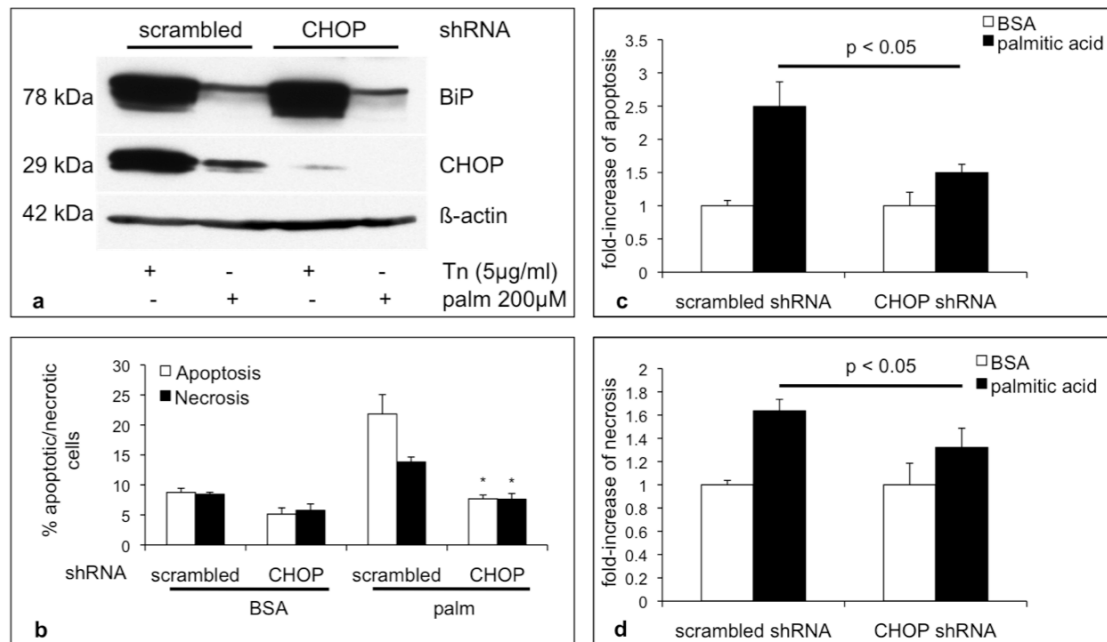


Figure 8: Gene-silencing of CHOP with a second shRNA sequence. a) CHOP shRNA suppresses tunicamycin- and palmitic acid-induced upregulation of CHOP. However, BiP levels remain unchanged. b-d) Gene-silencing of CHOP prevents palmitic acid-induced cell death. A scrambled sequence served as a control. b) Bar graphs show mean percentages \pm SD of apoptotic and necrotic cells ($n = 3$; $p < 0.05$). c,d) Bar graphs represent mean fold-increase \pm SD of apoptotic and necrotic cells, respectively. BSA controls were set to 1.

3.1.4 Chemical chaperones do not protect podocytes from palmitic acid-mediated death

The previous results clearly point to an active contribution of ER-stress in palmitic acid-induced podocyte apoptosis and necrosis. Treatment with small molecules, classified as chemical chaperones have been reported to enhance ER folding [115]. Although the mechanisms of action of these compounds are not completely understood they have been classified as such due to their ability to protect cells from ER-stress and to facilitate protein folding [116, 117]. Two of these molecules, 4-phenylbutyric acid (4-PBA) and tauroursodeoxycholic acid (TUDCA) have been demonstrated to reduce the induction of ER-stress in an obesity and type II diabetes mouse model [118]. To examine if chemical chaperones can reduce susceptibility towards palmitic acid-induced cell death, podocytes were treated with 4-PBA and TUDCA. 4-PBA worsened the effect of palmitic acid even at low concentrations (data not shown). On the other side TUDCA was not toxic itself but also had no clear beneficial effect on palmitic acid-induced apoptosis (Fig. 9; 0.5 mM TUDCA, $p =$

0.19). Palmitic acid-mediated ER-stress in podocytes might not be triggered by an accumulation of misfolded proteins but rather by impaired ER membrane integrity and ER-to-Golgi protein trafficking [87, 119].

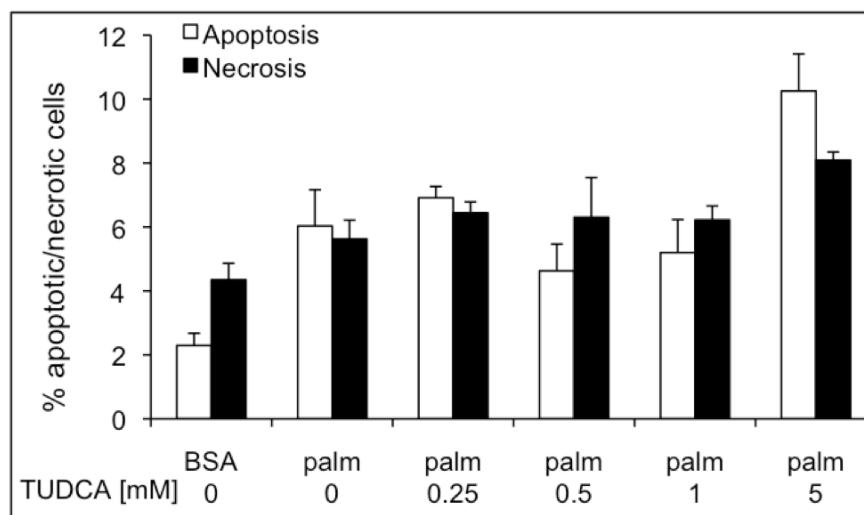


Figure 9: The chemical chaperone TUDCA has no protective effect on palmitic acid-induced cell death. Podocytes were pretreated with 0.25, 0.5, 1 and 5 mM TUDCA for 1 hour and incubated with 200 μ M palmitic acid for 48 hours. Bar graphs show mean percentages \pm SD of apoptotic and necrotic cells (n = 3).

3.1.5 Monounsaturated fatty acids prevent the induction of ER-stress and block palmitic acid-induced podocyte death

Unlike saturated fatty acids (SFAs) monounsaturated fatty acids (MUFAs) as palmitoleic and oleic acid show no toxic effects on several cell types and furthermore they could rescue cells from palmitic acid-induced cell death and ER-stress [92, 120]. Therefore, podocytes exposed to 500 μ M palmitic acid were coincubated with either 500 μ M palmitoleic or oleic acid. Induction of apoptosis and necrosis was analyzed after 38 hours. Both, palmitoleic and oleic acid could prevent podocyte death caused by palmitic acid (Fig. 10a, c). In line with this observation palmitoleic and oleic reduced the induction of CHOP and BiP (Fig. 10b, d).

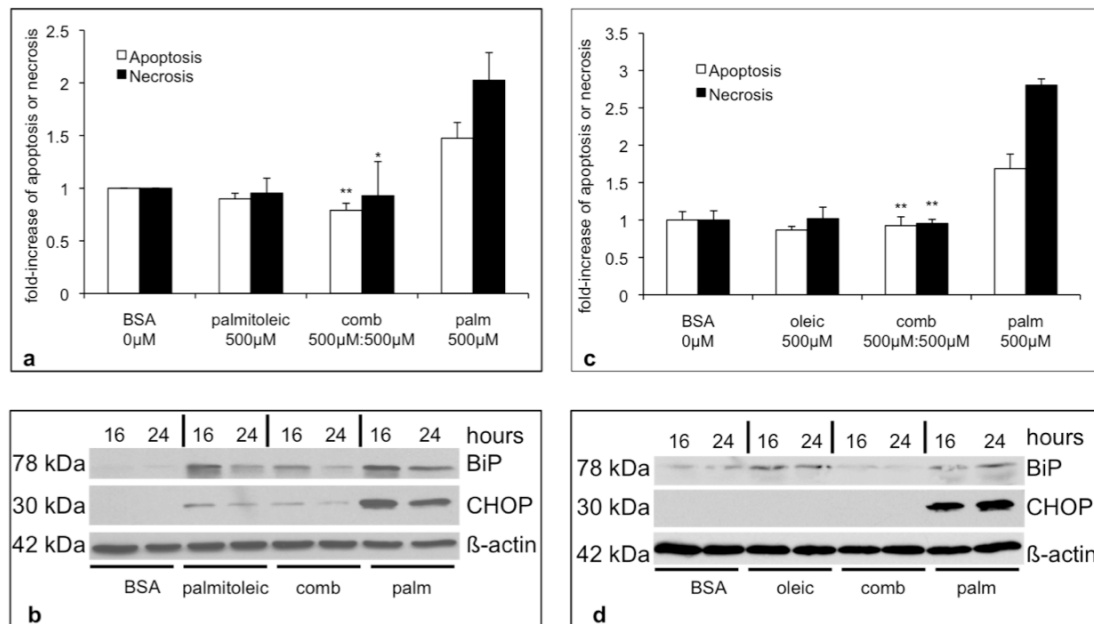


Figure 10: Palmitoleic and oleic acid prevent podocytes from palmitic acid-induced cell death and attenuate CHOP induction. a,c) palmitoleic and oleic acid block palmitic acid-induced cell death after 38 hours. Bar graphs represent mean fold-increase \pm SD of apoptotic and necrotic cells. BSA controls were set to 1 ($n = 3$; * $p < 0.05$ ** $p < 0.01$ compared with palmitic acid). b,d) palmitoleic and oleic acid block palmitic acid-induced upregulation of BiP and CHOP after 16 and 24 hours. β -actin was applied as a loading control.

3.1.6 Glomerular mRNA levels of BiP are induced in patients with DN

As shown before elevated SFA levels lead to ER-stress in podocytes *in vitro*. In addition induction of ER-stress has been observed in two rodent DN models [121, 122]. To evaluate an involvement of ER-stress in DN mRNA levels of the ER-stress markers BiP, CHOP and hypoxia-upregulated protein 1 (HYOU1) were quantified in glomerular extracts of patients with DN. They were compared to healthy controls and patients with minimal change disease (MCD). Consistent to the *in vitro* data the chaperone BiP was significantly upregulated in DN patients (Fig. 11). HYOU1 levels showed increased tendency but the data were not significant (Fig. 11). Interestingly, the proapoptotic factor CHOP was significantly down compared to both healthy controls and MCD patients (Fig. 11). These findings in one hand confirm a participation of ER-stress as BiP was up but on the other hand the downregulation of CHOP is opposing the *in vitro* data. It may be explained by the possibility that apoptotic podocytes detach and are not included in the analysis.

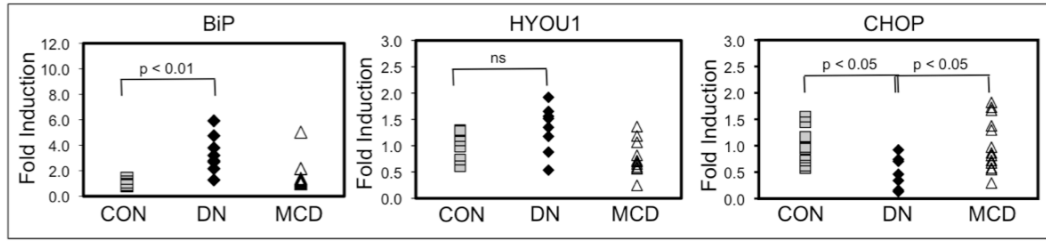


Figure 11: In DN patients mRNA expression levels of BiP are increased and CHOP levels are downregulated. mRNA levels of BiP, HYOU1 and CHOP were quantified in microdissected glomeruli from controls (CON; n = 6), patients with MCD (n = 12) and patients with established DN (n = 8). The graphs show expression ratios of each gene normalized to three reference genes (18S rRNA, hGAPDH and synaptopodin).

3.2 Role of Steroly-CoA Desaturases in palmitic acid-induced ER-stress and cell death in podocytes (Manuscript in preparation)

As MUFAs such as palmitoleic acid or oleic acid can reduce the induction of ER-stress and completely protect podocytes from palmitic acid-induced cell death, I explored in a next step whether stimulation of podocyte autonomous fatty acid desaturases can protect podocytes from palmitic acid-induced cell death.

Stearoyl-CoA desaturases (SCDs) catalyze the $\Delta 9$ -desaturation of SFA. Four SCD isoforms have been identified in mice [123-125]. In the current literature, SCD-1 and SCD-2 are ubiquitously expressed whereas SCD-3 expression is restricted to the skin, preputial gland and harderian gland and SCD-4 to the heart [125, 126]. The predominant isoform in most tissues including the kidney is SCD-1 [126] and SCD-1 is positively regulated by liver X receptor (LXR) binding to an LXR response element in the SCD-1 promoter [127] and by LXR-mediated stearoyl regulatory-element binding protein 1c (SREBP1c) transcription [128].

3.2.1 TO901317 (TO) ameliorates survival of palmitic acid-treated podocytes

To investigate the potentially beneficial action of SCDs on palmitic acid-induced lipotoxicity in podocytes it has been taken advantage of TO901317 (TO), an LXR agonist [129], which is known to induce SCD-1. Figure 12a shows that TO-treatment of podocytes for 14 hours led to a 2-3-fold increase in SCD-1 levels. To test the effect of TO on cell viability, podocytes were pretreated with 1 μ M TO for 14 hours and

subsequently incubated with 200 μ M palmitic acid for 48 hours. Incubation with TO reduced apoptosis by $38 \pm 6\%$ and necrosis by $30 \pm 8\%$ (Fig. 12b).

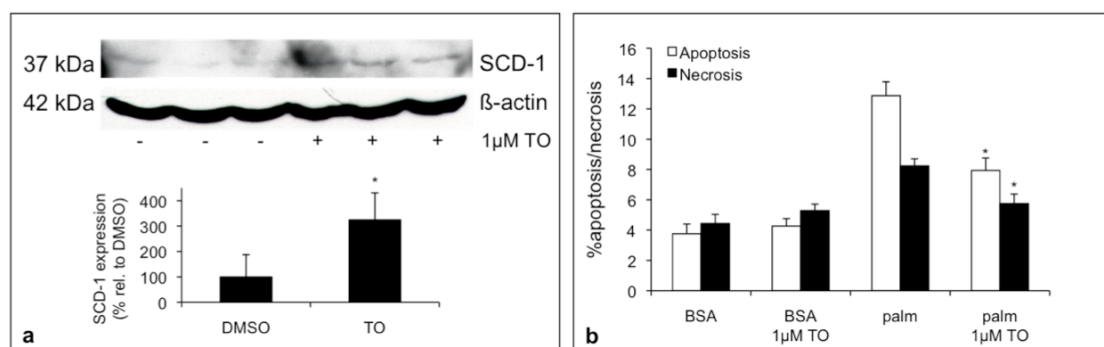


Figure 12: TO induces SCD-1 and ameliorates survival of palmitic acid-treated podocytes. a) 14 hours treatment with TO upregulates protein levels of SCD-1. β -actin was used as a control. Bar graph represents relative expression \pm SD of SCD-1. Vehicle (DMSO) treatment was set to 100% (n = 3, * p < 0.05). b) 14 hours pretreatment with TO protects podocytes from palmitic acid-induced death. Bar graphs represent mean percentages \pm SD of apoptotic and necrotic cells (n = 3, * p < 0.01).

3.2.2 In podocytes SCD-2 is the predominant SCD isoform and TO strongly induces SCD-1 and SCD-2

To investigate whether the protective effect of TO on palmitic acid-induced podocyte death may be related to the induction of SCDs the expression pattern of the various isoforms was evaluated in whole kidney lysates and podocytes. Real-time RT-PCR revealed that all four isoforms are expressed in the kidney (Fig. 13a) as well as in podocytes (Fig. 13b). Consistent with data from others [126] the most abundant isoform in the kidney is SCD-1 followed by SCD-2 (25% of SCD-1). Compared to SCD-1, SCD-3 (3%) and SCD-4 (< 1%) showed low expression levels in kidney lysates (Fig. 13a). Contrariwise, in podocytes SCD-2 was identified as the predominant isoform with 8-fold higher mRNA levels than SCD-1 (Fig. 13b). Similar to the expression in whole kidney lysates, expression levels of SCD-3 (22% of SCD-1), and SCD-4 (< 1%) were also low in podocytes (Fig. 13b). Next, the effect of TO on SCD mRNA expression has been examined in podocytes. Comparable to the effect of TO on SCD-1 protein levels (Fig. 12a), TO strongly induced SCD-1 (2.5 ± 0.4 -fold, p < 0.01), and to an even higher extent SCD-2 mRNA levels (5.0 ± 0.9 -fold, p < 0.01; Fig. 13c). Contrariwise, SCD-3 and SCD-4 mRNA levels were not significantly increased by TO (Fig. 13c).

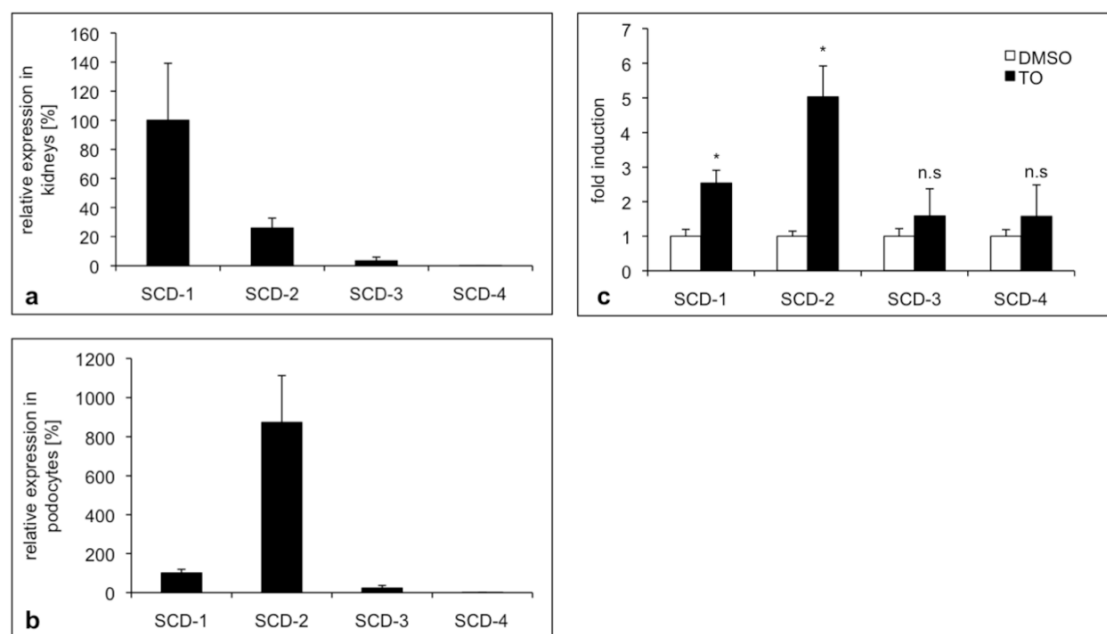


Figure 13: The expression pattern of SCD isoforms in the whole kidney differs from podocytes and TO strongly upregulates SCD-1 and SCD-2 in podocytes. a,b) SCD-1 is predominant in the kidney whereas in podocytes SCD-2 shows highest expression levels. Compared to SCD-1 and SCD-2 mRNA levels of SCD-3 and SCD-4 are low. Bar graphs represent relative expression \pm SD in the kidney (a) and in podocytes (b); each isoform was normalized to GAPDH and SCD-1 expression was set to 100%. c) Real-time RT-PCR analysis of SCD-1, SCD-2, SCD-3 and SCD-4 at 14 hours of TO-treatment. Bar graph represents fold induction \pm SD of each isoform normalized to GAPDH. Vehicle (DMSO) treatment was set to 1 (n = 3, * p < 0.01).

3.2.3 Gene-silencing of SCD-2 and SCD-1 reverts the protective effect of TO on palmitic acid-induced podocyte death

To investigate the role of desaturases in the protective action of TO, SCD-2 knockdown podocytes were generated as SCD-2 is the predominant isoform in podocytes and as SCD-2 is strongly induced by TO (Fig. 13a, c). SCD-2 knockdown podocytes were generated by lentiviral infection using a SCD-2-specific shRNA. A scrambled shRNA was used as a control. By RT-PCR, a marked suppression of SCD-2 expression (Fig. 14a) was observed in podocytes transduced with the SCD-2 silencing shRNA. To assess the effect of TO on podocytes deficient in SCD-2, podocytes were either pretreated with TO or vehicle for 14 hours before incubation with 200 μ M palmitic acid for 48 hours. SCD-2 silenced podocytes showed increased overall apoptosis and necrosis (data not shown) but SCD-2 silencing did not affect the

protective effect of TO on palmitic acid-treated podocytes (Fig. 14b-d). As shown in Figure 14, the protection of TO was not reduced in SCD-2-silenced podocytes, i.e. TO blocked palmitic acid-induced apoptosis to a similar degree in controls, and SCD-2 knockdown cells, by $26 \pm 10\%$, and by $29 \pm 7\%$, respectively (Fig. 14b). Similar findings were observed for necrosis as well as apoptosis and necrosis combined (Fig. 14c, d).

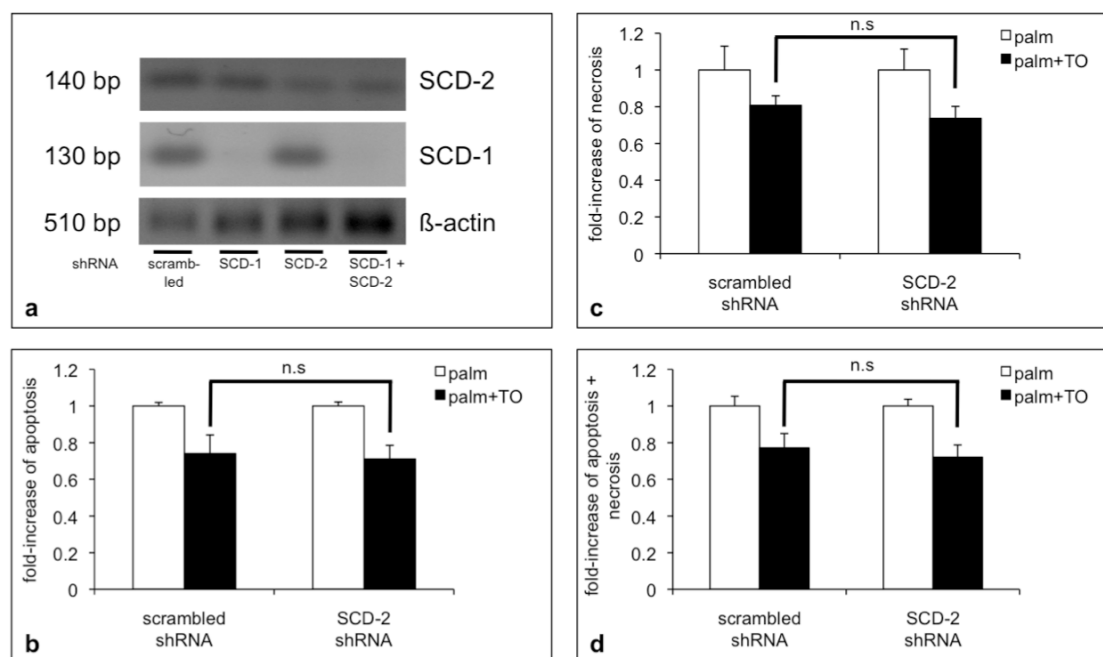


Figure 14: SCD-2 silencing does not affect the protective effect of TO on palmitic acid-induced podocyte death. a) SCD-1 and SCD-2 shRNA suppress the TO-mediated upregulation of SCD-1 and SCD-2 as analyzed by RT-PCR. β -actin served as a control. b-d) Podocytes were pretreated with $1 \mu\text{M}$ TO for 14 hours and incubated with $200 \mu\text{M}$ palmitic acid for 48 hours. Bar graphs represent mean fold-increase \pm SD of apoptosis (a), necrosis (b) and apoptosis+necrosis (c). Vehicle (DMSO) control was set to 1 ($n = 3$).

As SCD-1 might compensate for SCD-2 SCD-1/SCD-2 double-deficient podocytes were generated. As for SCD-2, efficiency of SCD-1 knockdown was assessed by RT-PCR (Fig. 14a). SCD-1/SCD-2 double-deficient podocytes were highly susceptible to palmitic acid-induced cell death and apoptotic cells increased from $8.5 \pm 1.0\%$ to $21.6 \pm 0.9\%$ in palmitic acid-treated controls and SCD-1/SCD-2 double-deficient cells, respectively (Fig. 15a), and most importantly the protective effect of TO was largely abrogated (Fig. 15a). In SCD-1/SCD-2 double-deficient podocytes the protective effect of TO on apoptosis was reduced from $40.3 \pm 4.0\%$ in control cells to $11.1 \pm$

7.7% ($p < 0.01$) in SCD-1/SCD-2 double-silenced cells (Fig. 15b). Similarly, the protective effect of TO on apoptosis and necrosis combined was reduced from $30.6 \pm 1.1\%$ in control cells to $11.6 \pm 7.9\%$ ($p < 0.05$) in SCD-1/SCD-2 double-silenced cells (Fig. 15d) whereas no significant impact was seen for necrosis (Fig. 15c). Together, these data indicate that SCD-1 and SCD-2 induction are mainly responsible for the protective effect of TO. Furthermore, SCD-1 and SCD-2 are presumably compensating for each other as a single-knockdown of SCD-1 (data not shown) and SCD-2 (Fig. 14) could not prevent the protective effect of TO on palmitic acid-induced podocyte apoptosis.

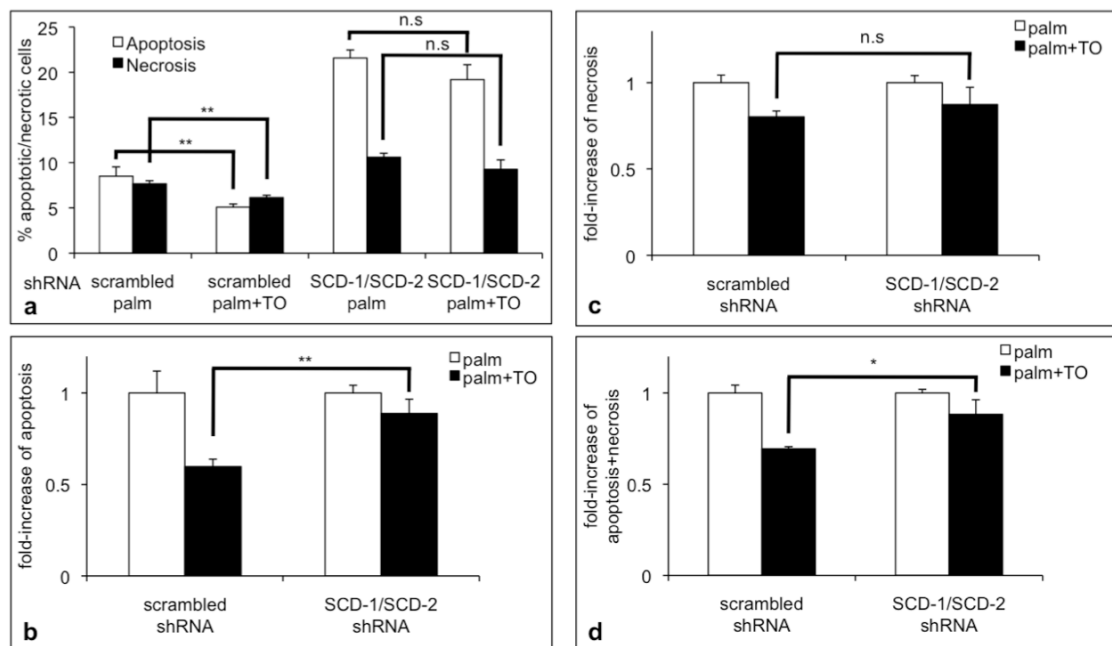


Figure 15: Combined silencing of SCD-1 and SCD-2 partially reverses the protective effect of TO on palmitic acid-induced apoptosis. Podocytes were pretreated with 1 μM TO for 14 hours and incubated with 200 μM palmitic acid for 48 hours. a) Bar graph represents mean percentages \pm SD of apoptotic and necrotic cells. b-d) Bar graphs represent mean fold-increase \pm SD of apoptosis (b), necrosis (c), and apoptosis + necrosis (d). Vehicle-treated (DMSO) control was set to 1. $n = 3$; * $p < 0.05$, ** $p < 0.01$.

3.2.4 Genetic overexpression of SCD-1 partially protects from palmitic acid-induced apoptosis

To further confirm the important role of SCDs on palmitic acid-induced apoptosis of podocytes a genetic approach, again by lentiviral transduction, was used by overexpressing SCD-1 in podocytes. Overexpression of SCD-1 was confirmed by

Western immunoblotting (Fig. 16a). Initially, GFP-overexpressing cells showed higher basal cell death that was associated with higher occurrence of ER-stress (data not shown). To overcome this problem podocyte transduction was carried out using lower virus titers and the cells were left to recover from ER-stress for 5 days before entering the experiment as BiP and CHOP levels were decreasing over time (data not shown). Treatment with BSA control for 48 hours showed comparable basal apoptosis and necrosis levels: $2.9 \pm 0.2\%$ apoptotic and $5.1 \pm 0.9\%$ necrotic cells in SCD-1 overexpressing cells versus $3.8 \pm 0.4\%$ apoptotic and $4.3 \pm 0.7\%$ necrotic cells in GFP-overexpressing cells (Fig. 16b). High levels of SCD-1 significantly prevented palmitic acid-induced apoptotic ($7.0 \pm 0.3\%$ vs. $10.3 \pm 0.7\%$, $p < 0.01$; Fig. 16b) and necrotic events ($5.7 \pm 0.4\%$ vs. $7.3 \pm 0.5\%$, $p < 0.05$; Fig. 16b). In Figure 16c and 16d the results of five independent experiments are pooled. Compared to GFP overexpression (set to 1), SCD-1 overexpression reduced the increase of apoptosis and necrosis after exposure to palmitic acid compared to podocytes incubated with BSA (control) by $16 \pm 9\%$ ($p < 0.0001$) and $12 \pm 18\%$ ($p < 0.05$), respectively (Fig. 16c, d). These data indicate that genetic overexpression of SCD-1 protects podocytes from palmitic acid-induced apoptosis, which is in complete accordance with the SCD-1 and SCD-2 dependent protective effect of TO (Fig. 15a-d).

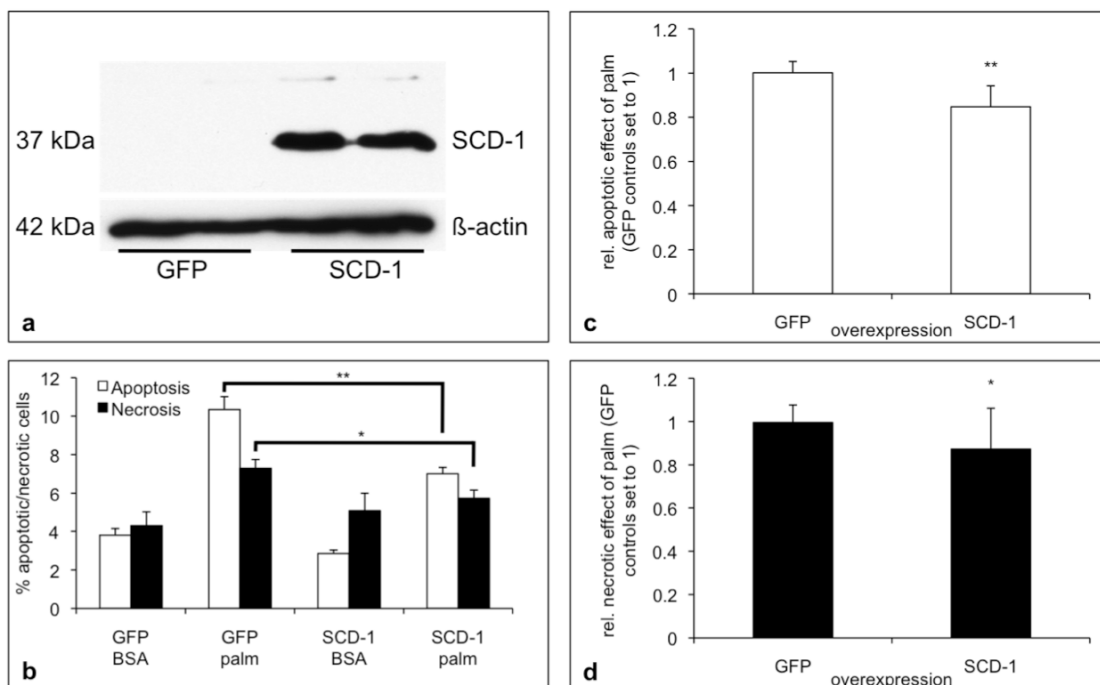


Figure 16: Overexpressing SCD-1 moderately protects from palmitic acid-induced apoptosis and necrosis. a) Western blot analysis of SCD-1 levels in GFP- or SCD-1 overexpressing podocytes. β -actin served as a loading control. b-d) SCD-1 overexpression

blocks palmitic acid-induced apoptosis and necrosis in podocytes. b) Bar graphs show mean percentages \pm SD of apoptotic and necrotic cells after exposure to 200 μ M palmitic acid for 48 h (representative experiment; n = 3, * p < 0.05, ** p < 0.01). c,d) Bar graphs represent the relative effect \pm SD of palmitic acid on apoptosis (c) and necrosis (d) in GFP- or SCD-1 overexpressing podocytes. GFP control was set to 1 (5 experiments pooled; n = 13, * p < 0.05, ** p < 0.0001).

3.2.5 MUFAs and TO shift palmitic acid into triglycerides (TGs) and MUFAs induce fatty acid β -oxidation

The mechanisms how MUFAs protect from SFA-mediated lipotoxicity are not completely understood. The protective effect of MUFAs is thought to be related to their stimulatory effect on fatty acid β -oxidation and on their ability to shift fatty acids into triglycerides (TGs) [50]. Both pathways are thought to prevent from harmful SFA metabolites either by getting rid of SFAs (β -oxidation) or by storing them away (TGs).

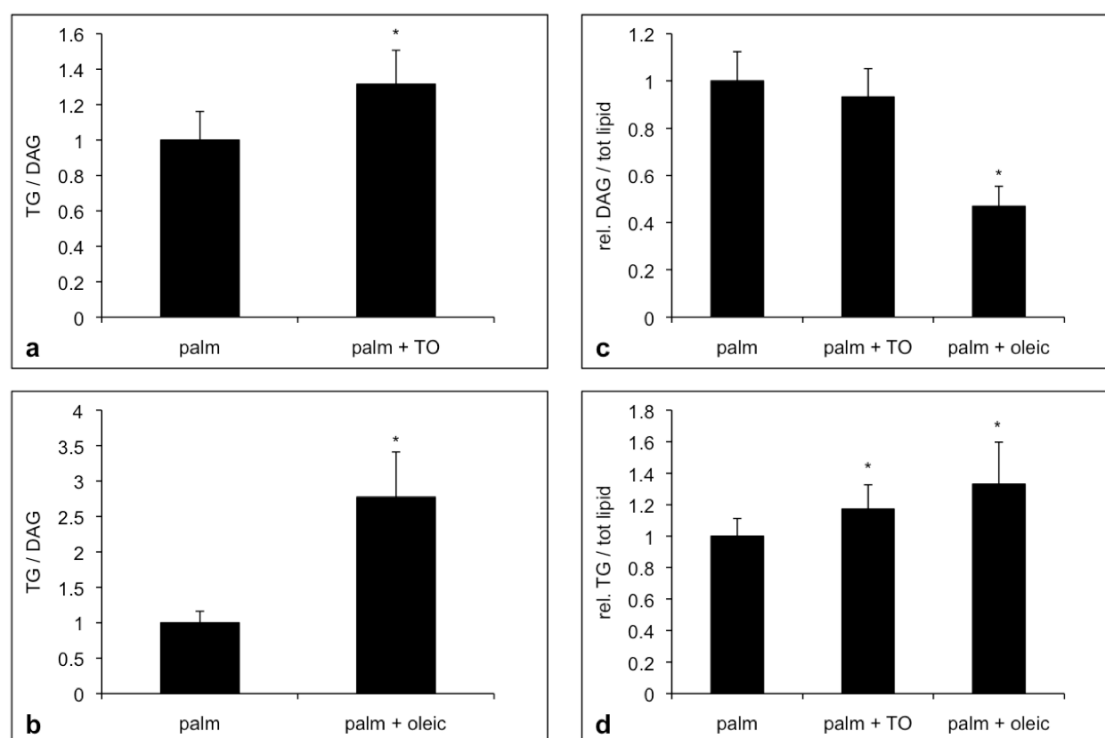


Figure 17: Oleic acid and TO increase palmitic acid incorporation into the TG fraction but only oleic acid reduces palmitic acid containing DAG levels in palmitic acid-treated podocytes. Podocytes were incubated for 5 hours in serum-free medium containing 0.5% FFA-free BSA and supplemented with 200 μ M palmitic acid (\pm 1 μ M TO) or oleic and palmitic acid (100 μ M each) in the presence of 0.5 μ Ci/ml [3 H]-palmitic acid. a-d) DAG and TG fractions were separated by thin layer chromatography and analyzed by a liquid

scintillation counter. a,b) Bar graphs represent the mean ratio of [³H]-palmitic acid-incorporated TGs to DAGs ± SD (n = 9; * p < 0.001). c,d) Bar graphs represent the relative incorporation ± SD of [³H]-palmitic acid into DAGs (c) and TGs (d) normalized to total lipid (n = 9; * p < 0.01). Vehicle-treatment was set to 1.

To investigate changes in lipid storage and fatty acid oxidation by MUFAs and TO tritium-labeled palmitic acid was used to trace incorporation of palmitic acid into diglycerides (DAGs) and TGs as well as to estimate levels of β-oxidation of palmitic acid. Analysis of the TG to DAG ratio revealed a shift of palmitic acid towards TG in the presence of oleic acid and TO. As shown in Figure 17b, coincubation with oleic acid strongly shifted the ratio towards the TG fraction (2.8 ± 0.6 -fold, $p < 0.001$). TO also increased the proportion of fatty acids derived from tritium-labeled palmitic acid incorporated in TGs in relation to DAGs but to a lower extent (1.3 ± 0.2 -fold, $p < 0.001$; Fig. 17a). Looking at the single fractions, the presence of oleic acid not only increased the radioactive-labeled TG fraction (Fig. 17d), but also markedly reduced the radioactive-labeled DAG fraction ($53 \pm 8\%$ of control cells, Fig. 17c). Interestingly, the latter could not be seen for cells treated with TO, although TO significantly increased the proportion of fatty acids derived from tritium-labeled palmitic acid incorporated in TGs (Fig. 17c, d). Further, the effect of oleic acid on β-oxidation of palmitic acid has been investigated. Podocytes were incubated with 200 μM palmitic acid along with 0.5 μCi/ml tritiated palmitic acid. In this assay the formation of [³H₂O] is utilized as a read out of β-oxidation of palmitic acid, and oxidation of palmitic acid is expressed as disintegrations per minute (DPM) normalized to the total protein of cell lysates. 5 hours cotreatment with oleic acid elevated β-oxidation by 30-40% when compared to palmitic acid-treated podocytes (Fig. 18). In contrast, the presence of TO revealed no detectable change in palmitic acid β-oxidation (Fig. 18). Together, these data indicate that oleic acid increases β-oxidation of palmitic acid in addition to shifting palmitic acid from DAGs to TGs.

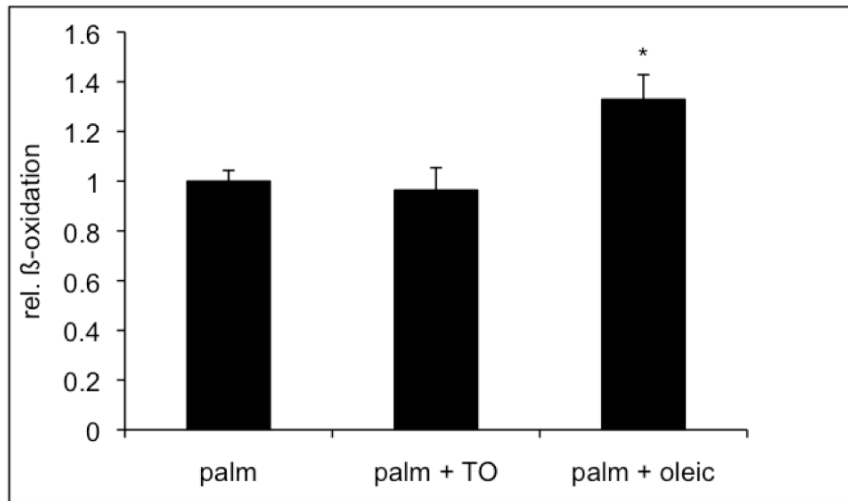


Figure 18: Cotreatment with oleic acid but not TO increases palmitic acid β -oxidation. Podocytes were incubated for 5 hours in serum-free medium containing 0.5% FFA-free BSA and supplemented with 200 μ M palmitic acid (\pm 1 μ M TO) or oleic and palmitic acid (100 μ M each) in the presence of 0.5 μ Ci/ml [3 H]-palmitic acid. β -oxidation was determined by counting [3 H $_2$ O] as a product of β -oxidation in the aqueous phase of the incubation medium. Bar graph represents relative β -oxidation \pm SD normalized to total lipid (n = 9, * p < 0.001). Vehicle-treatment was set to 1.

Taken together the LXR agonist TO partially protected podocytes from palmitic acid-induced death. The effect might be explained to a large part by induced expression of SCD-1 and SCD-2 as combined gene silencing almost completely reversed the beneficial effect of TO, and SCD-1 overexpression moderately but significantly suppressed palmitic acid-induced podocyte apoptosis. Mechanistically, the increased incorporation of palmitic acid into TGs that has been observed by the combination with oleic acid, but also by the treatment of podocytes with TO is indicating a potential benefit of lipid storage. The higher ability of oleic acid to increase lipid storage by comparison to TO, and its additional effect on β -oxidation might explain the stronger effect of oleic acid compared to TO.

3.3 The role of cAMP levels on palmitic acid-induced apoptosis in podocytes

The data described in part 3.1 are indicating that ER-stress has a crucial role in palmitic acid-induced podocyte death. In order to investigate how podocytes might be protected from palmitic acid-mediated lipotoxicity, molecular pathways have been

investigated that are preventing ER-stress or are inducing prosurvival pathways of the UPR response. The adenylate cyclase (AC) agonist forskolin [130] has been shown to ameliorate survival of palmitic acid-treated pancreatic β cells [131]. The effect of forskolin has been attributed basically to the upregulation of the ER chaperone BiP and the transcription factor JunB, which has been shown to be antiapoptotic in pancreatic β cells exposed to chemical ER-stressors [132].

3.3.1 Forskolin protects podocytes from palmitic acid-induced ER-stress and death by increasing cAMP levels

To examine the effect of forskolin on palmitic acid-induced death in podocytes, cells were pretreated with forskolin for 14 hours before incubation with 200 μ M palmitic acid for 48 hours. Analysis of apoptosis and necrosis revealed that palmitic acid-induced death was lower in forskolin-treated podocytes (Fig. 19a). Apoptosis was blocked by 40-60% ($p < 0.01$) and necrosis by 24% ($p < 0.05$; Fig. 19a and Fig. 20a). Forskolin is an agonist of AC that is converting ATP into cyclic AMP (cAMP). Therefore, the direct effect of elevated cAMP levels was tested on palmitic acid-induced cell death using 8-Br-cAMP, which is a cell permeable cAMP analogon with a higher resistance to phosphodiesterases. Indeed, pretreatment with 8-Br-cAMP of podocytes treated with 200 μ M palmitic acid for 48 hours protected from apoptosis and necrosis to a similar extent as forskolin (Fig. 20a), i.e 100 respectively 200 μ M of 8-Br-cAMP suppressed apoptosis by $54 \pm 5\%$ ($p < 0.001$) and $63 \pm 6\%$ ($p < 0.001$).

To examine if reduced induction of apoptosis and necrosis is due to higher levels of the ER chaperone BiP whole cell lysates were analyzed by Western blot. Contradictory to pancreatic β cells, forskolin reduced the induction of BiP in podocytes treated with palmitic acid for 24 hours (Fig. 19b). Even at early time points, 4 and 9 hours, BiP expression was lower (data not shown). In addition, CHOP levels were significantly lower (Fig. 19b). Thus, consistent with the effect on apoptosis and necrosis, forskolin is reducing palmitic acid-induced CHOP induction in podocytes, which may indicate that forskolin is directly influencing ER-stress.

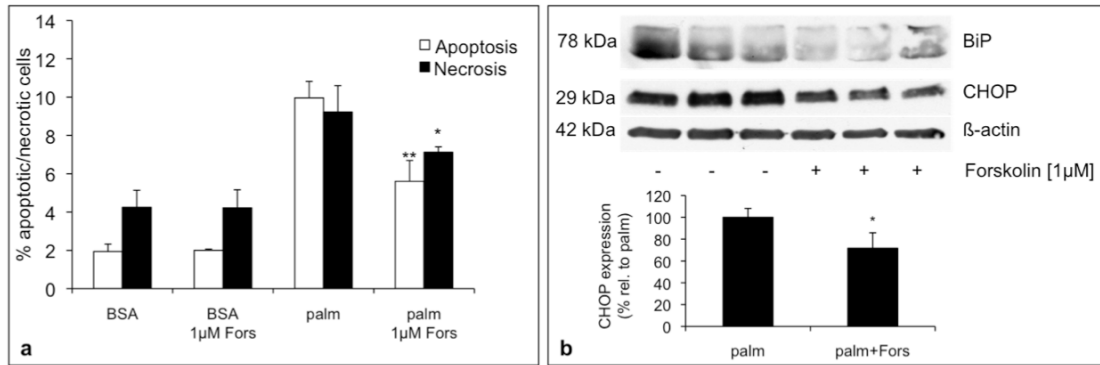


Figure 19: Forskolin protects from palmitic acid-induced apoptosis and reduces the induction of ER-stress. a) 14 hours pretreatment of forskolin decreases palmitic acid-induced cell death. Bar graph represents mean percentages \pm SD of apoptotic and necrotic cells ($n = 3$, * $p < 0.05$, ** $p < 0.01$). b) Forskolin-treatment reduces palmitic acid-induced upregulation of BiP and CHOP at 24 hours. Bar graph shows relative CHOP expression, vehicle (DMSO) control was set to 100% (* $p < 0.05$).

3.3.2 8-CPT-2Me-cAMP is less potent than 8-Br-cAMP in preventing palmitic acid-induced podocyte death

Besides cAMP-gated ion channels the effects of cAMP are attributed to activation of protein kinase A (PKA) and Epac (exchange protein directly activated by cAMP) [133]. Enserink and colleagues [134] generated a cAMP analogon, 8-CPT-2Me-cAMP, that is reported to activate Epac specifically. In order to discriminate between both pathways the effect of 8-CPT-2Me-cAMP was compared to 8-Br-cAMP (Fig. 20b). As already shown above 200 μ M 8-Br-cAMP that is activating PKA and Epac suppressed apoptosis by $57 \pm 6\%$ ($p < 0.001$) and necrosis by $24 \pm 7\%$ ($p < 0.05$). By contrast 8-CPT-2Me-cAMP showed a moderate but not significant protection compared to palmitic acid-treated controls: $15 \pm 11\%$ ($p < 0.08$) less apoptotic and $13 \pm 7\%$ ($p < 0.1$) less necrotic cells (Fig. 20b). Together these results indicate that the effect of forskolin and thereby cAMP on palmitic acid-induced apoptosis and necrosis may mainly involve PKA.

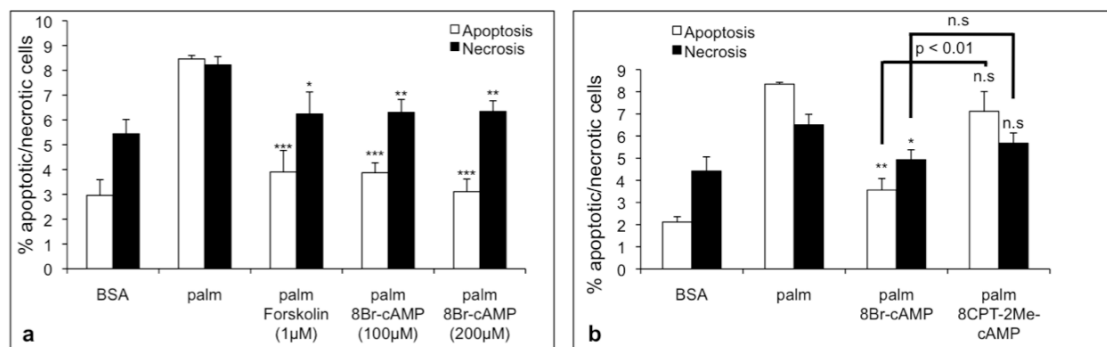


Figure 20: The positive effect of forskolin on palmitic acid-induced apoptosis is caused by elevating levels of cAMP. a) 14 hours pretreatment of 8-Br-cAMP (100 and 200 μ M) mimicks the effect of forskolin. b) 8-CPT-2Me-cAMP (200 μ M) is less potent than 8-Br-cAMP. 8-CPT-2Me-cAMP tends to slightly suppress (not significant) cell death. Bar graphs represent mean percentages \pm SD of apoptotic and necrotic cells exposed to 200 μ M palmitic acid for 48 hours. (n = 3; * p < 0.05, ** p < 0.01, *** p < 0.001).

3.3.3 H89 partially reverts the protective effect of forskolin on palmitic acid-induced apoptosis but is itself enhancing the effect of palmitic acid

To further investigate if the protective effect of forskolin on palmitic acid-induced podocyte death is mediated by PKA signaling the effect of forskolin had been studied in the presence of the PKA inhibitor H89. Podocytes were pretreated with 1 μ M forskolin for 14 hours in the presence or absence of various dosages of H89 before treatment with 200 μ M palmitic acid for 48 hours (Fig. 21). H89 partially reverted the favorable result of forskolin in a dose-dependent manner. However, 10 μ M H89 was itself aggravating the effect of palmitic acid-induced apoptosis and necrosis (Fig. 21). Thus, even though H89 is reducing the beneficial effect of forskolin on palmitic acid-induced cell death, the H89 experiment cannot firmly establish that the favorable effect of forskolin involves PKA signaling as H89 itself had a deleterious effect on palmitic acid-treated podocytes. Nevertheless, PKA signaling seems to exhibit prosurvival effects in palmitic acid-induced podocyte death.

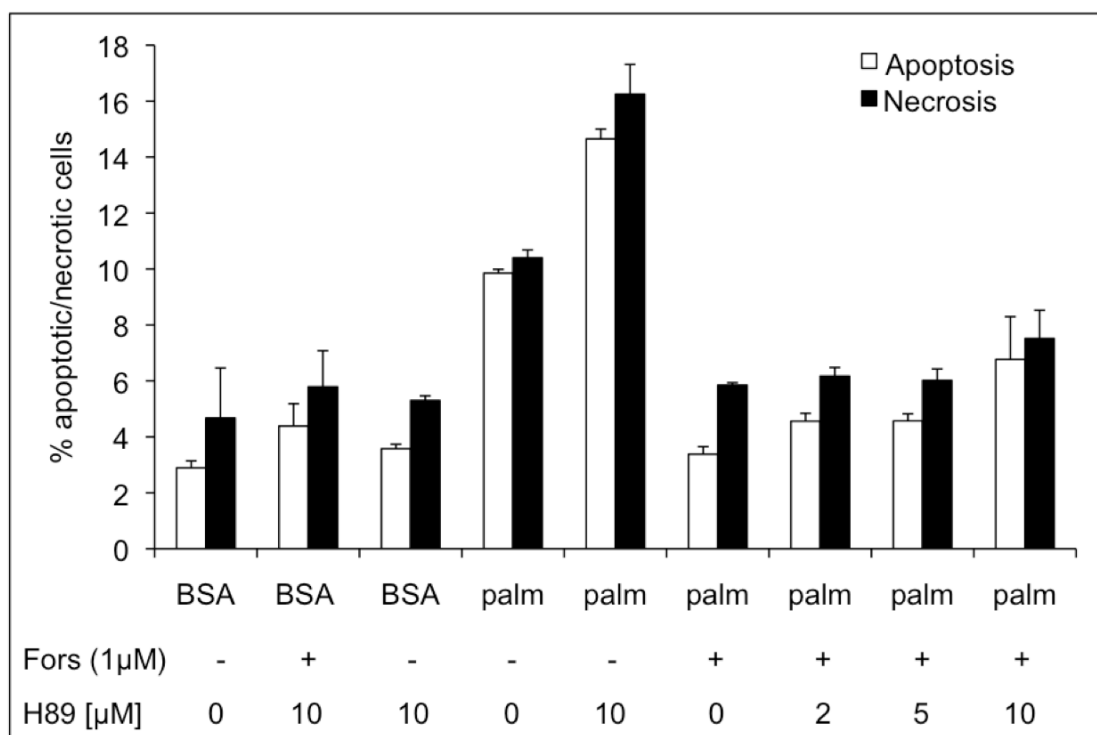


Figure 21: H89 is partially reverting the beneficial effect of forskolin on palmitic acid-induced apoptosis and necrosis but is enhancing itself the effect of palmitic acid. Podocytes were pretreated with forskolin in the absence or presence of H89 and subsequently treated with 200 μ M palmitic acid for 48 hours. Bar graphs represent mean percentages \pm SD of apoptotic and necrotic cells (n = 2).

3.3.4 Forskolin is activating the transcription factor CREB

The most characterized signal transduction cascade of cAMP downstream of PKA involves the transcription factor cAMP response element binding protein (CREB). Phosphorylation by PKA leads to dimerization of CREB and transcriptional regulation of various proteins [135, 136]. Activation of CREB was confirmed in podocytes treated with forskolin for 0.5, 1, 2 and 24 hours. P-CREB formation peaked at 0.5 hours and decreased over time with no detectable signal after 24 hours (Fig. 22a). Since signal transduction is apparently rapid pretreatment with forskolin was reduced to 2 hours and removed during the following treatment with 200 μ M palmitic acid. After 48 hours podocyte survival was again ameliorated by $31 \pm 13\%$ less apoptotic and by $24 \pm 6\%$ less necrotic events (Fig. 22b).

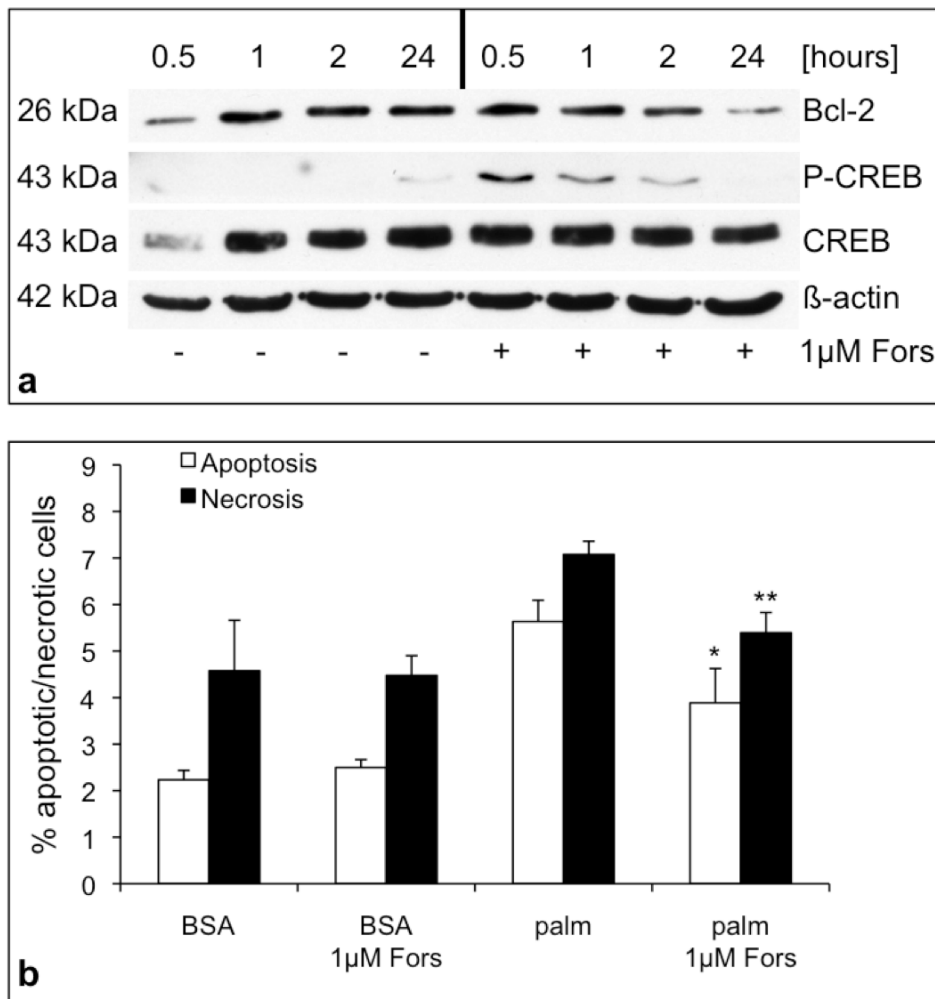


Figure 22: Forskolin activates CREB in podocytes and induces its downstream target Bcl-2 at an early time point. a) Phosphorylation of CREB is an early event in forskolin-treatment and decreases over time. Levels of Bcl-2 are induced after 30 min but are comparable to DMSO control treatment at later timepoints. Total CREB and β -actin served as loading controls. b) In addition, 2 hours preincubation of forskolin and removal during palmitic acid exposure is enough to significantly block palmitic acid-induced cell death. Bar graphs represent mean percentages \pm SD of apoptotic and necrotic cells ($n = 3$; * $p < 0.05$, ** $p < 0.01$).

To further examine a potential contribution of CREB, a dominant negative form (ACREB) was overexpressed in podocytes [102] (Fig. 23a). Podocytes expressing ACREB were preincubated with forskolin for 14 hours and treated with 200 μ M palmitic acid for 48 hours. Either GFP or the empty vector was used as a control. Apoptotic and necrotic levels were lower in ACREB expressing cells compared to controls. Nevertheless, ACREB could not revert the beneficial effect of forskolin, e.g forskolin prevented apoptosis by $30 \pm 7\%$ in empty vector-transduced podocytes and

by $34 \pm 1\%$ in ACREB overexpressing podocytes (Fig. 23b-d), respectively, indicating that the PKA-CREB is not directly involved in the beneficial effect of forskolin on palmitic acid-induced podocyte death. However, ACREB overexpressing podocytes showed increased levels of CREB, which might be explained by a compensatory mechanism and might be responsible for the ineffectiveness of ACREB in reversing the protective effect of forskolin (Fig. 23a).

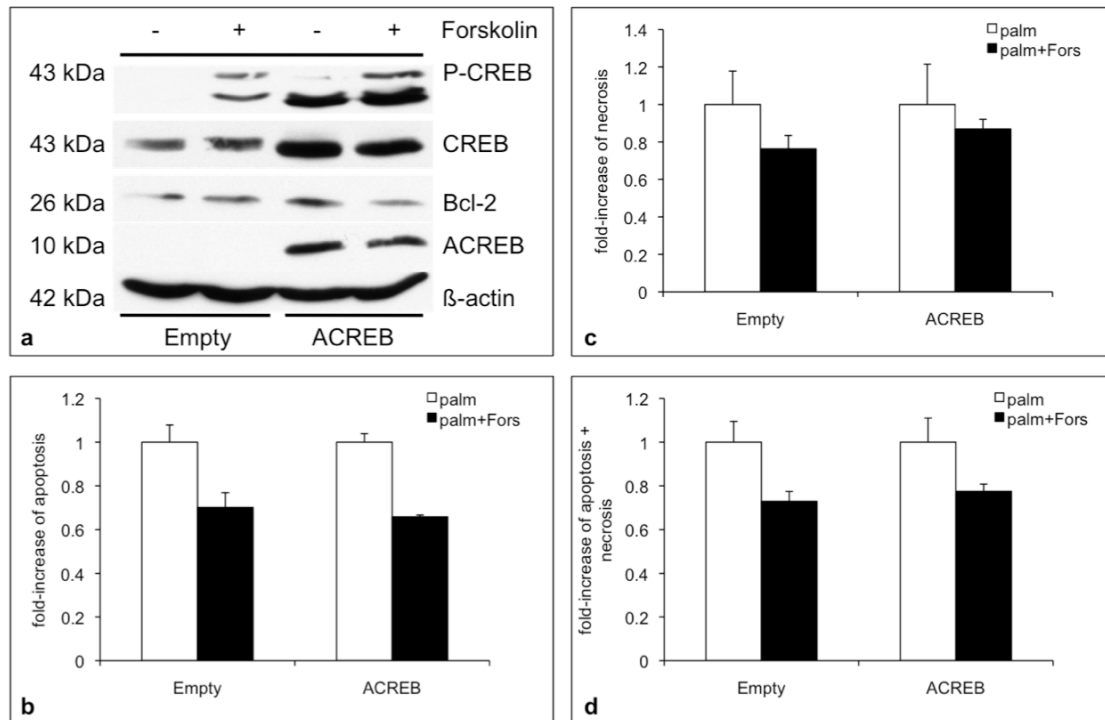


Figure 23: A dominant negative CREB does not impair the effect of forskolin on palmitic acid-induced cell death. a) Western blot analysis of ACREB expression in ACREB overexpressing and control (empty vector) podocytes. b-d) ACREB overexpression does not revert the effect of forskolin on palmitic acid-induced podocyte death. Bar graphs represent mean fold-increase \pm SD of apoptotic (a), necrotic (b) and apoptotic + necrotic (c) cells. Vehicle (DMSO)-treatment was set to 1.

3.3.5 Forskolin is obviously acting not directly on the intrinsic apoptotic pathway

Considering the fact that 16 hours treatment with 250 μ M palmitic acid led to increased cytosolic cytochrome c (Fig. 5c) a potential candidate induced by CREB that might be involved in the protective effect of forskolin is the antiapoptotic Bcl-2 [137]. Bcl-2 prevents mitochondrial cytochrome c release by direct interaction with proapoptotic Bax/Bak and by inhibition of mitochondrial membrane permeability

transition (MPT) [138]. To examine a possible involvement of Bcl-2 protein levels were analyzed after 0.5, 1, 2 and 24 hours of forskolin-treatment. Comparable to CREB phosphorylation Bcl-2 levels were most enhanced after 30 minutes followed by a gradual decrease (Fig. 22a). Surprisingly, DMSO (vehicle)-treatment was increasing Bcl-2 content over time (Fig. 22a). Furthermore, no significant changes in Bcl-2 expression levels were determined in forskolin-treated podocytes incubated with palmitic acid for 24 hours (data not shown). These results do not support a crucial role for Bcl-2 in the prevention of forskolin from palmitic acid-induced apoptosis and necrosis. Consistent to the Bcl-2 data, forskolin did not affect mitochondrial cytochrome c release in palmitic acid-treated podocytes (data not shown).

3.3.6 Forskolin generally protects podocytes from ER-stress-induced apoptosis and necrosis

The protective effect of forskolin and the different effect of the two cAMP analogs are indicating an involvement of PKA. However, data are indicating that forskolin is not acting via PKA-CREB and furthermore is not affecting the mitochondrial apoptotic pathway. Nevertheless, forskolin is reducing the induction of ER-stress, which has been shown to be crucially involved in mediating palmitic acid-induced podocyte death. In order to examine a direct effect of forskolin on attenuating the induction of ER-stress, it has been investigated if forskolin could prevent from tunicamycin- and thapsigargin-induced podocyte death. Podocytes were pretreated with 1 μ M forskolin for 14 hours and subsequently treated with either 1 μ M thapsigargin or 2 μ g/ml tunicamycin for 48 hours. Annexin V and PI staining revealed that forskolin moderately prevented the cytotoxic effect of both thapsigargin and tunicamycin (Fig. 24a, b). Forskolin suppressed apoptosis and necrosis in thapsigargin-treated cells by $25 \pm 9\%$ ($p < 0.01$) and $27 \pm 7\%$ ($p < 0.01$), respectively (Fig. 24a). The beneficial effect on tunicamycin-treatment was less pronounced: $22 \pm 9\%$ ($p < 0.05$) less necrosis but not significantly less apoptosis ($21 \pm 17\%$; $p = 0.1$; Fig. 24b).

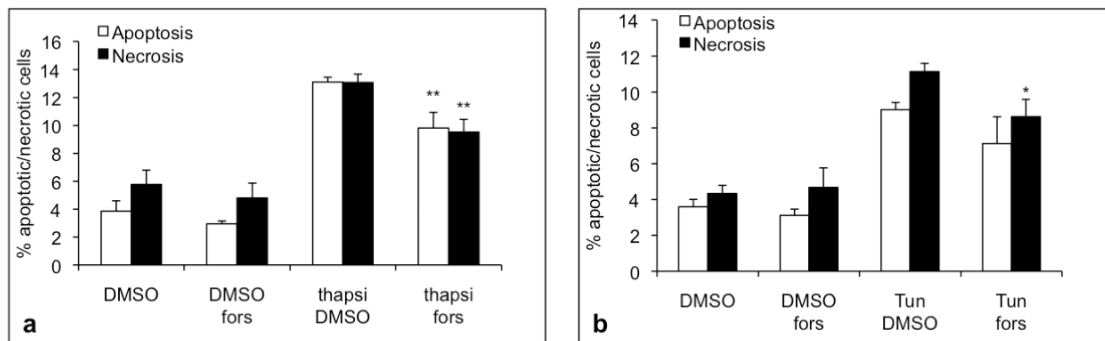


Figure 24: Forskolin ameliorates survival of thapsigargin- and tunicamycin-treated podocytes. Podocytes were pretreated with 1 μ M forskolin or DMSO for 14 hours and subsequently treated with 1 μ M thapsigargin (a) or 2 μ g/ml tunicamycin (b). Vehicle (DMSO)-treatment was used as control. Bar graphs represent mean percentages \pm SD of apoptotic and necrotic podocytes (n = 3; * p < 0.05, **p < 0.01).

Taken together, these data indicate that forskolin protects from palmitic acid-induced cell death not involving an upregulation of Bcl-2 or an attenuation of cytochrome c release. In addition the lack of an effect of ACREB overexpression in podocytes does not support a causal role of CREB in podocytes treated with forskolin. Interestingly, forskolin is ameliorating podocyte survival when treated with two other independent ER-stress inducers, thapsigargin and tunicamycin, indicating a direct interference with the apoptotic cascades of the UPR.

4. DISCUSSION

4.1 Palmitic acid induces podocytes death; involvement of ER-stress and CHOP

The present study uncovered that the saturated palmitic acid induces podocyte cell death (Fig. 3 and Fig. 4). These findings are of clinical interest because insulin resistance is associated with increased plasma levels of long-chain FFAs, and DN is characterized by apoptosis and loss of podocytes that precede albuminuria and renal dysfunction in DN, both in type I and type II diabetes [10, 11, 16, 25, 139].

Previous studies found that high glucose [25], TGF- β [36, 140], the RAAS system [32, 141], and AGEs [28, 29] can also induce apoptosis of podocytes.

The identification of palmitic acid as another proapoptotic factor for podocytes may be of clinical relevance in the setting of type II diabetes because FFAs are elevated in patients with obesity and insulin resistance even before hyperglycemia arises [142]. FFAs can also be elevated in type I diabetic subjects [143]. Moreover, similar to DN, obesity-related glomerulonephropathy is characterized by a decreased density of podocytes [144], raising the intriguing possibility that FFA-induced podocyte apoptosis may also contribute to the development and progression of obesity-related glomerular disease.

The detection of palmitic acid-induced ER-stress in podocytes is in line with similar findings in other cell types [52, 54, 56, 61, 62]. In pancreatic β cells, overexpression of the ER chaperone BiP can partially prevent palmitic acid-induced apoptosis [55], implying that the upregulation of BiP (Fig. 6a) is part of an adaptive podocyte-protective mechanism. In contrast, the strong upregulation of CHOP (Fig. 6b, c) makes CHOP a good candidate as mediator of palmitic acid-induced podocyte apoptosis because CHOP is critically involved in ER-stress induced apoptosis [98, 145]. Consistent with the strong induction of CHOP we also observed palmitic acid-induced XBP-1 splicing (Fig. 6d), which is directly involved in transcriptional regulation of CHOP [112].

In further experiments we could definitely establish a causative role for CHOP in palmitic acid-induced podocyte apoptosis, as gene-silencing of CHOP protects podocytes from palmitic acid-induced death (Fig. 7d-f and Fig. 8b-d). This outcome is consistent with the known role of CHOP in ER-stress induced apoptosis [98, 145].

Importantly, ER-stress has been implicated in podocyte apoptosis caused by AGEs [29] or excessive protein loading [146], but a causative role of CHOP under these conditions remains to be established.

We also tested the chemical chaperones 4-PBA and TUDCA. TUDCA did not show a protective effect on palmitic acid-induced cell death (Fig. 9), whereas 4-PBA was even deleterious (data not shown). Interestingly, these results are in line with observations in pancreatic β cells [93]. It might be explained by the fact that palmitic acid overload is shifting the ER fatty acid composition and is directly disrupting ER integrity and structure [87]. Moreover, in pancreatic β cells it has been shown that palmitic acid is not leading to increased mis- or unfolded proteins in the ER but rather to impaired ER-to-Golgi protein trafficking, which may trigger ER-stress [119].

The notion that CHOP plays a pathogenic role in experimental DN is supported by the observation that CHOP is upregulated in two rodent models of DN [121, 122], and CHOP-deficient mice are protected from DN as well as age-related albuminuria [122]. However, in patients with DN, although we found an upregulation of BiP by quantitative RT-PCR analysis in microdissected glomeruli (Fig. 11) as previously reported in the tubulointerstitial compartment [147], CHOP mRNA expression was unchanged in the tubulointerstitial compartment [147] and down regulated in glomeruli (Fig. 11). Clearly, future studies will be required to address potential differences between our *in vitro* data and results in murine models with that of human DN to determine the precise role of CHOP in patients with DN.

An interesting additional finding was the observation that proapoptotic stimuli such as high glucose and TGF- β did not lead to an induction of CHOP in podocytes (Fig. 6d), suggesting that ER-stress is not involved in apoptosis caused by high glucose and TGF- β . However, high glucose was able to amplify the induction of BiP and CHOP by palmitic acid (Fig. 6d), and high glucose enhances apoptosis mediated by palmitic acid in podocytes (Kapil Kampe, unpublished data) similarly as in pancreatic β cells [53].

4.2 Palmitoleic and oleic acid attenuate palmitic acid-induced ER-stress and prevent palmitic acid-induced podocyte death

Palmitoleic and oleic acid could prevent palmitic acid-induced podocyte apoptosis and necrosis (Fig. 10). The antagonistic effects of palmitic acid and the

monounsaturated palmitoleic and oleic acid on cell death in podocytes (Fig. 10) are analogous to data from other cell types [52, 53, 62, 92]. Consistent with the outcome that CHOP is an important player in mediating palmitic acid-induced apoptosis the addition of MUFAs also prevented from the induction of CHOP (Fig. 10). In addition, palmitoleic and oleic acid increased protein levels of the chaperone BiP (Fig. 10), which is known to prevent palmitic acid-induced apoptosis [55], thus BiP production might partially explain the protective effects of MUFAs.

4.3 Stearoyl-CoA desaturases protect from palmitic acid-induced cell death

Consistent with the protective effects of MUFAs on palmitic acid-induced cell death induction of cell autonomous fatty acid desaturases ameliorates survival of palmitic acid-treated podocytes. First, we could demonstrate that TO901317 (TO), an LXR agonist [129] that is leading to increased levels of desaturases, partially prevents palmitic acid-induced cell death (Fig. 12b), which is in line with results from other cell types [89, 148]. TO is strongly inducing SCD-1 and SCD-2 in podocytes (Fig. 13c), whereas the effect of TO on SCD-3 and SCD-4 was not significant (Fig. 13c). Gene-silencing (Fig. 15) and overexpression (Fig. 16) experiments indicate that the protective effect of TO can be largely attributed to the induction of SCD-1 and SCD-2. Moreover, SCD-1 and SCD-2 are able to compensate for each other as only combined silencing of both isoforms can revert the beneficial effect of TO on palmitic acid-induced podocyte apoptosis (Fig. 14 and Fig. 15).

An interesting finding was that SCD-2 is apparently predominant in cultured podocytes (Fig. 13b), which differs from whole kidney expression where SCD-1 is the commonest isoform (Fig. 13a) as previously reported [126].

Although the mechanisms of how MUFAs are protecting from SFA-induced lipotoxicity are not completely understood, data are indicating that increased fatty acid storage as TGs and fatty acid oxidation may help cells to reduce biological active SFAs and to avoid the formation of cytotoxic metabolites such as DAGs and ceramides [50]. Using palmitic acid tracing experiments we observed that TO increases the ratio of [³H]-palmitic acid-containing TGs to DAGs (Fig. 17a). The effect was even more pronounced in podocytes coincubated with oleic acid (Fig. 17b). Whereas the effect of TO is mainly due to an increase in TGs, oleic acid decreased

[³H]-palmitic acid recovered in the DAG fraction and increased [³H]-palmitic acid in the TG fraction (Fig. 17c, d). Previously, increased TG synthesis has been associated with a reduction in intracellular levels of DAGs and ceramides and it has been suggested that this is preventing from their harmful actions [65, 149]. In this study we did not measure [³H]-palmitic acid integrated into ceramides as fumonisin B1, a ceramide synthetase inhibitor, showed no protection from palmitic acid-induced lipotoxicity in podocytes (data not shown). As TO-treatment has no significant effect on palmitic acid-derived FFA incorporated into DAGs, the beneficial action on palmitic acid-induced podocyte death cannot be explained by this mechanism (Fig. 17c). However, there is data indicating that DAG-mediated lipotoxicity might be depending on the saturation of fatty acids incorporated in DAGs [150], and we speculate that TO might have increased palmitic acid-derived MUFAs incorporated in DAGs. In addition, the increased amount of [³H]-palmitic acid recovered in TGs after treatment with TO is likely protective as palmitic acid is stored away in a “safe lipid pool” [50].

Even though a shift to increased TG synthesis and lipid storage may help the cells to cope with lipotoxicity, the role of SCDs and increased TG content is rather debated. SCD-1 deficiency in mice is attenuating high fat diet-induced obesity and insulin resistance [151] but is as well promoting inflammation and atherosclerosis [152]. Importantly, the favorable effect of SCD-1 deficiency is mainly associated with altered skin lipid composition leading to decreased skin insulation and a resulting substantial increase in energy expenditure, which may mainly explain the decreased insulin resistance in this genetic model [153].

The role of ectopic TG storage in non-adipose tissue is controversial. Insulin resistant obese rodents [154, 155] show increased intramuscular TG content and synthesis rates whereas in humans the so-called ‘athletes paradox’ indicates that ectopic fat accumulation is not *per se* negative as endurance trained people have higher insulin-sensitivity but as well increased intramuscular TG stores [156, 157]. Furthermore transgenic mice overexpressing the TG-synthesizing enzyme DAG acyltransferase 1 (DGAT1) in the heart show increased TG content associated with improved heart function [158].

In addition, we evaluated the effect of TO and oleic acid on oxidation of palmitic acid using [³H]-palmitic acid. Whereas oleic acid induces β -oxidation no increase results from the treatment with TO (Fig. 18). These differences in the synthesis of TGs and

the upregulation of β -oxidation may explain the more potent effect of oleic acid in protecting podocytes from palmitic acid-induced death. In summary, the *in vitro* observations of this study indicate that induction of desaturases might prevent podocyte apoptosis and thus glomerular podocyte loss and attenuate the pathogenesis of DN. However, further studies are necessary to delineate the exact role of desaturases in the development and pathogenesis of DN.

The importance of fatty acid oxidation in ameliorating the detrimental effect of palmitic acid is supported by additional experiments using Aicar, an AMP-activated protein kinase (AMPK) agonist, to increase fatty acid oxidation and etomoxir, an inhibitor of the carnitine palmitoyl transferase 1 (CPT1), which is the rate-limiting enzyme in β -oxidation. Stimulation of fatty acid oxidation by Aicar is protective, whereas inhibition of fatty acid oxidation is detrimental for palmitic acid-induced podocyte damage (Kapil Kampe, unpublished data).

Importantly, the potentially critical contribution of reduced β -oxidation in the pathogenesis of DN is strongly supported by a recent large-scale genome wide association study in patients with type II diabetes and DN [159]. This study found a polymorphism in a noncoding region of acetyl-CoA carboxylase β (ACCB) with a strong association with proteinuria. ACCB activity inhibits fatty acid oxidation and the DN-risk single nucleotide polymorphism (SNP) of ACCB results in a higher ACCB expression [159] indicating that impaired fatty metabolism in addition to elevated free fatty acid levels may be critical in the pathogenesis of DN. The original finding of this association in Japanese patients has been confirmed in independent cohorts including a large cohort from China [160].

4.4 The protective effect of increased cAMP levels on palmitic acid-induced podocyte death

The present study uncovered that the adenylate cyclase agonist forskolin is ameliorating survival of palmitic acid-treated podocytes (Fig. 19a and Fig. 20a). Similarly, the constitutively active cAMP analogon Br-cAMP is protective (Fig. 20a), which suggests that increased cAMP levels are responsible for the favorable effect of forskolin. In pancreatic β cells the protective effect of forskolin on palmitic acid-induced lipotoxicity has been attributed to increased expression levels of the ER chaperone BiP [131]. Contrariwise, forskolin reduces the induction of BiP in

podocytes exposed to palmitic acid (Fig. 19b) and the favorable effect of forskolin cannot be explained by a protective upregulation of BiP. However, forskolin prevented upregulation of the proapoptotic transcription factor CHOP (Fig. 19b), which certainly contributes to its protective effect although further studies need to be done to elucidate the underlying mechanisms.

Experiments using 8-CPT-2Me-cAMP, a cAMP analogon favoring Epac [134], are indicating that the beneficial effect of forskolin and cAMP is mainly resulting from PKA signaling (Fig. 20b), though we can not completely exclude that the less protective effect compared to 8-Br-cAMP (Fig. 20b) results from unspecific lack of equipotency. The PKA inhibitor H89 is reversing the protective effect of forskolin to some extent (Fig. 21). However, as H89 is itself aggravating palmitic acid-induced podocyte death, an essential involvement of PKA in the protective effect of forskolin needs confirmation, though the deleterious effect of H89 indicates a prosurvival action of PKA.

Looking downstream of PKA, forskolin leads to phosphorylation of the transcription factor CREB and induction of its downstream target Bcl-2 (Fig. 22a) [136, 161]. However, the protective effect of forskolin seems not to involve this pathway as forskolin does not prevent cytochrome c release into the cytoplasm (data not shown), and genetic overexpression of a dominant negative form of CREB, ACREB [102] is not affecting the effect of forskolin on palmitic acid-induced podocyte apoptosis and necrosis (Fig. 23).

An interesting finding is the fact that forskolin is protecting from the distinct and independent ER-stressors tunicamycin and thapsigargin (Fig. 24). This observation is indicating that forskolin and elevated levels of cAMP have a more general effect on the induction of ER-stress and the UPR in podocytes.

Increased cAMP levels have also been attributed to glomeruloprotective effects *in vivo*. Rolipram, an inhibitor of the type IV phosphodiesterase, the major cAMP metabolizing enzyme in podocytes, has been effective in the prevention and treatment of experimental crescentic glomerulonephritis, a proteinuric kidney disease, which often progresses rapidly to ESRD [162]. In addition, inactivation of AC1 is resulting in increased susceptibility to experimental proteinuria induced by intraperitoneal injections of BSA, which is associated with increased local foot process effacement [163]. Forskolin has been shown to rearrange the actin cytoskeleton and reinforce the integrity of cell-cell contacts in podocytes [164], and PKA inhibition has been shown

to prevent actin cytoskeleton formation [165]. In addition, it has been observed that synaptopodin, an actin-associated protein [166], is phosphorylated directly by PKA and thus prevented from degradation [167]. As a consequence it would be reasonable to test the effect of forskolin and increased cAMP levels on synaptopodin stability and its subsequent influence on the actin cytoskeleton in palmitic acid-treated podocytes, which might be a link to the favorable effect of forskolin on palmitic acid-induced podocyte death. Moreover, it would be of interest to investigate the effect of forskolin and increased cAMP levels on the pathogenesis DN.

5. CONCLUSION

The uncovering of the saturated palmitic acid as another proapoptotic factor of the diabetic milieu, which is causally linked to ER-stress induction, might be of clinical relevance as podocyte apoptosis is an early event in the development and pathogenesis of DN and as plasma FFA levels are elevated in obese and insulin resistant patients before the onset of hyperglycemia [10, 11, 16, 25, 36, 142].

However, the fact that MUFAs prevented SFA-mediated podocyte death and that *in vivo* FFAs consist of both, SFAs and MUFAs, makes it difficult to evaluate the contribution of elevated FFAs in the pathogenesis of DN. Nevertheless, increased SFA intake may lead in the longterm to increased podocyte apoptosis and thus contribute to the development and pathogenesis of DN.

Examining mechanisms to rescue podocytes from palmitic acid-induced death *in vitro* revealed two promising strategies. First, induction of cellular autonomous desaturases, converting SFAs into MUFAs and subsequently leading to increased TG levels, protected podocytes from palmitic acid-induced apoptosis. Second, raising intracellular cAMP levels ameliorated survival of podocytes treated with palmitic acid. So far, the beneficial effect could be linked to a general reduction of ER-stress initiation.

Together, further studies are necessary to unravel the mechanisms how palmitic acid is inducing ER-stress and apoptosis in podocytes and to delineate the role of desaturases and cAMP levels in preventing this process. Moreover, it would be of interest to interfere with these pathways in mice, in particular podocyte-specifically, to learn more about its relevance *in vivo*.

6. REFERENCES

1. USRDS, *The United States Renal Data System 2011 Annual Data Report: Atlas of Chronic Kidney Disease and End-Stage Renal Disease in the United States*. 2011, Institutes of Health, National Institute of Diabetes and Digestive and Kidney Diseases, Bethesda, MD, 2011.
2. Foley, R.N., P.S. Parfrey, and M.J. Sarnak, *Epidemiology of cardiovascular disease in chronic renal disease*. *J Am Soc Nephrol*, 1998. **9**(12 Suppl): p. S16-23.
3. Locatelli, F., P. Pozzoni, and L. Del Vecchio, *Renal replacement therapy in patients with diabetes and end-stage renal disease*. *J Am Soc Nephrol*, 2004. **15 Suppl 1**: p. S25-9.
4. Kimmelstiel P, W.C., *Intercapillary lesions in the glomeruli of the kidney*. *Am J Pathol*, 1936. **12**: p. 82-97.
5. Pavenstadt, H., W. Kriz, and M. Kretzler, *Cell biology of the glomerular podocyte*. *Physiol Rev*, 2003. **83**(1): p. 253-307.
6. Kriz, W., *The pathogenesis of 'classic' focal segmental glomerulosclerosis-lessons from rat models*. *Nephrol Dial Transplant*, 2003. **18 Suppl 6**: p. vi39-44.
7. Reidy, K. and F.J. Kaskel, *Pathophysiology of focal segmental glomerulosclerosis*. *Pediatr Nephrol*, 2007. **22**(3): p. 350-4.
8. Shankland, S.J., *The podocyte's response to injury: role in proteinuria and glomerulosclerosis*. *Kidney Int*, 2006. **69**(12): p. 2131-47.
9. Berg, U.B., et al., *Kidney morphological changes in relation to long-term renal function and metabolic control in adolescents with IDDM*. *Diabetologia*, 1998. **41**(9): p. 1047-56.
10. Dalla Vestra, M., et al., *Is podocyte injury relevant in diabetic nephropathy? Studies in patients with type 2 diabetes*. *Diabetes*, 2003. **52**(4): p. 1031-5.
11. Pagtalunan, M.E., et al., *Podocyte loss and progressive glomerular injury in type II diabetes*. *J Clin Invest*, 1997. **99**(2): p. 342-8.
12. Steffes, M.W., et al., *Glomerular cell number in normal subjects and in type I diabetic patients*. *Kidney Int*, 2001. **59**(6): p. 2104-13.

13. White, K.E. and R.W. Bilous, *Type 2 diabetic patients with nephropathy show structural-functional relationships that are similar to type 1 disease*. J Am Soc Nephrol, 2000. **11**(9): p. 1667-73.
14. White, K.E., et al., *Podocyte number in normotensive type 1 diabetic patients with albuminuria*. Diabetes, 2002. **51**(10): p. 3083-9.
15. White, K.E. and R.W. Bilous, *Structural alterations to the podocyte are related to proteinuria in type 2 diabetic patients*. Nephrol Dial Transplant, 2004. **19**(6): p. 1437-40.
16. Meyer, T.W., P.H. Bennett, and R.G. Nelson, *Podocyte number predicts long-term urinary albumin excretion in Pima Indians with Type II diabetes and microalbuminuria*. Diabetologia, 1999. **42**(11): p. 1341-4.
17. Marshall, C.B. and S.J. Shankland, *Cell cycle and glomerular disease: a minireview*. Nephron Exp Nephrol, 2006. **102**(2): p. e39-48.
18. Petermann, A.T., et al., *Viable podocytes detach in experimental diabetic nephropathy: potential mechanism underlying glomerulosclerosis*. Nephron Exp Nephrol, 2004. **98**(4): p. e114-23.
19. Vogelmann, S.U., et al., *Urinary excretion of viable podocytes in health and renal disease*. Am J Physiol Renal Physiol, 2003. **285**(1): p. F40-8.
20. Nakamura, T., et al., *Urinary excretion of podocytes in patients with diabetic nephropathy*. Nephrol Dial Transplant, 2000. **15**(9): p. 1379-83.
21. Adler, S., *Integrin receptors in the glomerulus: potential role in glomerular injury*. Am J Physiol, 1992. **262**(5 Pt 2): p. F697-704.
22. Hemler, M.E., *Dystroglycan versatility*. Cell, 1999. **97**(5): p. 543-6.
23. Chen, H.C., et al., *Altering expression of alpha3beta1 integrin on podocytes of human and rats with diabetes*. Life Sci, 2000. **67**(19): p. 2345-53.
24. Makino, H., et al., *Altered gene expression related to glomerulogenesis and podocyte structure in early diabetic nephropathy of db/db mice and its restoration by pioglitazone*. Diabetes, 2006. **55**(10): p. 2747-56.
25. Susztak, K., et al., *Glucose-induced reactive oxygen species cause apoptosis of podocytes and podocyte depletion at the onset of diabetic nephropathy*. Diabetes, 2006. **55**(1): p. 225-33.

26. Brownlee, M., A. Cerami, and H. Vlassara, *Advanced glycosylation end products in tissue and the biochemical basis of diabetic complications*. N Engl J Med, 1988. **318**(20): p. 1315-21.
27. Wendt, T.M., et al., *RAGE drives the development of glomerulosclerosis and implicates podocyte activation in the pathogenesis of diabetic nephropathy*. Am J Pathol, 2003. **162**(4): p. 1123-37.
28. Chuang, P.Y., et al., *Advanced glycation endproducts induce podocyte apoptosis by activation of the FOXO4 transcription factor*. Kidney Int, 2007. **72**(8): p. 965-76.
29. Chen, Y., et al., *Effect of taurine-conjugated ursodeoxycholic acid on endoplasmic reticulum stress and apoptosis induced by advanced glycation end products in cultured mouse podocytes*. Am J Nephrol, 2008. **28**(6): p. 1014-22.
30. Welsh, G.I., et al., *Insulin signaling to the glomerular podocyte is critical for normal kidney function*. Cell Metab. **12**(4): p. 329-40.
31. Singh, R., et al., *Role of angiotensin II in glucose-induced inhibition of mesangial matrix degradation*. Diabetes, 1999. **48**(10): p. 2066-73.
32. Ding, G., et al., *Angiotensin II induces apoptosis in rat glomerular epithelial cells*. Am J Physiol Renal Physiol, 2002. **283**(1): p. F173-80.
33. Yamamoto, T., et al., *Expression of transforming growth factor beta is elevated in human and experimental diabetic nephropathy*. Proc Natl Acad Sci U S A, 1993. **90**(5): p. 1814-8.
34. Border, W.A. and N.A. Noble, *Transforming growth factor beta in tissue fibrosis*. N Engl J Med, 1994. **331**(19): p. 1286-92.
35. Kopp, J.B., et al., *Transgenic mice with increased plasma levels of TGF-beta 1 develop progressive renal disease*. Lab Invest, 1996. **74**(6): p. 991-1003.
36. Schiffer, M., et al., *Apoptosis in podocytes induced by TGF-beta and Smad7*. J Clin Invest, 2001. **108**(6): p. 807-16.
37. Opie, L.H. and P.G. Walfish, *Plasma free fatty acid concentrations in obesity*. N Engl J Med, 1963. **268**: p. 757-60.
38. Mokdad, A.H., et al., *Prevalence of obesity, diabetes, and obesity-related health risk factors, 2001*. JAMA, 2003. **289**(1): p. 76-9.

39. Randle, P.J., et al., *The glucose fatty-acid cycle. Its role in insulin sensitivity and the metabolic disturbances of diabetes mellitus*. Lancet, 1963. **1**(7285): p. 785-9.
40. Hue, L. and H. Taegtmeyer, *The Randle cycle revisited: a new head for an old hat*. Am J Physiol Endocrinol Metab, 2009. **297**(3): p. E578-91.
41. Engfeldt, P. and P. Arner, *Lipolysis in human adipocytes, effects of cell size, age and of regional differences*. Horm Metab Res Suppl, 1988. **19**: p. 26-9.
42. Campbell, P.J., M.G. Carlson, and N. Nurjhan, *Fat metabolism in human obesity*. Am J Physiol, 1994. **266**(4 Pt 1): p. E600-5.
43. Arner, P., *Human fat cell lipolysis: biochemistry, regulation and clinical role*. Best Pract Res Clin Endocrinol Metab, 2005. **19**(4): p. 471-82.
44. Lionetti, L., et al., *From chronic overnutrition to insulin resistance: the role of fat-storing capacity and inflammation*. Nutr Metab Cardiovasc Dis, 2009. **19**(2): p. 146-52.
45. Delarue, J. and C. Magnan, *Free fatty acids and insulin resistance*. Curr Opin Clin Nutr Metab Care, 2007. **10**(2): p. 142-8.
46. Kusminski, C.M., et al., *Diabetes and apoptosis: lipotoxicity*. Apoptosis, 2009. **14**(12): p. 1484-95.
47. Boni-Schnetzler, M., et al., *Free fatty acids induce a proinflammatory response in islets via the abundantly expressed interleukin-1 receptor I*. Endocrinology, 2009. **150**(12): p. 5218-29.
48. Zhou, Y.P. and V.E. Grill, *Long-term exposure of rat pancreatic islets to fatty acids inhibits glucose-induced insulin secretion and biosynthesis through a glucose fatty acid cycle*. J Clin Invest, 1994. **93**(2): p. 870-6.
49. Hagenfeldt, L., et al., *Uptake of individual free fatty acids by skeletal muscle and liver in man*. J Clin Invest, 1972. **51**(9): p. 2324-30.
50. Nolan, C.J. and C.Z. Larter, *Lipotoxicity: why do saturated fatty acids cause and monounsaturates protect against it?* J Gastroenterol Hepatol, 2009. **24**(5): p. 703-6.
51. Lundgren, M. and J.W. Eriksson, *No in vitro effects of fatty acids on glucose uptake, lipolysis or insulin signaling in rat adipocytes*. Horm Metab Res, 2004. **36**(4): p. 203-9.

52. Guo, W., et al., *Palmitate modulates intracellular signaling, induces endoplasmic reticulum stress, and causes apoptosis in mouse 3T3-L1 and rat primary preadipocytes*. Am J Physiol Endocrinol Metab, 2007. **293**(2): p. E576-86.
53. Maedler, K., et al., *Distinct effects of saturated and monounsaturated fatty acids on beta-cell turnover and function*. Diabetes, 2001. **50**(1): p. 69-76.
54. Kharroubi, I., et al., *Free fatty acids and cytokines induce pancreatic beta-cell apoptosis by different mechanisms: role of nuclear factor-kappaB and endoplasmic reticulum stress*. Endocrinology, 2004. **145**(11): p. 5087-96.
55. Laybutt, D.R., et al., *Endoplasmic reticulum stress contributes to beta cell apoptosis in type 2 diabetes*. Diabetologia, 2007. **50**(4): p. 752-63.
56. Martinez, S.C., et al., *Inhibition of Foxo1 protects pancreatic islet beta-cells against fatty acid and endoplasmic reticulum stress-induced apoptosis*. Diabetes, 2008. **57**(4): p. 846-59.
57. Turpin, S.M., et al., *Apoptosis in skeletal muscle myotubes is induced by ceramides and is positively related to insulin resistance*. Am J Physiol Endocrinol Metab, 2006. **291**(6): p. E1341-50.
58. Henique, C., et al., *Increased mitochondrial fatty acid oxidation is sufficient to protect skeletal muscle cells from palmitate-induced apoptosis*. J Biol Chem. **285**(47): p. 36818-27.
59. Peterson, J.M., et al., *Bax signaling regulates palmitate-mediated apoptosis in C(2)C(12) myotubes*. Am J Physiol Endocrinol Metab, 2008. **295**(6): p. E1307-14.
60. Eckel, J., B. Asskamp, and H. Reinauer, *Induction of insulin resistance in primary cultured adult cardiac myocytes*. Endocrinology, 1991. **129**(1): p. 345-52.
61. Wei, Y., et al., *Saturated fatty acids induce endoplasmic reticulum stress and apoptosis independently of ceramide in liver cells*. Am J Physiol Endocrinol Metab, 2006. **291**(2): p. E275-81.
62. Wei, Y., et al., *Reduced endoplasmic reticulum luminal calcium links saturated fatty acid-mediated endoplasmic reticulum stress and cell death in liver cells*. Mol Cell Biochem, 2009. **331**(1-2): p. 31-40.
63. Nakamura, S., et al., *Palmitate induces insulin resistance in H4IIEC3 hepatocytes through reactive oxygen species produced by mitochondria*. J Biol Chem, 2009. **284**(22): p. 14809-18.

64. Staiger, K., et al., *Saturated, but not unsaturated, fatty acids induce apoptosis of human coronary artery endothelial cells via nuclear factor-kappaB activation*. *Diabetes*, 2006. **55**(11): p. 3121-6.
65. Hardy, S., et al., *Saturated fatty acid-induced apoptosis in MDA-MB-231 breast cancer cells. A role for cardiolipin*. *J Biol Chem*, 2003. **278**(34): p. 31861-70.
66. Solinas, G., et al., *Saturated fatty acids inhibit induction of insulin gene transcription by JNK-mediated phosphorylation of insulin-receptor substrates*. *Proc Natl Acad Sci U S A*, 2006. **103**(44): p. 16454-9.
67. Turban, S. and E. Hajdouch, *Protein kinase C isoforms: mediators of reactive lipid metabolites in the development of insulin resistance*. *FEBS Lett*. **585**(2): p. 269-74.
68. Holzer, R.G., et al., *Saturated Fatty Acids Induce c-Src Clustering within Membrane Subdomains, Leading to JNK Activation*. *Cell*. **147**(1): p. 173-84.
69. Listenberger, L.L., D.S. Ory, and J.E. Schaffer, *Palmitate-induced apoptosis can occur through a ceramide-independent pathway*. *J Biol Chem*, 2001. **276**(18): p. 14890-5.
70. Keller, H., et al., *Fatty acids and retinoids control lipid metabolism through activation of peroxisome proliferator-activated receptor-retinoid X receptor heterodimers*. *Proc Natl Acad Sci U S A*, 1993. **90**(6): p. 2160-4.
71. Hihi, A.K., L. Michalik, and W. Wahli, *PPARs: transcriptional effectors of fatty acids and their derivatives*. *Cell Mol Life Sci*, 2002. **59**(5): p. 790-8.
72. Ricchi, M., et al., *Differential effect of oleic and palmitic acid on lipid accumulation and apoptosis in cultured hepatocytes*. *J Gastroenterol Hepatol*, 2009. **24**(5): p. 830-40.
73. Schroder, M., *Endoplasmic reticulum stress responses*. *Cell Mol Life Sci*, 2008. **65**(6): p. 862-94.
74. Gaut, J.R. and L.M. Hendershot, *The modification and assembly of proteins in the endoplasmic reticulum*. *Curr Opin Cell Biol*, 1993. **5**(4): p. 589-95.
75. Szegezdi, E., et al., *Mediators of endoplasmic reticulum stress-induced apoptosis*. *EMBO Rep*, 2006. **7**(9): p. 880-5.
76. Harding, H.P., Y. Zhang, and D. Ron, *Protein translation and folding are coupled by an endoplasmic-reticulum-resident kinase*. *Nature*, 1999. **397**(6716): p. 271-4.

77. Harding, H.P., et al., *An integrated stress response regulates amino acid metabolism and resistance to oxidative stress*. Mol Cell, 2003. **11**(3): p. 619-33.
78. Shamu, C.E. and P. Walter, *Oligomerization and phosphorylation of the Ire1p kinase during intracellular signaling from the endoplasmic reticulum to the nucleus*. EMBO J, 1996. **15**(12): p. 3028-39.
79. Rasheva, V.I. and P.M. Domingos, *Cellular responses to endoplasmic reticulum stress and apoptosis*. Apoptosis, 2009. **14**(8): p. 996-1007.
80. Travers, K.J., et al., *Functional and genomic analyses reveal an essential coordination between the unfolded protein response and ER-associated degradation*. Cell, 2000. **101**(3): p. 249-58.
81. Lee, A.H., N.N. Iwakoshi, and L.H. Glimcher, *XBP-1 regulates a subset of endoplasmic reticulum resident chaperone genes in the unfolded protein response*. Mol Cell Biol, 2003. **23**(21): p. 7448-59.
82. Acosta-Alvear, D., et al., *XBP1 controls diverse cell type- and condition-specific transcriptional regulatory networks*. Mol Cell, 2007. **27**(1): p. 53-66.
83. Shen, J., et al., *ER stress regulation of ATF6 localization by dissociation of BiP/GRP78 binding and unmasking of Golgi localization signals*. Dev Cell, 2002. **3**(1): p. 99-111.
84. Ye, J., et al., *ER stress induces cleavage of membrane-bound ATF6 by the same proteases that process SREBPs*. Mol Cell, 2000. **6**(6): p. 1355-64.
85. Kim, I., W. Xu, and J.C. Reed, *Cell death and endoplasmic reticulum stress: disease relevance and therapeutic opportunities*. Nat Rev Drug Discov, 2008. **7**(12): p. 1013-30.
86. Tabas, I. and D. Ron, *Integrating the mechanisms of apoptosis induced by endoplasmic reticulum stress*. Nat Cell Biol. **13**(3): p. 184-90.
87. Borradaile, N.M., et al., *Disruption of endoplasmic reticulum structure and integrity in lipotoxic cell death*. J Lipid Res, 2006. **47**(12): p. 2726-37.
88. Peter, A., et al., *Individual stearyl-coa desaturase 1 expression modulates endoplasmic reticulum stress and inflammation in human myotubes and is associated with skeletal muscle lipid storage and insulin sensitivity in vivo*. Diabetes, 2009. **58**(8): p. 1757-65.

89. Peter, A., et al., *Induction of stearoyl-CoA desaturase protects human arterial endothelial cells against lipotoxicity*. Am J Physiol Endocrinol Metab, 2008. **295**(2): p. E339-49.
90. Busch, A.K., et al., *Increased fatty acid desaturation and enhanced expression of stearoyl coenzyme A desaturase protects pancreatic beta-cells from lipoapoptosis*. Diabetes, 2005. **54**(10): p. 2917-24.
91. Cunha, D.A., et al., *Initiation and execution of lipotoxic ER stress in pancreatic beta-cells*. J Cell Sci, 2008. **121**(Pt 14): p. 2308-18.
92. Diakogiannaki, E., H.J. Welters, and N.G. Morgan, *Differential regulation of the endoplasmic reticulum stress response in pancreatic beta-cells exposed to long-chain saturated and monounsaturated fatty acids*. J Endocrinol, 2008. **197**(3): p. 553-63.
93. Cnop, M., et al., *Causes and cures for endoplasmic reticulum stress in lipotoxic beta-cell dysfunction*. Diabetes Obes Metab. **12 Suppl 2**: p. 76-82.
94. Pfaffenbach, K.T., et al., *Linking endoplasmic reticulum stress to cell death in hepatocytes: roles of C/EBP homologous protein and chemical chaperones in palmitate-mediated cell death*. Am J Physiol Endocrinol Metab. **298**(5): p. E1027-35.
95. Peng, G., et al., *Oleate blocks palmitate-induced abnormal lipid distribution, endoplasmic reticulum expansion and stress, and insulin resistance in skeletal muscle*. Endocrinology. **152**(6): p. 2206-18.
96. Oyadomari, S., et al., *Targeted disruption of the Chop gene delays endoplasmic reticulum stress-mediated diabetes*. J Clin Invest, 2002. **109**(4): p. 525-32.
97. Song, B., et al., *Chop deletion reduces oxidative stress, improves beta cell function, and promotes cell survival in multiple mouse models of diabetes*. J Clin Invest, 2008. **118**(10): p. 3378-89.
98. Zinszner, H., et al., *CHOP is implicated in programmed cell death in response to impaired function of the endoplasmic reticulum*. Genes Dev, 1998. **12**(7): p. 982-95.
99. Mundel, P., et al., *Rearrangements of the cytoskeleton and cell contacts induce process formation during differentiation of conditionally immortalized mouse podocyte cell lines*. Exp Cell Res, 1997. **236**(1): p. 248-58.
100. Shankland, S.J., et al., *Podocytes in culture: past, present, and future*. Kidney Int, 2007. **72**(1): p. 26-36.

101. Asanuma, K., et al., *Nuclear relocation of the nephrin and CD2AP-binding protein dendrin promotes apoptosis of podocytes*. Proc Natl Acad Sci U S A, 2007. **104**(24): p. 10134-9.
102. Herzig, S., et al., *CREB regulates hepatic gluconeogenesis through the coactivator PGC-1*. Nature, 2001. **413**(6852): p. 179-83.
103. Dittgen, T., et al., *Lentivirus-based genetic manipulations of cortical neurons and their optical and electrophysiological monitoring in vivo*. Proc Natl Acad Sci U S A, 2004. **101**(52): p. 18206-11.
104. Nozaki, J., et al., *The endoplasmic reticulum stress response is stimulated through the continuous activation of transcription factors ATF6 and XBP1 in Ins2+/Akita pancreatic beta cells*. Genes Cells, 2004. **9**(3): p. 261-70.
105. Han, L.Q., et al., *mRNA abundance and expression of SLC27A, ACC, SCD, FADS, LPIN, INSIG, and PPARGC1 gene isoforms in mouse mammary glands during the lactation cycle*. Genet Mol Res. **9**(2): p. 1250-7.
106. Cohen, C.D., et al., *Quantitative gene expression analysis in renal biopsies: a novel protocol for a high-throughput multicenter application*. Kidney Int, 2002. **61**(1): p. 133-40.
107. Schmid, H., et al., *Gene expression profiles of podocyte-associated molecules as diagnostic markers in acquired proteinuric diseases*. J Am Soc Nephrol, 2003. **14**(11): p. 2958-66.
108. Vara, E., et al., *Palmitate dependence of insulin secretion, "de novo" phospholipid synthesis and 45Ca²⁺-turnover in glucose stimulated rat islets*. Diabetologia, 1988. **31**(9): p. 687-93.
109. Sieber, J., et al., *Regulation of podocyte survival and endoplasmic reticulum stress by fatty acids*. Am J Physiol Renal Physiol. **299**(4): p. F821-9.
110. Yamagishi, S., et al., *Palmitate-induced apoptosis of microvascular endothelial cells and pericytes*. Mol Med, 2002. **8**(4): p. 179-84.
111. Mandal, D., et al., *Caspase 3 regulates phosphatidylserine externalization and phagocytosis of oxidatively stressed erythrocytes*. FEBS Lett, 2002. **513**(2-3): p. 184-8.
112. Oyadomari, S. and M. Mori, *Roles of CHOP/GADD153 in endoplasmic reticulum stress*. Cell Death Differ, 2004. **11**(4): p. 381-9.

113. Yoshida, H., et al., *XBPI mRNA is induced by ATF6 and spliced by IRE1 in response to ER stress to produce a highly active transcription factor*. Cell, 2001. **107**(7): p. 881-91.
114. Shang, J. and M.A. Lehrman, *Discordance of UPR signaling by ATF6 and Ire1p-XBPI with levels of target transcripts*. Biochem Biophys Res Commun, 2004. **317**(2): p. 390-6.
115. Welch, W.J. and C.R. Brown, *Influence of molecular and chemical chaperones on protein folding*. Cell Stress Chaperones, 1996. **1**(2): p. 109-15.
116. Xie, Q., et al., *Effect of tauroursodeoxycholic acid on endoplasmic reticulum stress-induced caspase-12 activation*. Hepatology, 2002. **36**(3): p. 592-601.
117. Gregor, M.F. and G.S. Hotamisligil, *Thematic review series: Adipocyte Biology. Adipocyte stress: the endoplasmic reticulum and metabolic disease*. J Lipid Res, 2007. **48**(9): p. 1905-14.
118. Ozcan, U., et al., *Chemical chaperones reduce ER stress and restore glucose homeostasis in a mouse model of type 2 diabetes*. Science, 2006. **313**(5790): p. 1137-40.
119. Preston, A.M., et al., *Reduced endoplasmic reticulum (ER)-to-Golgi protein trafficking contributes to ER stress in lipotoxic mouse beta cells by promoting protein overload*. Diabetologia, 2009. **52**(11): p. 2369-73.
120. Morgan, N.G., et al., *The cytoprotective actions of long-chain mono-unsaturated fatty acids in pancreatic beta-cells*. Biochem Soc Trans, 2008. **36**(Pt 5): p. 905-8.
121. Liu, G., et al., *Apoptosis induced by endoplasmic reticulum stress involved in diabetic kidney disease*. Biochem Biophys Res Commun, 2008. **370**(4): p. 651-6.
122. Wu, J., et al., *Induction of diabetes in aged C57B6 mice results in severe nephropathy: an association with oxidative stress, endoplasmic reticulum stress, and inflammation*. Am J Pathol. **176**(5): p. 2163-76.
123. Ntambi, J.M., et al., *Differentiation-induced gene expression in 3T3-L1 preadipocytes. Characterization of a differentially expressed gene encoding stearoyl-CoA desaturase*. J Biol Chem, 1988. **263**(33): p. 17291-300.
124. Kaestner, K.H., et al., *Differentiation-induced gene expression in 3T3-L1 preadipocytes. A second differentially expressed gene encoding stearoyl-CoA desaturase*. J Biol Chem, 1989. **264**(25): p. 14755-61.

125. Miyazaki, M., et al., *Identification and characterization of murine SCD4, a novel heart-specific stearyl-CoA desaturase isoform regulated by leptin and dietary factors*. J Biol Chem, 2003. **278**(36): p. 33904-11.
126. Ntambi, J.M. and M. Miyazaki, *Recent insights into stearyl-CoA desaturase-1*. Curr Opin Lipidol, 2003. **14**(3): p. 255-61.
127. Chu, K., et al., *Stearyl-coenzyme A desaturase 1 deficiency protects against hypertriglyceridemia and increases plasma high-density lipoprotein cholesterol induced by liver X receptor activation*. Mol Cell Biol, 2006. **26**(18): p. 6786-98.
128. Shimomura, I., et al., *Nuclear sterol regulatory element-binding proteins activate genes responsible for the entire program of unsaturated fatty acid biosynthesis in transgenic mouse liver*. J Biol Chem, 1998. **273**(52): p. 35299-306.
129. Schultz, J.R., et al., *Role of LXRs in control of lipogenesis*. Genes Dev, 2000. **14**(22): p. 2831-8.
130. Seamon, K.B., W. Padgett, and J.W. Daly, *Forskolin: unique diterpene activator of adenylate cyclase in membranes and in intact cells*. Proc Natl Acad Sci U S A, 1981. **78**(6): p. 3363-7.
131. Cunha, D.A., et al., *Glucagon-like peptide-1 agonists protect pancreatic beta-cells from lipotoxic endoplasmic reticulum stress through upregulation of BiP and JunB*. Diabetes, 2009. **58**(12): p. 2851-62.
132. Gurzov, E.N., et al., *JunB Inhibits ER Stress and Apoptosis in Pancreatic Beta Cells*. PLoS One, 2008. **3**(8): p. e3030.
133. Gloerich, M. and J.L. Bos, *Epac: defining a new mechanism for cAMP action*. Annu Rev Pharmacol Toxicol. **50**: p. 355-75.
134. Enserink, J.M., et al., *A novel Epac-specific cAMP analogue demonstrates independent regulation of Rap1 and ERK*. Nat Cell Biol, 2002. **4**(11): p. 901-6.
135. Montminy, M.R., G.A. Gonzalez, and K.K. Yamamoto, *Regulation of cAMP-inducible genes by CREB*. Trends Neurosci, 1990. **13**(5): p. 184-8.
136. Mayr, B. and M. Montminy, *Transcriptional regulation by the phosphorylation-dependent factor CREB*. Nat Rev Mol Cell Biol, 2001. **2**(8): p. 599-609.

137. Kim, S.J., et al., *Glucose-dependent insulinotropic polypeptide-mediated up-regulation of beta-cell antiapoptotic Bcl-2 gene expression is coordinated by cyclic AMP (cAMP) response element binding protein (CREB) and cAMP-responsive CREB coactivator 2*. *Mol Cell Biol*, 2008. **28**(5): p. 1644-56.
138. Tsujimoto, Y. and S. Shimizu, *Role of the mitochondrial membrane permeability transition in cell death*. *Apoptosis*, 2007. **12**(5): p. 835-40.
139. Toyoda, M., et al., *Podocyte detachment and reduced glomerular capillary endothelial fenestration in human type 1 diabetic nephropathy*. *Diabetes*, 2007. **56**(8): p. 2155-60.
140. Ziyadeh, F.N., et al., *Long-term prevention of renal insufficiency, excess matrix gene expression, and glomerular mesangial matrix expansion by treatment with monoclonal antitransforming growth factor-beta antibody in db/db diabetic mice*. *Proc Natl Acad Sci U S A*, 2000. **97**(14): p. 8015-20.
141. Durvasula, R.V. and S.J. Shankland, *Activation of a local renin angiotensin system in podocytes by glucose*. *Am J Physiol Renal Physiol*, 2008. **294**(4): p. F830-9.
142. Boden, G., *Fatty acid-induced inflammation and insulin resistance in skeletal muscle and liver*. *Curr Diab Rep*, 2006. **6**(3): p. 177-81.
143. Mevorach, M., et al., *Hormone-independent activation of EGP during hypoglycemia is absent in type 1 diabetes mellitus*. *Am J Physiol Endocrinol Metab*, 2000. **278**(3): p. E421-9.
144. Chen, H.M., et al., *Podocyte lesions in patients with obesity-related glomerulopathy*. *Am J Kidney Dis*, 2006. **48**(5): p. 772-9.
145. Marciniak, S.J., et al., *CHOP induces death by promoting protein synthesis and oxidation in the stressed endoplasmic reticulum*. *Genes Dev*, 2004. **18**(24): p. 3066-77.
146. Inagi, R., et al., *Involvement of endoplasmic reticulum (ER) stress in podocyte injury induced by excessive protein accumulation*. *Kidney Int*, 2005. **68**(6): p. 2639-50.
147. Lindenmeyer, M.T., et al., *Proteinuria and hyperglycemia induce endoplasmic reticulum stress*. *J Am Soc Nephrol*, 2008. **19**(11): p. 2225-36.
148. Hellemans, K.H., et al., *Susceptibility of pancreatic beta cells to fatty acids is regulated by LXR/PPARalpha-dependent stearoyl-coenzyme A desaturase*. *PLoS One*, 2009. **4**(9): p. e7266.

149. Listenberger, L.L., et al., *Triglyceride accumulation protects against fatty acid-induced lipotoxicity*. Proc Natl Acad Sci U S A, 2003. **100**(6): p. 3077-82.
150. Bergman, B.C., et al., *Increased intramuscular lipid synthesis and low saturation relate to insulin sensitivity in endurance-trained athletes*. J Appl Physiol. **108**(5): p. 1134-41.
151. Miyazaki, M., et al., *Stearoyl-CoA desaturase-1 deficiency attenuates obesity and insulin resistance in leptin-resistant obese mice*. Biochem Biophys Res Commun, 2009. **380**(4): p. 818-22.
152. MacDonald, M.L., et al., *Despite antiatherogenic metabolic characteristics, SCD1-deficient mice have increased inflammation and atherosclerosis*. Arterioscler Thromb Vasc Biol, 2009. **29**(3): p. 341-7.
153. Sampath, H., et al., *Skin-specific deletion of stearoyl-CoA desaturase-1 alters skin lipid composition and protects mice from high fat diet-induced obesity*. J Biol Chem, 2009. **284**(30): p. 19961-73.
154. Guo, Z.K. and M.D. Jensen, *Accelerated intramyocellular triglyceride synthesis in skeletal muscle of high-fat-induced obese rats*. Int J Obes Relat Metab Disord, 2003. **27**(9): p. 1014-9.
155. Zhang, X.J., et al., *The synthetic rate of muscle triglyceride but not phospholipid is increased in obese rabbits*. Metabolism, 2009. **58**(11): p. 1649-56.
156. Mittendorfer, B., *Origins of metabolic complications in obesity: adipose tissue and free fatty acid trafficking*. Curr Opin Clin Nutr Metab Care.
157. Goodpaster, B.H., et al., *Skeletal muscle lipid content and insulin resistance: evidence for a paradox in endurance-trained athletes*. J Clin Endocrinol Metab, 2001. **86**(12): p. 5755-61.
158. Liu, L., et al., *DGAT1 expression increases heart triglyceride content but ameliorates lipotoxicity*. J Biol Chem, 2009. **284**(52): p. 36312-23.
159. Maeda, S., et al., *A single nucleotide polymorphism within the acetyl-coenzyme A carboxylase beta gene is associated with proteinuria in patients with type 2 diabetes*. PLoS Genet. **6**(2): p. e1000842.
160. Tang, S.C., et al., *The acetyl-coenzyme A carboxylase beta (ACACB) gene is associated with nephropathy in Chinese patients with type 2 diabetes*. Nephrol Dial Transplant. **25**(12): p. 3931-4.

161. Riccio, A., et al., *Mediation by a CREB family transcription factor of NGF-dependent survival of sympathetic neurons*. Science, 1999. **286**(5448): p. 2358-61.
162. Tam, F.W., et al., *Development of scarring and renal failure in a rat model of crescentic glomerulonephritis*. Nephrol Dial Transplant, 1999. **14**(7): p. 1658-66.
163. Xiao, Z., et al., *Glomerular podocytes express type 1 adenylate cyclase: inactivation results in susceptibility to proteinuria*. Nephron Exp Nephrol. **118**(3): p. e39-48.
164. Gao, S.Y., et al., *Rho-family small GTPases are involved in forskolin-induced cell-cell contact formation of renal glomerular podocytes in vitro*. Cell Tissue Res, 2007. **328**(2): p. 391-400.
165. Oh, J., et al., *Stimulation of the calcium-sensing receptor stabilizes the podocyte cytoskeleton, improves cell survival, and reduces toxin-induced glomerulosclerosis*. Kidney Int. **80**(5): p. 483-92.
166. Mundel, P., et al., *Synaptopodin: an actin-associated protein in telencephalic dendrites and renal podocytes*. J Cell Biol, 1997. **139**(1): p. 193-204.
167. Faul, C., et al., *The actin cytoskeleton of kidney podocytes is a direct target of the antiproteinuric effect of cyclosporine A*. Nat Med, 2008. **14**(9): p. 931-8.

7. ACKNOWLEDGEMENT

I would like to express my deep gratitude and appreciation to my supervisor, PD Dr. Andreas Jehle, for giving me the opportunity to do my Ph.D in his research group, for the great support during the whole project, for all the interesting and constructive discussions and, most importantly, for the highly pleasant and stimulating atmosphere in the lab, which is promoting creative and independent research.

Also, I would like to thank my colleague, Kapil Kampe, for all the input and discussions and for contributing to the nice environment in the lab.

I would also like to thank to Dr. Maja Linenmeyer and PD Dr. med. Clemens Cohen for the collaboration and for analyzing microdissected glomeruli of human patients.

In addition, I am very grateful to Dr. Kirk Campbell and Prof. Peter Mundel for helping me to establish the lentiviral knockdown system in our lab.

I am very grateful to Prof. Ed Palmer for being my faculty representative and to Prof. Marc Donath for co-reporting the thesis.

I am also thankful to the Donath group for all the input and suggestions during the group meetings.

Furthermore, I would like to thank Dr. Stefan Gruber for helping me to establish the TLC in our lab.

I would also like to thank all my friends for distracting me from work and for helping me to recharge my batteries.

Last but not least I want to thank my parents, Markus and Beatrice, and my sisters, Nora, Noemi and Deborah, for all the support during my life and for everything they have done for me.

APPENDIX

Regulation of podocyte survival and endoplasmic reticulum stress by free fatty acids. *Am J Physiol Renal Physiol*. 2010 Oct;299(4):F821-9.

7.1.1 - Am J Physiol Renal Physiol Article

Regulation of podocyte survival and endoplasmic reticulum stress by fatty acids

Jonas Sieber, Maja Tamara Lindenmeyer, Kapil Kampe, Kirk Nicholas Campbell, Clemens David Cohen, Helmut Hoyer, Peter Mundel and Andreas Werner Jehle
Am J Physiol Renal Physiol 299:F821-F829, 2010. First published 28 July 2010;
doi:10.1152/ajprenal.00196.2010

You might find this additional info useful...

Supplemental material for this article can be found at:

<http://ajprenal.physiology.org/content/suppl/2010/08/09/ajprenal.00196.2010.DC1.html>

This article cites 62 articles, 30 of which can be accessed free at:

<http://ajprenal.physiology.org/content/299/4/F821.full.html#ref-list-1>

Updated information and services including high resolution figures, can be found at:

<http://ajprenal.physiology.org/content/299/4/F821.full.html>

Additional material and information about *AJP - Renal Physiology* can be found at:

<http://www.the-aps.org/publications/ajprenal>

This information is current as of April 19, 2011.

AJP - Renal Physiology publishes original manuscripts on a broad range of subjects relating to the kidney, urinary tract, and their respective cells and vasculature, as well as to the control of body fluid volume and composition. It is published 12 times a year (monthly) by the American Physiological Society, 9650 Rockville Pike, Bethesda MD 20814-3991. Copyright © 2010 by the American Physiological Society. ISSN: 0363-6127, ESN: 1522-1466. Visit our website at <http://www.the-aps.org/>.

Regulation of podocyte survival and endoplasmic reticulum stress by fatty acids

Jonas Sieber,¹ Maja Tamara Lindenmeyer,^{2,3} Kapil Kampe,¹ Kirk Nicholas Campbell,⁴ Clemens David Cohen,^{2,3} Helmut Hopfer,⁵ Peter Mundel,⁴ and Andreas Werner Jehle^{1,6}

¹Department of Biomedicine, Molecular Nephrology, University Hospital, Basel; ²Institute of Physiology with Center of Integrative Human Physiology, University of Zurich, and ³Division of Nephrology, University Hospital Zurich, Zurich;

⁴Department of Medicine, Miller School of Medicine, University of Miami, Miami, Florida; and ⁵Institute of Clinical Pathology, University Hospital, and ⁶Department of Internal Medicine, Kantonsspital Bruderholz, University of Basel, Basel, Switzerland

Submitted 6 April 2010; accepted in final form 21 July 2010

Sieber J, Lindenmeyer MT, Kampe K, Campbell KN, Cohen CD, Hopfer H, Mundel P, Jehle AW. Regulation of podocyte survival and endoplasmic reticulum stress by fatty acids. *Am J Physiol Renal Physiol* 299: F821–F829, 2010. First published July 28, 2010; doi:10.1152/ajprenal.00196.2010.—Apoptosis of podocytes is considered critical in the pathogenesis of diabetic nephropathy (DN). Free fatty acids (FFAs) are critically involved in the pathogenesis of diabetes mellitus type 2, in particular the regulation of pancreatic β cell survival. The objectives of this study were to elucidate the role of palmitic acid, palmitoleic, and oleic acid in the regulation of podocyte cell death and endoplasmic reticulum (ER) stress. We show that palmitic acid increases podocyte cell death, both apoptosis and necrosis of podocytes, in a dose and time-dependent fashion. Palmitic acid induces podocyte ER stress, leading to an unfolded protein response as reflected by the induction of the ER chaperone immunoglobulin heavy chain binding protein (BiP) and proapoptotic C/EBP homologous protein (CHOP) transcription factor. Of note, the monounsaturated palmitoleic and oleic acid can attenuate the palmitic acid-induced upregulation of CHOP, thereby preventing cell death. Similarly, gene silencing of CHOP protects against palmitic acid-induced podocyte apoptosis. Our results offer a rationale for interventional studies aimed at testing whether dietary shifting of the FFA balance toward unsaturated FFAs can delay the progression of DN.

diabetic nephropathy; apoptosis; endoplasmic reticulum; stress; palmitic acid

DIABETIC NEPHROPATHY (DN) is the major cause of end-stage renal disease (ESRD) in many industrialized countries, and as the prevalence of type 2 diabetes is much greater, most diabetic patients starting renal replacement therapy today have type 2 diabetes (1, 25). Podocyte injury and loss are critical events in the course of DN (58) and precede albuminuria and renal dysfunction (9, 35, 42, 50, 53). Type 2 diabetes mellitus is characterized by hyperglycemia and dyslipidemia with increased plasma levels of long-chain free fatty acids (FFAs) (43, 55). Saturated FFAs such as palmitic acid are proapoptotic factors in other cell types, including pancreatic β -cells (28, 33, 48) and hepatocytes (29, 57). Monounsaturated FFAs such as palmitoleic or oleic acid are able to prevent/attenuate palmitic acid-induced impaired insulin secretion and increased apoptosis of pancreatic β -cells (27), and diets rich in unsaturated FFAs were shown to lower glucose levels in type 2 diabetic

mic (54). It is now widely accepted that a disbalance between saturated and unsaturated FFAs critically contributes to the pathogenesis of type 2 diabetes (37).

Previous studies with cultured human mesangial cells demonstrated that palmitic acid stimulates apoptosis that can be prevented by unsaturated FFAs (36). However, as it stands, the role of FFAs in the pathogenesis of DN and their role in podocyte viability are largely unknown. In cultured podocytes, palmitic acid leads to insulin resistance and blockade of insulin-dependent glucose uptake (21), reflecting profound alterations in podocyte function. In proteinuric kidney disease, FFAs bound to albumin are filtered and reabsorbed by the proximal tubule, which may contribute to tubulointerstitial inflammation and fibrosis (51, 52).

The endoplasmic reticulum (ER) is the organelle where secretory and membrane proteins are folded. Correctly folded proteins exit the ER and are transported to the Golgi and other destinations within the cell, but mis- or unfolded proteins are retained in the ER (44). The accumulation of unfolded proteins constitutes a form of cellular stress that has been termed ER stress. Importantly, the aforementioned toxicity of palmitic acid involves ER stress (15, 18, 33, 56, 57). As a result of ER stress, several signaling pathways, collectively known as the unfolded protein response (UPR), are being activated, thereby maintaining proper ER function. This involves attenuation of translation and transcriptional induction of ER chaperones, whose functions are to increase the folding capacity of the ER and to prevent protein aggregation (17, 26). Under conditions with severe ER stress, however, the protective mechanisms activated by the UPR are not sufficient and a particular branch of the UPR evolves leading to induction of the proapoptotic transcription factor C/EBP homologous protein (CHOP; also known as DDIT3), which can trigger apoptosis (61). The expression of CHOP is mainly regulated at the transcriptional level by several transcription factors, including X-box binding protein-1 (XBP-1) (41). Of note, only the spliced form of XBP-1 has transcriptional activity (60).

The induction of ER stress markers has been described in human kidney biopsies of different glomerulopathies, including membranous nephropathy, focal segmental glomerulosclerosis, and minimal change disease (3, 32). Gene expression analysis of the tubulointerstitial compartment of renal biopsies obtained from patients with DN found a significant upregulation of major genes involved in the UPR, including the ER chaperones BiP (also known as HSPA5 or GRP78) and hyp-

Address for reprint requests and other correspondence: A. W. Jehle, Dept. of Biomedicine, Molecular Nephrology, Rm 303, Univ. Hospital Basel, Hebelstrasse 20, 4031 Basel, Switzerland (e-mail: andreas.jehle@unibas.ch).

oxia-upregulated 1, but no changes in the expression of proapoptotic CHOP (22).

The objectives of the present study were to investigate the effects of palmitic acid, a saturated FFA, and monounsaturated FFAs such as palmitoleic or oleic acid on podocyte cell death and the involvement of ER stress in this process. In addition, we explored the mechanistic role of the proapoptotic transcription factor CHOP in palmitic acid-induced podocyte cell death by gene silencing of CHOP using a specific short-hairpin (sh) RNA.

MATERIALS AND METHODS

Materials. Palmitic acid, palmitoleic acid, oleic acid, and essential fatty acid-free BSA were purchased from Sigma, anti-BiP and anti-activated caspase 3 antibodies from Cell Signaling, anti-CHOP from Santa-Cruz Biotechnology, and anti- β -actin from Sigma. The horseradish peroxidase-conjugated secondary antibodies were obtained from Dako and Jackson. The primary antibodies were applied at dilutions of 1:1,000 in blocking solution (5% milk in TBS-Tween) except anti-CHOP (1:200) and anti- β -actin (1:100,000). Alexa 647 annexin V and propidium iodide (PI) were purchased from Invitrogen.

Cell culture. Podocytes were cultured as described before (39). Briefly, conditionally immortalized mouse podocytes were cultured under permissive conditions (33°C) in RPMI-1640 supplemented with 10% FBS, penicillin/streptomycin (all from Invitrogen), and interferon- γ (Cell Sciences) on type I collagen (BD Biosciences). Differentiation was induced by thermoshift to 37°C without interferon- γ in six-well plates (apoptosis assays) and 10-cm dishes (protein isolation). All experiments were performed with cells that had been allowed to differentiate for at least 11 days.

Fatty acid preparation. Fatty acids were prepared as described previously (23). In brief, 20 mM solutions of palmitic, palmitoleic, or oleic acids in 0.01 M NaOH (vehicle) were incubated at 70°C for 30 min and complexed to 10% BSA in a molar ratio of 6.6:1, shaken overnight at 37°C under N₂-atmosphere, sonicated for 10 min, sterile filtrated, and stored at -20°C. Before use, the complexes were heated at 60°C for 15 min followed by dilution in medium. The fatty acid concentrations were determined with a commercial kit according to the manufacturer's instructions (Wako). The endotoxin concentration was measured using a commercial kit (GenScript), and the final concentration in all experiments was equal or below 0.5 ng/ml. BSA used for control experiments was prepared and handled exactly the same as BSA complexed to FFAs.

Apoptosis assay. Podocyte apoptosis and necrosis were determined by flow cytometry exactly as recently reported (2). Briefly, podocytes were trypsinized and resuspended in annexin V binding buffer (10 mM HEPES, 140 mM NaCl, 2.5 mM CaCl₂, pH 7.4). Annexin V staining was applied for 15 min at room temperature (see producer protocol) and before analysis 0.5 μ g PI was added. For the assay, 20,000–25,000 cells were analyzed by flow cytometry (Dako).

RT-PCR analysis of XBP-1 mRNA splicing. Total RNA was extracted with a Nucleospin kit (Macherey-Nagel), and first-strand cDNA was synthesized using oligo(dT) primers (Fermentas). Amplification (initial denaturation at 94°C for 1 min, 30 cycles of PCR at 94°C for 30 s, 58°C for 30 s, and 72°C for 1 min, and a final extension at 72°C for 10 min) was performed with a pair of primers corresponding to nucleotides 392–415 (TGAGAACCAGGAGTTAAGAA-CACGC) and 720–696 (TTCTGGGTAGACCTCTGGGAGTTC) of mouse XBP-1 cDNA (AF027963) (40). PCR products were separated by electrophoresis on 2.5% agarose gels and visualized by ethidium bromide staining.

Western blotting. Podocytes were washed with ice-cold PBS and scraped into 200 μ l RIPA lysis buffer (50 mM Tris-HCl, pH 7.5, 200 mM NaCl, 1% Triton, 0.25% deoxycholic acid, 1 mM EDTA, 1 mM EGTA) containing EDTA-free protease inhibitors (Roche) and phos-

phatase inhibitors (Pierce). To include the floating and detached cells, the culture medium and PBS (the cells were washed with) were collected, centrifuged (530 g), and resuspended in 20 μ l lysis buffer. The pooled cells were lysed mechanically and rotated for 1 h at 4°C. To remove nuclei, the samples were spun down (10,000 rpm, 10 min) and the protein concentration of the supernatant was determined by D_C protein assay (Bio-Rad). Then, 30–80 μ g of protein/well were loaded on 12 or 15% gels and separated by SDS-PAGE. Transfer to nitrocellulose membranes was applied at 100 V in the cold room for 1 h, and the blots were blocked for 2 h with 5% milk powder in TBS-Tween. Primary antibodies were applied overnight, secondary antibodies for 1 h. The immunoblots were detected by enhanced chemiluminescence (Pierce) on Kodak BioMax light films (Sigma).

Lentivirus production and CHOP knockdown. A CHOP-specific oligonucleotide (GGAAACGAAGAGGAAGAATCA) (11) was cloned into a FUGW vector coexpressing green fluorescent protein under a ubiquitin promoter. A 21-nt scrambled sequence (GACCGCGACTCGC-CGTCTGCG) with no murine homology served as a nonsilencing control (2). Lentivirus production was performed as previously reported (13). In brief, HEK293 cells were transfected using Fugene (Roche) with the FUGW vector and two helper plasmids, vesicular stomatitis virus (VSV) G protein and Δ 8.9. After 72 h, the supernatant was spun down at 780 g and filtered using a filter with 0.45- μ m pore size. Podocytes were transduced by adding virus-containing medium after 5-min pretreatment with 10 μ g/ml polybrene (Sigma). All experiments were performed 4 days after viral transduction (2).

Statistical analysis. Data are expressed as means \pm SD unless otherwise indicated. The significance of differences was calculated with a two-sided, unpaired *t*-test unless otherwise indicated.

RESULTS

Palmitic acid induces podocyte cell death. First, we investigated whether palmitic acid may also induce podocyte cell death as reported for other cell types, e.g., pancreatic β -cells (28, 33, 48). Palmitic acid complexed to BSA in concentrations from 125 to 500 μ M enhanced cell death of podocytes in a concentration-dependent manner (Fig. 1). Figure 1A shows representative flow cytometry data with the abscissa and ordinate representing the fluorescence intensity of annexin V and PI, respectively. In BSA not complexed to palmitic acid (BSA containing control medium), 5.2 \pm 0.1% of podocytes were annexin V-positive/PI-negative cells, representing early apoptotic podocytes, and 5.9 \pm 0.9% were annexin V positive/PI positive, representing late apoptotic/necrotic cells (Fig. 1B). Palmitic acid increased apoptosis significantly at 250 (9.1 \pm 0.9%, $P < 0.01$; Fig. 1B) and at 500 μ M (14.0 \pm 0.2%, $P < 0.01$; Fig. 1B). We also found a dose-dependent increase in necrotic cells (at 500 μ M, 17.3 \pm 1.2%, $P < 0.01$; Fig. 1B). To be able to detect an effect of low palmitic acid concentrations (125 and 250 μ M), a relatively long incubation time (38 h) was chosen for the experiments displayed in Fig. 1. Next, we tested the time dependency of palmitic acid-induced podocyte apoptosis by analyzing cell death over time after exposure to 500 μ M palmitic acid (Fig. 2A). Palmitic acid induced cell death, both apoptosis and necrosis, in a time-dependent manner, and significant differences became apparent at 24 h (Fig. 2, B and C). After 48 h, a 2.5- to 3-fold increase in apoptotic and necrotic podocytes was observed ($P < 0.01$; Fig. 2, B and C). Of note, the increase in annexin V/PI double-positive late apoptotic/necrotic cells was underestimated by flow cytometry, as more floating cellular debris were formed in the supernatants of cell pellets used for flow experiments over time. This was reflected

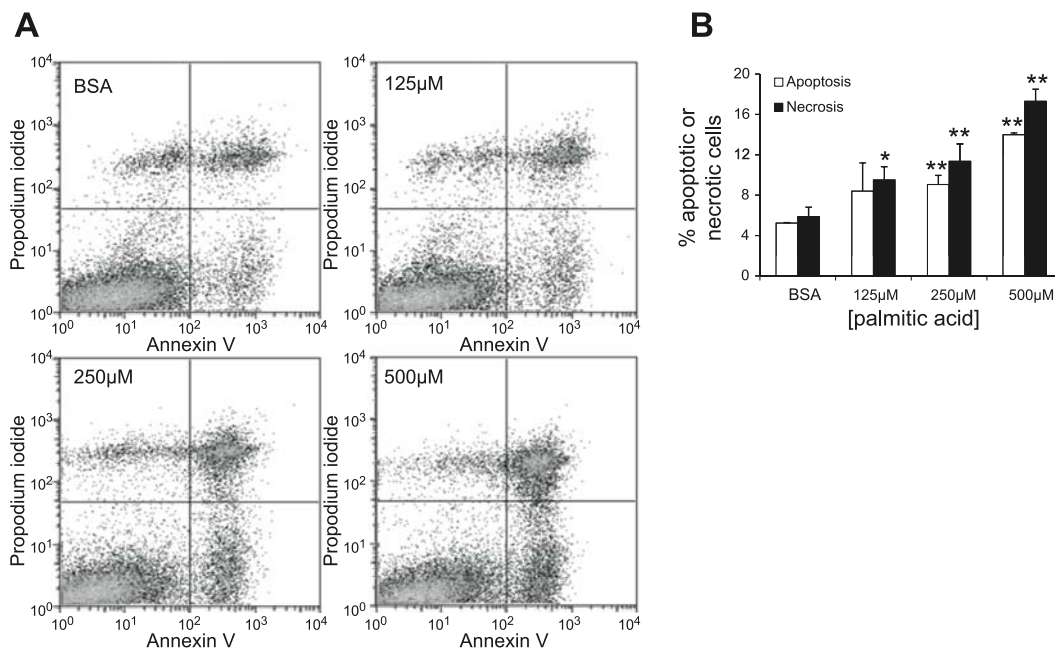


Fig. 1. Palmitic acid induces apoptosis and necrosis of podocytes in a dose-dependent manner. *A*: representative flow cytometry results for podocytes exposed to increasing concentrations of palmitic acid (125–500 μM) or BSA (at a concentration equivalent to cells treated with 500 μM palmitic acid complexed to BSA) for 38 h. The abscissa and ordinate represent the fluorescence intensity of annexin V Alexa 647 and propidium iodide (PI), respectively. *B*: quantitative analysis of palmitic acid-induced podocyte cell death. Bar graph represents the mean percentages \pm SD of annexin V-positive/PI-negative (early apoptotic) and annexin V-positive/PI-positive (late apoptotic/necrotic) podocytes ($n = 3$). * $P < 0.05$, ** $P < 0.01$.

in a decreased total number of cells recovered in cell pellets after 34 and 48 h ($P < 0.05$; Fig. 2D).

Palmitic acid activates effector caspase 3. To confirm the effect of palmitic acid on podocyte apoptosis with a second, independent approach, we examined the activation of effector caspase 3 by Western immunoblotting using an antibody specific for cleaved and therefore activated caspase 3 (49) (Fig. 3). As activation of caspase 3 typically occurs before externalization of phosphatidylserine (30) as assessed by annexin V staining in the flow cytometry assay, we incubated podocytes with 500 μM palmitic acid for 1 or 16 h (Fig. 3A). For staurosporine (positive control), a faint band for cleaved caspase 3 was seen as early as after 1 h, whereas for palmitic acid a band for cleaved caspase 3 was seen after 16 h (Fig. 3A). Consistent with the flow cytometry data (Fig. 1), cleaved caspase 3 could be observed at lower concentrations of palmitic acid with a faint band at a concentration of 125 μM and a strong band at 250 and 500 μM (Fig. 3B).

Palmitic acid induces ER stress in podocytes. The toxicity of palmitic acid has been attributed to the induction of ER stress (15, 18, 33, 56, 57). Therefore, we studied the effect of palmitic acid on protein levels of BiP, an ER chaperone that is upregulated during ER stress (19). We observed a strong upregulation of BiP protein expression after incubation with 500 μM palmitic acid for 16 and 24 h ($P < 0.01$, Fig. 4A, and Supplemental Fig. S1A; supplemental material for this article is available online at the Journal website). In addition, the proapoptotic transcription factor CHOP, which is typically upregulated during severe ER stress (61), was increased ninefold after 24 h ($P < 0.01$, Fig. 4B).

As the effect of palmitic acid on podocyte cell death started to become visible at a concentration of 125 μM and even more at 250 μM (Fig. 1), we tested whether palmitic acid at 125 and 250 μM could also upregulate BiP and CHOP expression. Indeed, already lower concentrations of palmitic acid upregulated CHOP (Fig. 4C) and BiP expression (Supplemental Fig. S1B). Moreover, as the induction of CHOP expression should precede palmitic acid-induced cell death, we explored changes in CHOP expression at an earlier time point (6 h). Taken together, we found a dose- and time-dependent increase in CHOP protein levels as early as after 6 h (Fig. 4C).

XBP-1 is involved in the transcriptional activation of CHOP in ER stress, but only the spliced form of XBP-1 (sXBP-1) has transcriptional activity (60). Therefore, we used RT-PCR to amplify fragments of XBP-1 representing both the unspliced (uXBP-1) and the spliced (sXBP-1) forms of XBP-1 mRNA. Palmitic acid and tunicamycin (Tn), an established inducer of ER stress, strongly induced sXBP-1 and an additional slowly migrating band (Fig. 4D). The slowly migrating band represents a hybrid form of uXBP-1 and sXBP-1 (hXBP-1), which can form during annealing in the last PCR step (47). XBP-1 splicing was increased as early as after 4 h after exposure to palmitic acid (data not shown), implying a potential role for XBP-1 splicing in transcriptional activation of CHOP.

High glucose concentrations (50) and TGF- β at a concentration of 5 ng/ml (62) can also induce podocyte injury and death. Therefore, we tested whether high glucose or TGF- β can induce BiP or CHOP expression. Neither high glucose (22 mM) nor TGF- β induced CHOP (Fig. 4E), but TGF- β (5

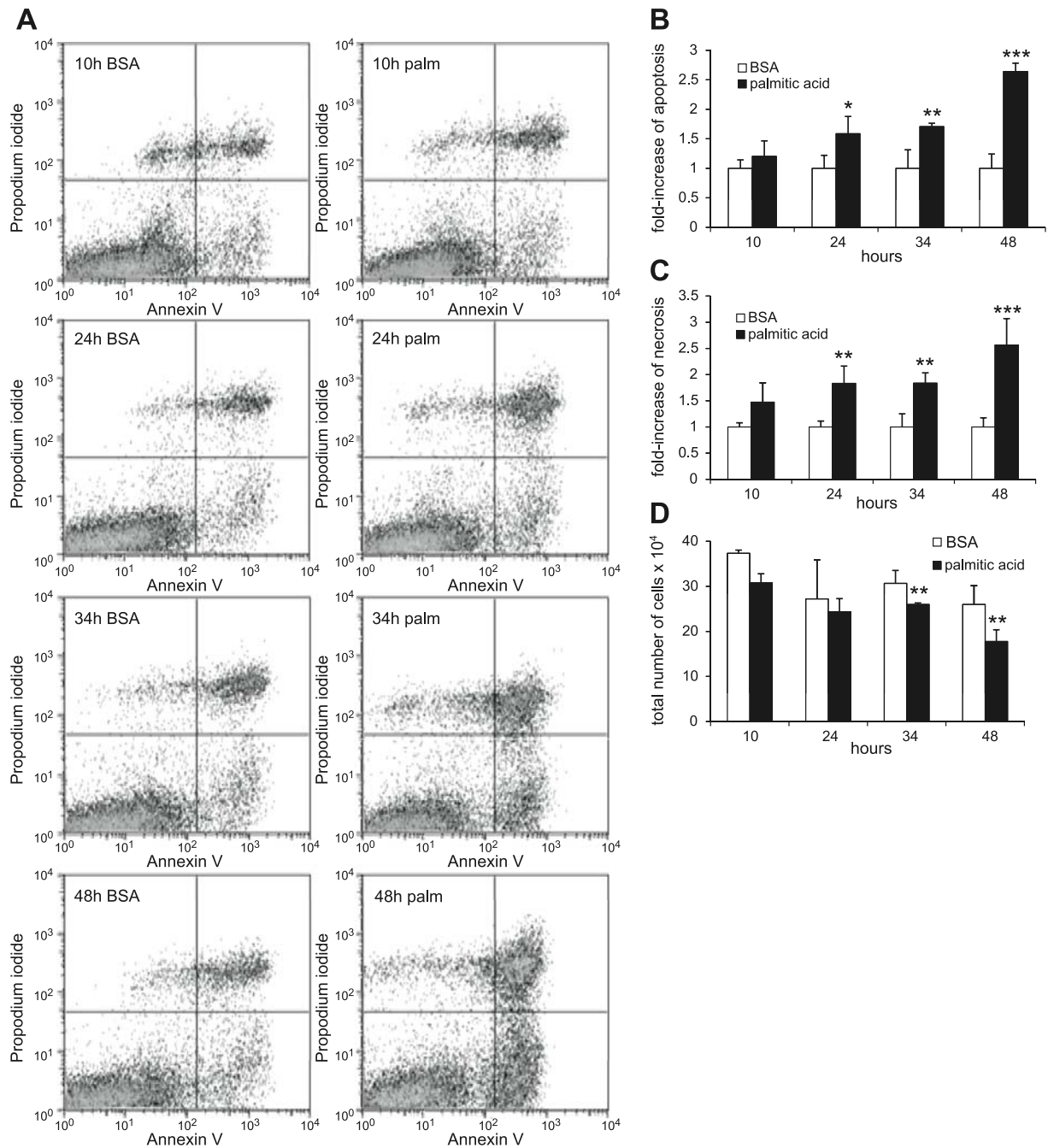


Fig. 2. Palmitic acid induces time-dependent podocyte apoptosis. *A*: palmitic acid-induced podocyte cell death was determined by annexin V/PI staining followed by flow cytometry. *B*: quantitative analysis. Bar graph represents the mean fold-increase \pm SD in annexin V-positive/PI-negative (apoptotic) cells incubated with palmitic acid or BSA for indicated time points ($n = 3$). * $P = 0.05$, ** $P < 0.05$, *** $P < 0.01$. *C*: bar graph representing the mean fold-increase \pm SD in annexin V-positive/PI-positive (necrotic) cells incubated with palmitic acid or BSA for indicated time points ($n = 3$). ** $P < 0.05$, *** $P < 0.01$. *D*: bar graphs representing intact cells recovered in cell pellets (= total cells in culture dishes minus floating cellular debris in supernatant after centrifugation at 550g), which were used for flow experiments shown in *A–C*. Palmitic acid significantly decreased the number of recovered cells after 34 and 48 h (** $P < 0.05$), reflecting the increase in necrotic cellular debris that could not be recovered in cell pellets.

ng/ml) alone or in combination with high glucose induced BiP (Fig. 4E). The weak effect of high glucose on BiP expression was similar to the effect of mannitol, which was used to adjust osmolality to the high-glucose condition, and therefore, the

difference in osmolality rather than a high glucose concentration may account for this observation. Staurosporine, a strong inducer of podocyte apoptosis (2), did not increase BiP or CHOP expression (Fig. 4E).

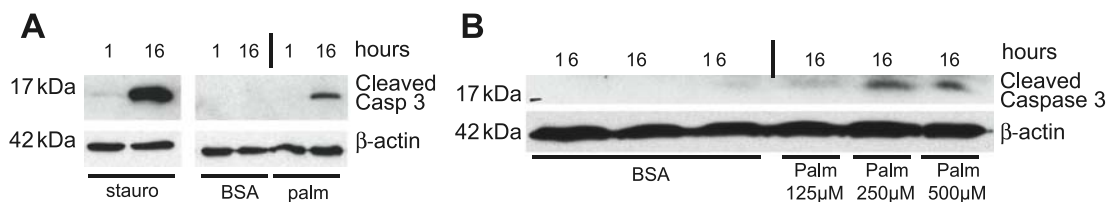


Fig. 3. Palmitic acid activates caspase 3 in podocytes. Western blot analysis of active, cleaved caspase 3 protein steady-state levels in podocytes exposed to staurosporine (stauro), fatty acid-free BSA (BSA), or palmitic acid (palm) is shown. *A*: 0.25 μ M staurosporine (serving as a positive control) and palmitic acid caused a strong activation of caspase 3 after 16 h. No signal was seen after 1-h exposure to palmitic acid or after treatment with BSA (negative control). β -Actin served as a loading control. Representative results of 3 independent experiments are shown. *B*: dose-dependent activation of caspase 3 by palmitic acid. For control condition (BSA), the BSA concentration equivalent to cells exposed to 500 μ M palmitic acid complexed to BSA was used. β -Actin served as a loading control. Representative results of 2 independent experiments are shown.

Palmitoleic or oleic acid attenuates palmitic acid-induced UPR and prevents podocyte cell death. In β cells of the pancreas, certain monounsaturated FFAs can activate antiapoptotic mechanisms (38) and suppress CHOP expression (10), and diets rich in unsaturated FFAs can lower glucose levels in type 2 diabetic mice (54). Therefore, we explored the effect of 500 μ M palmitoleic acid (C16:1) or oleic acid (C18:1) on palmitic acid-induced podocyte cell death and CHOP induction. Palmitoleic acid and oleic acid could prevent podocyte apoptosis and necrosis (Fig. 5, *A* and *C*). Palmitoleic acid alone or in combination with palmitic acid also induced BiP but strongly attenuated the induction of CHOP (Fig. 5*B*). Similar

results were observed when oleic acid was used instead of palmitoleic acid (Fig. 5*D*).

Gene silencing of CHOP attenuates palmitic acid-induced cell death in podocytes. CHOP is a proapoptotic transcription factor, and CHOP deletion can protect from ER-stressed induced apoptosis (61). To test whether the marked upregulation of CHOP (Fig. 4, *B* and *C*) is mechanistically involved in palmitic acid-induced podocyte cell death, we generated CHOP knockdown podocytes by lentiviral infection using a CHOP-specific shRNA (11). By immunoblotting, we observed a marked suppression of CHOP (Fig. 6*B*, $P < 0.01$) and BiP (Fig. 6*B*, $P < 0.05$) protein expression in podocytes transduced

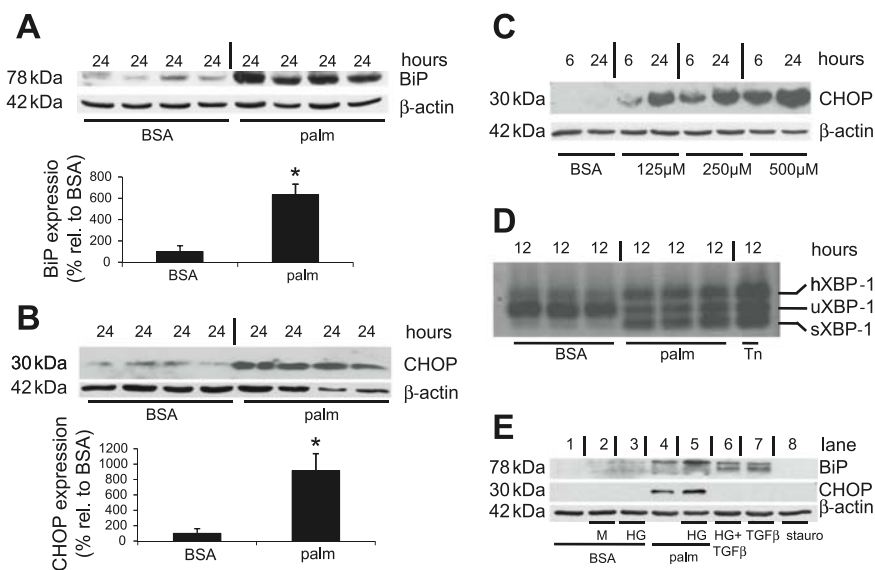
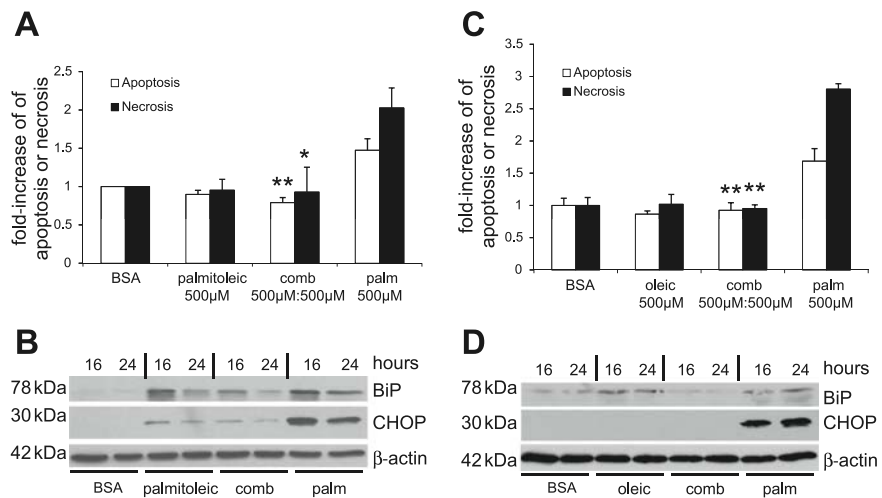


Fig. 4. Palmitic acid induced the endoplasmic reticulum (ER) chaperone immunoglobulin heavy chain binding protein (BiP) and C/EBP homologous protein (CHOP) in podocytes. *A*: palmitic acid-induced upregulation of BiP (*top*) and quantitative analysis of BiP levels normalized to β -actin (*bottom*). The expression level of the control condition (BSA) was set to 100%; $n = 4$. $*P < 0.01$. *B*: palmitic acid induced upregulation of CHOP (*top*) and quantitative analysis of CHOP levels normalized to β -actin (*bottom*). The expression level of the control condition (BSA) was set to 100%; $n = 4$. $*P < 0.01$. *C*: time- and dose-dependent upregulation of CHOP protein levels by palmitic acid. For the control condition (BSA), the BSA concentration was equivalent to cells exposed to 500 μ M palmitic acid complexed to BSA. β -Actin served as a loading control. Representative results of 3 independent experiments are shown. *D*: RT-PCR of X-box binding protein-1 (XBP-1) mRNA in podocytes treated with 500 μ M palmitic acid for 12 h. Tunicamycin (Tn; 5 ng/ml) was used as a positive control. In the control condition (BSA), a strong band for unspliced (u) XBP-1 is visible, whereas sXBP-1 and hXBP-1 are strongly increased after treatment with palmitic acid or tunicamycin. Representative results of 3 independent experiments. *E*: BiP and CHOP expression after exposure for 24 h as follows. Lane 1, control medium containing 5 mM glucose and fatty acid free BSA (BSA); lane 2, control medium (BSA) supplemented with additional 17 mM mannitol (M); lane 3, control medium (BSA) supplemented with additional 17 mM glucose [high glucose (HG)]; lane 4, BSA complexed with 500 μ M palmitic acid (palm); lane 5, palmitic acid (palm) and HG; lane 6, 5 ng/ml TGF- β with HG; lane 7, 5 ng/ml TGF- β ; lane 8, 0.25 μ M staurosporine (stauro). Upregulation of CHOP is only seen with palmitic acid, whereas BiP is induced by palmitic acid and TGF- β (faint band also for HG and M). β -Actin served as a loading control. Representative results of 4 independent experiments are shown.

Fig. 5. Palmitoleic or oleic acid prevent palmitic acid-induced podocyte death and attenuate CHOP induction. *A*: palmitoleic acid blocks palmitic acid-induced podocyte cell death ($n = 3$, $*P < 0.05$, $**P < 0.01$, compared with palmitic acid). *B*: palmitoleic acid blocks palmitic acid-induced upregulation of BiP and CHOP protein steady-state levels. β -Actin served as a loading control. Representative result of 2 independent experiments is shown. *C*: oleic acid blocks palmitic acid-induced podocyte cell death ($n = 3$, $*P < 0.01$ compared with palmitic acid). *D*: oleic acid blocks palmitic acid-induced upregulation of BiP and CHOP protein steady-state levels. β -Actin served as a loading control. Representative result of 2 independent experiments is shown.



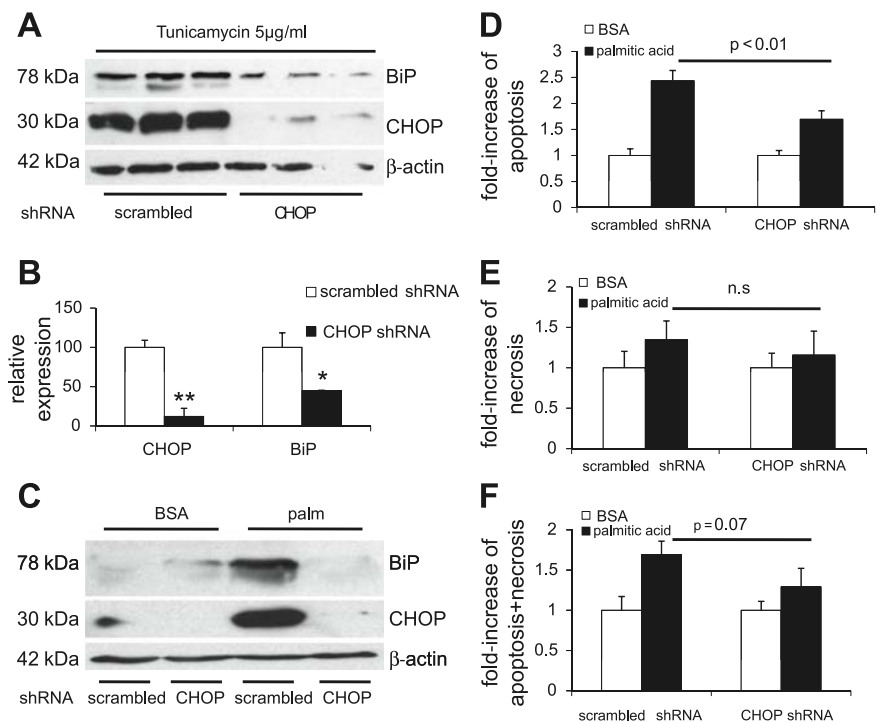
with CHOP-silencing shRNA after stimulation with tunicamycin, an established inducer of the UPR (Fig. 6, *A* and *B*) or palmitic acid (Fig. 6*C*). The suppression of BiP upregulation (Fig. 6, *A–C*) was expected as CHOP knockdown leads to lower levels of the UPR as a result of reduced translation, resulting in decreased expression of BiP (31). Functionally, the knockdown of CHOP significantly attenuated the palmitic acid-induced cell death of podocytes (Fig. 6, *D* and *F*). These findings are completely consistent with the important role of CHOP in a murine model of DN as well as age-related albuminuria (59). However, the role of CHOP may be more complicated in humans with DN, as CHOP was not upregu-

lated by quantitative RT-PCR in the tubulointerstitial compartment of patients with DN (22). Similarly, we found no upregulation of CHOP mRNA expression in glomerular extracts from eight patients with established DN where CHOP expression was even reduced (Supplemental Fig. S2C).

DISCUSSION

The present study uncovered that saturated palmitic acid induces podocyte cell death. Our findings are of clinical interest because insulin resistance is associated with increased plasma levels of long-chain FFAs, and DN is characterized by

Fig. 6. Gene silencing of CHOP protects against palmitic acid-induced podocyte cell death. *A*: gene-silencing of CHOP suppresses the tunicamycin-induced upregulation of BiP and CHOP protein levels. β -Actin served as a loading control. Representative result of 3 independent experiments are shown. *B*: quantitative analysis showing a significant reduction of tunicamycin-induced upregulation of CHOP and BiP in cells infected with CHOP short-hairpin (sh) RNA ($*P < 0.01$, $**P < 0.001$). *C*: gene silencing of CHOP suppresses the palmitic acid-induced upregulation of CHOP and BiP protein levels. Representative result of 3 independent experiments is shown. *D–F*: gene silencing of CHOP protects against palmitic acid-induced apoptosis (*D*) and overall increase in cell death (*F*).



apoptosis and loss of podocytes that precede albuminuria and renal dysfunction in DN, both in type 1 and type 2 diabetes (9, 35, 42, 50, 53). Previous studies found that high glucose (50), TGF- β (62), the renin-angiotensin-aldosterone system (12, 14), and advanced glycation end products (7) can also induce apoptosis of podocytes.

The identification of palmitic acid as another proapoptotic factor for podocytes may be of clinical relevance in the setting of type 2 diabetes because FFAs are elevated in patients with obesity and insulin resistance even before hyperglycemia arises (4). FFAs can also be elevated in type 1 diabetic subjects (34). Moreover, similar to DN, obesity-related glomerulonephropathy is characterized by a decreased density of podocytes (5), raising the intriguing possibility that FFA-induced podocyte apoptosis may also contribute to the development and progression of obesity-related glomerular disease.

The detection of palmitic acid-induced ER stress in podocytes is in line with similar findings in other cell types (15, 18, 33, 56, 57). In pancreatic β cells, the overexpression of the ER-chaperon BiP can reduce palmitic acid-induced apoptosis (20), implying that the upregulation of BiP (Fig. 4A) is part of an adaptive podocyte-protective mechanism. In contrast, the strong upregulation of CHOP (Fig. 4, B and C) makes CHOP a good candidate as a mediator of palmitic acid-induced podocyte apoptosis because CHOP is critically involved in ER stress-induced apoptosis (31, 61). Consistent with the strong induction of CHOP, we also observed palmitic acid-induced XBP-1 splicing (Fig. 4D), which is directly involved in transcriptional regulation of CHOP (41). Together, our data indicate that the palmitic acid-induced upregulation of CHOP in podocytes results, at least in part, from transcriptional activation of CHOP.

Another interesting outcome of the current study was the finding that neither high glucose nor TGF- β at a concentration previously shown to induce podocyte apoptosis (45) caused an upregulation of CHOP (Fig. 4E), suggesting that CHOP is not involved in podocyte apoptosis induced by high glucose or TGF- β .

The antagonistic effects of palmitic acid and monounsaturated palmitoleic acid or oleic acid on ER stress and apoptosis of podocytes (Fig. 5) are in line with studies in other cells (10, 15, 28, 56). The addition of the monounsaturated FFAs to palmitic acid could suppress the induction of CHOP (Fig. 5, B and C), which may explain, at least in part, the prevention of palmitic acid-induced podocyte apoptosis. In addition, we consistently observed an increase in the ER chaperone BiP in podocytes treated with monounsaturated palmitoleic or oleic acid (Fig. 5, B and C). As BiP is known to protect from palmitic acid-induced apoptosis (20), this may explain the protective effect of monounsaturated FFAs.

The gene silencing of CHOP reduces palmitic acid-induced podocyte death (Fig. 6, D–F), thereby establishing a causative role for CHOP in palmitic acid-induced podocyte apoptosis. This outcome is consistent with the known role of CHOP in ER stress-induced apoptosis (31, 61). ER stress has been implicated in podocyte apoptosis caused by advanced glycation end products (6) or excessive protein loading (16), but a causative role of CHOP under these conditions remains to be established.

The notion that CHOP plays a pathogenic role in experimental DN is supported by the observation that CHOP is upregulated in two rodent models of DN (24, 59), and CHOP-

deficient mice are protected from DN as well as age-related albuminuria (59). However, in patients with DN, although we found an upregulation of BiP by quantitative RT-PCR analysis in the tubulointerstitial compartment (22) as well as in microdissected glomeruli (Supplemental Fig. S2A), CHOP mRNA expression was unchanged in the tubulointerstitial compartment (22) and downregulated in glomeruli (Supplemental Fig. 2C). Clearly, future studies will be required to address potential differences between our in vitro data, results in murine models, and human DN to determine the precise role of CHOP in patients with DN.

In conclusion, our results unveil the antagonistic effects of palmitic acid vs. monounsaturated FFAs on podocyte survival, ER stress, and the UPR. They support an important role of CHOP in the regulation of podocyte cell death by FFAs. The observed opposing effects of long-chain saturated and unsaturated FFAs on ER stress and podocyte viability provide a rationale for interventional studies that will test whether the progression of DN can be delayed by dietary shifting the FFA balance toward unsaturated FFAs, e.g., by consumption of peanuts and olive oil.

ACKNOWLEDGMENTS

We thank Dr. Marc Y. Donath, Dr. R. Krapf, and Dr. Alan R. Tall for comments on the manuscript.

We thank all participating centers of the European Renal cDNA Bank-Kroener-Fresenius Biopsy Bank (ERCB-KFB) and patients for cooperation. Active members at the time of the study were as follows: Clemens David Cohen, Holger Schmid, Michael Fischeder, Lutz Weber, Matthias Kretzler, and Detlef Schlöndorff (Munich/Zurich/AnnArbor/New York); Jean Daniel Sraer and Pierre Ronco (Paris); Maria Pia Rastaldi and Giuseppe D'Amico (Milan); Peter Doran and Hugh Brady (Dublin); Detlev Mönks and Christoph Wanner (Würzburg); Andrew Rees (Aberdeen); Frank Strutz and Gerhard Anton Müller (Göttingen); Peter Mertens and Jürgen Floege (Aachen); Norbert Braun and Teut Risler (Tübingen); Loreto Gesualdo and Francesco Paolo Schena (Bari); Jens Gerth and Gunter Wolf (Jena); Rainer Oberbauer and Dentscho Kerjaschki (Vienna); Bernhard Banas and Bernhard Krämer (Regensburg); Moin Saleem (Bristol); Rudolf Wüthrich (Zurich); Walter Samtleben (Munich); Harm Peters and Hans-Hellmut Neumayer (Berlin); Mohamed Doha (Leiden); Katrin Ivens and Bernd Grabensee (Düsseldorf); Francisco Mampaso (Madrid); Jun Oh, Franz Schaefer, Martin Zeier, and Hermann-Joseph Gröne (Heidelberg); Peter Gross (Dresden); Giancarlo Tonolo (Sassari); Vladimír Tesar (Prague); Harald Rupprecht (Bayreuth); Hermann Pavenstädt (Münster); and Hans-Peter Marti (Bern).

GRANTS

This study was supported by Swiss National Science Foundation Grant 31003A-119974 (A. W. Jehle), a grant from Freie Akademische Gesellschaft Basel (A. W. Jehle), National Institutes of Health Grants DK62472 and DK57683 (P. Mundel), and the Else-Kröner-Fresenius Foundation (C. D. Cohen).

DISCLOSURES

No conflicts of interest, financial or otherwise, are declared by the authors.

REFERENCES

1. USRDS. The United States Renal Data System. *Am J Kidney Dis* 42: 1–230, 2003.
2. Asanuma K, Campbell KN, Kim K, Faul C, Mundel P. Nuclear relocation of the nephrin and CD2AP-binding protein dendrin promotes apoptosis of podocytes. *Proc Natl Acad Sci USA* 104: 10134–10139, 2007.
3. Bek MF, Bayer M, Muller B, Greiber S, Lang D, Schwab A, August C, Springer E, Rohrbach R, Huber TB, Benzing T, Pavenstädt H. Expression and function of C/EBP homology protein (GADD153) in podocytes. *Am J Pathol* 168: 20–32, 2006.

4. **Boden G.** Fatty acid-induced inflammation and insulin resistance in skeletal muscle and liver. *Curr Diab Rep* 6: 177–181, 2006.
5. **Chen HM, Liu ZH, Zeng CH, Li SJ, Wang QW, Li LS.** Podocyte lesions in patients with obesity-related glomerulopathy. *Am J Kidney Dis* 48: 772–779, 2006.
6. **Chen Y, Liu CP, Xu KF, Mao XD, Lu YB, Fang L, Yang JW, Liu C.** Effect of taurine-conjugated ursodeoxycholic acid on endoplasmic reticulum stress and apoptosis induced by advanced glycation end products in cultured mouse podocytes. *Am J Nephrol* 28: 1014–1022, 2008.
7. **Chuang PY, Yu Q, Fang W, Urbarri J, He JC.** Advanced glycation endproducts induce podocyte apoptosis by activation of the FOXO4 transcription factor. *Kidney Int* 72: 965–976, 2007.
8. **Cohen CD, Frach K, Schlondorff D, Kretzler M.** Quantitative gene expression analysis in renal biopsies: a novel protocol for a high-throughput multicenter application. *Kidney Int* 61: 133–140, 2002.
9. **Dalla Vestra M, Masiero A, Roiter AM, Saller A, Crepaldi G, Fioretto P.** Is podocyte injury relevant in diabetic nephropathy? Studies in patients with type 2 diabetes. *Diabetes* 52: 1031–1035, 2003.
10. **Diakogiannaki E, Welters HJ, Morgan NG.** Differential regulation of the endoplasmic reticulum stress response in pancreatic beta-cells exposed to long-chain saturated and monounsaturated fatty acids. *J Endocrinol* 197: 553–563, 2008.
11. **Di Nardo A, Kramvis I, Cho N, Sadowski A, Meikle L, Kwiatkowski DJ, Sahin M.** Tuberous sclerosis complex activity is required to control neuronal stress responses in an mTOR-dependent manner. *J Neurosci* 29: 5926–5937, 2009.
12. **Ding G, Reddy K, Kapasi AA, Franki N, Gibbons N, Kasinath BS, Singhal PC.** Angiotensin II induces apoptosis in rat glomerular epithelial cells. *Am J Physiol Renal Physiol* 283: F173–F180, 2002.
13. **Dittgen T, Nimmerjahn A, Komai S, Licznarski P, Waters J, Margrie TW, Helmchen F, Denk W, Brecht M, Osten P.** Lentivirus-based genetic manipulations of cortical neurons and their optical and electrophysiological monitoring in vivo. *Proc Natl Acad Sci USA* 101: 18206–18211, 2004.
14. **Durvasula RV, Petermann AT, Hiromura K, Blonski M, Pippin J, Mundel P, Pichler R, Griffin S, Couser WG, Shankland SJ.** Activation of a local tissue angiotensin system in podocytes by mechanical strain. *Kidney Int* 65: 30–39, 2004.
15. **Guo W, Wong S, Xie W, Lei T, Luo Z.** Palmitate modulates intracellular signaling, induces endoplasmic reticulum stress, and causes apoptosis in mouse 3T3-L1 and rat primary preadipocytes. *Am J Physiol Endocrinol Metab* 293: E576–E586, 2007.
16. **Inagi R, Nangaku M, Onogi H, Ueyama H, Kitao Y, Nakazato K, Ogawa S, Kurokawa K, Couser WG, Miyata T.** Involvement of endoplasmic reticulum (ER) stress in podocyte injury induced by excessive protein accumulation. *Kidney Int* 68: 2639–2650, 2005.
17. **Kaufman RJ.** Orchestrating the unfolded protein response in health and disease. *J Clin Invest* 110: 1389–1398, 2002.
18. **Kharroubi I, Ladriere L, Cardozo AK, Dogusan Z, Cnop M, Eizirik DL.** Free fatty acids and cytokines induce pancreatic beta-cell apoptosis by different mechanisms: role of nuclear factor-kappaB and endoplasmic reticulum stress. *Endocrinology* 145: 5087–5096, 2004.
19. **Kozutsumi Y, Segal M, Normington K, Gething MJ, Sambrook J.** The presence of misfolded proteins in the endoplasmic reticulum signals the induction of glucose-regulated proteins. *Nature* 332: 462–464, 1988.
20. **Laybutt DR, Preston AM, Akerfeldt MC, Kench JG, Busch AK, Biankin AV, Biden TJ.** Endoplasmic reticulum stress contributes to beta cell apoptosis in type 2 diabetes. *Diabetologia* 50: 752–763, 2007.
21. **Lennon R, Pons D, Sabin MA, Wei C, Shield JP, Coward RJ, Tavare JM, Mathieson PW, Saleem MA, Welsh GI.** Saturated fatty acids induce insulin resistance in human podocytes: implications for diabetic nephropathy. *Nephrol Dial Transplant* 24: 3288–3296, 2009.
22. **Lindenmeyer MT, Rastaldi MP, Ikehata M, Neusser MA, Kretzler M, Cohen CD, Schlondorff D.** Proteinuria and hyperglycemia induce endoplasmic reticulum stress. *J Am Soc Nephrol* 19: 2225–2236, 2008.
23. **Listenberger LL, Ory DS, Schaffer JE.** Palmitate-induced apoptosis can occur through a ceramide-independent pathway. *J Biol Chem* 276: 14890–14895, 2001.
24. **Liu G, Sun Y, Li Z, Song T, Wang H, Zhang Y, Ge Z.** Apoptosis induced by endoplasmic reticulum stress involved in diabetic kidney disease. *Biochem Biophys Res Commun* 370: 651–656, 2008.
25. **Locatelli F, Pozzoni P, Del Vecchio L.** Renal replacement therapy in patients with diabetes and end-stage renal disease. *J Am Soc Nephrol* 15, Suppl 1: S25–S29, 2004.
26. **Ma Y, Hendershot LM.** The unfolding tale of the unfolded protein response. *Cell* 107: 827–830, 2001.
27. **Maedler K, Oberholzer J, Bucher P, Spinas GA, Donath MY.** Monounsaturated fatty acids prevent the deleterious effects of palmitate and high glucose on human pancreatic beta-cell turnover and function. *Diabetes* 52: 726–733, 2003.
28. **Maedler K, Spinas GA, Dyntar D, Moritz W, Kaiser N, Donath MY.** Distinct effects of saturated and monounsaturated fatty acids on beta-cell turnover and function. *Diabetes* 50: 69–76, 2001.
29. **Malhi H, Bronk SF, Werneburg NW, Gores GJ.** Free fatty acids induce JNK-dependent hepatocyte lipoapoptosis. *J Biol Chem* 281: 12093–12101, 2006.
30. **Mandal D, Moitra PK, Saha S, Basu J.** Caspase 3 regulates phosphatidylserine externalization and phagocytosis of oxidatively stressed erythrocytes. *FEBS Lett* 513: 184–188, 2002.
31. **Marciniak SJ, Yun CY, Oyadomari S, Novoa I, Zhang Y, Jungreis R, Nagata K, Harding HP, Ron D.** CHOP induces death by promoting protein synthesis and oxidation in the stressed endoplasmic reticulum. *Genes Dev* 18: 3066–3077, 2004.
32. **Markan S, Kohli HS, Joshi K, Minz RW, Sud K, Ahuja M, Anand S, Khullar M.** Up regulation of the GRP-78 and GADD-153 and down regulation of Bcl-2 proteins in primary glomerular diseases: a possible involvement of the ER stress pathway in glomerulonephritis. *Mol Cell Biochem* 324: 131–138, 2009.
33. **Martinez SC, Tanabe K, Cras-Meneur C, Abumrad NA, Bernal-Mizrachi E, Permutt MA.** Inhibition of Foxo1 protects pancreatic islet beta-cells against fatty acid and endoplasmic reticulum stress-induced apoptosis. *Diabetes* 57: 846–859, 2008.
34. **Mevorach M, Kaplan J, Chang CJ, Rossetti L, Shamooh H.** Hormone-independent activation of EGP during hypoglycemia is absent in type 1 diabetes mellitus. *Am J Physiol Endocrinol Metab* 278: E421–E429, 2000.
35. **Meyer TW, Bennett PH, Nelson RG.** Podocyte number predicts long-term urinary albumin excretion in Pima Indians with type II diabetes and microalbuminuria. *Diabetologia* 42: 1341–1344, 1999.
36. **Mishra R, Simonson MS.** Saturated free fatty acids and apoptosis in microvascular mesangial cells: palmitate activates pro-apoptotic signaling involving caspase 9 and mitochondrial release of endonuclease G. *Cardiovasc Diabetol* 4: 2, 2005.
37. **Morgan NG.** Fatty acids and beta-cell toxicity. *Curr Opin Clin Nutr Metab Care* 12: 117–122, 2009.
38. **Morgan NG, Dhayal S, Diakogiannaki E, Welters HJ.** The cytoprotective actions of long-chain mono-unsaturated fatty acids in pancreatic beta-cells. *Biochem Soc Trans* 36: 905–908, 2008.
39. **Mundel P, Reiser J, Zuniga Mejia Borja A, Pavenstadt H, Davidson GR, Kriz W, Zeller R.** Rearrangements of the cytoskeleton and cell contacts induce process formation during differentiation of conditionally immortalized mouse podocyte cell lines. *Exp Cell Res* 236: 248–258, 1997.
40. **Nozaki J, Kubota H, Yoshida H, Naitoh M, Goji J, Yoshinaga T, Mori K, Koizumi A, Nagata K.** The endoplasmic reticulum stress response is stimulated through the continuous activation of transcription factors ATF6 and XBP1 in Ins2+/Akita pancreatic beta cells. *Genes Cells* 9: 261–270, 2004.
41. **Oyadomari S, Mori M.** Roles of CHOP/GADD153 in endoplasmic reticulum stress. *Cell Death Differ* 11: 381–389, 2004.
42. **Pagtalunan ME, Miller PL, Jumping-Eagle S, Nelson RG, Myers BD, Renke HG, Coplon NS, Sun L, Meyer TW.** Podocyte loss and progressive glomerular injury in type II diabetes. *J Clin Invest* 99: 342–348, 1997.
43. **Randle PJ, Garland PB, Hales CN, Newsholme EA.** The glucose fatty-acid cycle. Its role in insulin sensitivity and the metabolic disturbances of diabetes mellitus. *Lancet* 1: 785–789, 1963.
44. **Rasheva VI, Domingos PM.** Cellular responses to endoplasmic reticulum stress and apoptosis. *Apoptosis* 14: 996–1007, 2009.
45. **Schiffer M, Mundel P, Shaw AS, Bottinger EP.** A novel role for the adaptor molecule CD2-associated protein in transforming growth factor-beta-induced apoptosis. *J Biol Chem* 279: 37004–37012, 2004.
46. **Schmid H, Henger A, Cohen CD, Frach K, Grone HJ, Schlondorff D, Kretzler M.** Gene expression profiles of podocyte-associated molecules as diagnostic markers in acquired proteinuric diseases. *J Am Soc Nephrol* 14: 2958–2966, 2003.
47. **Shang J, Lehrman MA.** Discordance of UPR signaling by ATF6 and Ire1p-XBP1 with levels of target transcripts. *Biochem Biophys Res Commun* 317: 390–396, 2004.

48. Shimabukuro M, Zhou YT, Levi M, Unger RH. Fatty acid-induced beta cell apoptosis: a link between obesity and diabetes. *Proc Natl Acad Sci USA* 95: 2498–2502, 1998.
49. Slee EA, Adrain C, Martin SJ. Serial killers: ordering caspase activation events in apoptosis. *Cell Death Differ* 6: 1067–1074, 1999.
50. Susztak K, Raff AC, Schiffer M, Bottinger EP. Glucose-induced reactive oxygen species cause apoptosis of podocytes and podocyte depletion at the onset of diabetic nephropathy. *Diabetes* 55: 225–233, 2006.
51. Thomas ME, Harris KP, Walls J, Furness PN, Brunskill NJ. Fatty acids exacerbate tubulointerstitial injury in protein-overload proteinuria. *Am J Physiol Renal Physiol* 283: F640–F647, 2002.
52. Thomas ME, Schreiner GF. Contribution of proteinuria to progressive renal injury: consequences of tubular uptake of fatty acid bearing albumin. *Am J Nephrol* 13: 385–398, 1993.
53. Toyoda M, Najafian B, Kim Y, Caramori ML, Mauer M. Podocyte detachment and reduced glomerular capillary endothelial fenestration in human type 1 diabetic nephropathy. *Diabetes* 56: 2155–2160, 2007.
54. Vassiliou EK, Gonzalez A, Garcia C, Tadros JH, Chakraborty G, Toney JH. Oleic acid and peanut oil high in oleic acid reverse the inhibitory effect of insulin production of the inflammatory cytokine TNF-alpha both in vitro and in vivo systems. *Lipids Health Dis* 8: 25, 2009.
55. Wahba IM, Mak RH. Obesity and obesity-initiated metabolic syndrome: mechanistic links to chronic kidney disease. *Clin J Am Soc Nephrol* 2: 550–562, 2007.
56. Wei Y, Wang D, Gentile CL, Pagliassotti MJ. Reduced endoplasmic reticulum luminal calcium links saturated fatty acid-mediated endoplasmic reticulum stress and cell death in liver cells. *Mol Cell Biochem* 331: 31–40, 2009.
57. Wei Y, Wang D, Topczewski F, Pagliassotti MJ. Saturated fatty acids induce endoplasmic reticulum stress and apoptosis independently of ceramide in liver cells. *Am J Physiol Endocrinol Metab* 291: E275–E281, 2006.
58. Wolf G, Chen S, Ziyadeh FN. From the periphery of the glomerular capillary wall toward the center of disease: podocyte injury comes of age in diabetic nephropathy. *Diabetes* 54: 1626–1634, 2005.
59. Wu J, Zhang R, Torreggiani M, Ting A, Xiong H, Striker GE, Vlassara H, Zheng F. Induction of diabetes in aged C57B6 mice results in severe nephropathy: an association with oxidative stress, endoplasmic reticulum stress, and inflammation. *Am J Pathol* 176: 2163–2176, 2010.
60. Yoshida H, Matsui T, Yamamoto A, Okada T, Mori K. XBP1 mRNA is induced by ATF6 and spliced by IRE1 in response to ER stress to produce a highly active transcription factor. *Cell* 107: 881–891, 2001.
61. Zinszner H, Kuroda M, Wang X, Batchvarova N, Lightfoot RT, Remotti H, Stevens JL, Ron D. CHOP is implicated in programmed cell death in response to impaired function of the endoplasmic reticulum. *Genes Dev* 12: 982–995, 1998.
62. Ziyadeh FN, Hoffman BB, Han DC, Iglesias-De La Cruz MC, Hong SW, Isono M, Chen S, McGowan TA, Sharma K. Long-term prevention of renal insufficiency, excess matrix gene expression, and glomerular mesangial matrix expansion by treatment with monoclonal antitransforming growth factor-beta antibody in db/db diabetic mice. *Proc Natl Acad Sci USA* 97: 8015–8020, 2000.



7.1.2 - Supplemental material

SUPPORTING MATERIAL: Regulation of podocyte survival by fatty acids 1

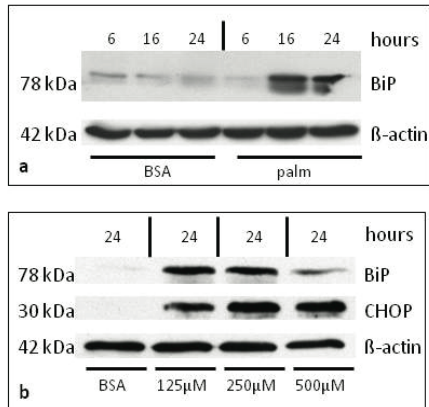
SUPPORTING MATERIAL

MATERIALS AND METHODS

Quantitative real-time PCR of renal biopsies - Human renal biopsy specimens were procured in an international multicenter study, the European Renal cDNA Bank-Kroener-Fresenius Biopsy bank (ERCB-KFB). Biopsies were obtained from patients after informed consent and with approval of the local ethics committees. Following renal biopsy, the tissue was transferred to RNase inhibitor and microdissected into glomerular and tubular fragments. Total RNA was isolated from micro-dissected glomeruli as described previously (1). Reverse transcription and real-time RT-PCR were performed as reported earlier (1). Pre-developed TaqMan reagents were used for human BiP (NM_005347.2), HYOU1 (NM_006389.2), CHOP (NM_004083.4), as well as the reference genes (Applied Biosystems). The expression of BiP, HYOU1 and CHOP was normalized to the mean of three reference genes, GAPDH, 18S rRNA, and synaptopodin. The mRNA expression was analyzed by standard curve quantification (4). For the real time RT-PCR data statistical analysis was performed using Kruskal-Wallis and Mann-Whitney U tests.

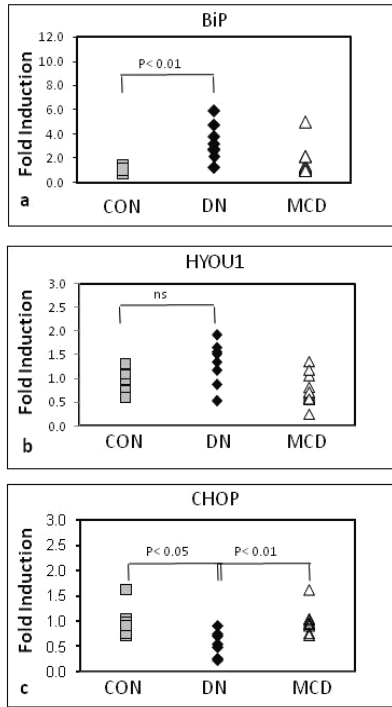
SUPPLEMENTAL RESULTS

SFig 1.: Dose and time-dependent induction of the ER-chaperons BiP and CHOP



A. Time-dependent upregulation of BiP protein levels by palmitic acid. β -actin serves as loading control. Representative results of 3 independent experiments. B. Upregulation of BiP and CHOP at 125 μ M, 250 μ M, and 500 μ M palmitic acid. For the control condition (BSA) the BSA concentration was equivalent to cells exposed to 500 μ M palmitic acid complexed to BSA. β -actin serves as loading control. Representative results of 2 independent experiments.

SFig 2.: Induction of UPR gene mRNA expression in glomeruli of patients with DN



(A-C) mRNA expression levels of (A) BiP, (B) HYOU1, and (C) CHOP were quantified in microdissected glomeruli from controls (CON, n = 6), patients with established DN (DN, n=8) and patients with MCD (n=12). BiP (A) was upregulated and CHOP (C) was downregulated in patients with DN compared to control samples. (B) No significant changes were found for HYOU1. The changes between controls and MCD were not significant for all three genes. The graphs for BiP, HYOU1, and CHOP show expression ratios of each gene normalized to three reference genes (18S rRNA, hGAPDH, and synaptotodin).

Supplemental Table 1: Clinical data from living donors and patients with DN or MCD analyzed by real time RT-PCR

Biopsy Group	Number	Age [years]	Creatinine [mg/dl]	Proteinuria [g/day]	Hypertension	HbA1c [%]	RR syst.	RR diast.
Living donor								
Mean ±	6	46.2 ±	<1.1	<0.2	0/6	NA	NA	NA
SEM		13.8						
Diabetic Nephropathy								
Mean ±	8	60.4 ±	2.5 ±	4.8 ± 3.8	8/8	8.2 ± 2.6	157.9 ±	85.9 ±
SEM		8.4	1.8				11.2	4.0
Minimal Change Disease								
Mean ±	12	33.3 ±	1.1 ±	6.7 ± 4.5	4/12	NA	129.2 ±	75.3 ±
SEM		13.6	0.3				4.9	3.1

1. Cohen CD, Frach K, Schlondorff D, and Kretzler M. Quantitative gene expression analysis in renal biopsies: a novel protocol for a high-throughput multicenter application. *Kidney Int* 61: 133-140, 2002.
2. Lindenmeyer MT, Rastaldi MP, Ikehata M, Neusser MA, Kretzler M, Cohen CD, and Schlondorff D. Proteinuria and hyperglycemia induce endoplasmic reticulum stress. *J Am Soc Nephrol* 19: 2225-2236, 2008.
3. Liu G, Sun Y, Li Z, Song T, Wang H, Zhang Y, and Ge Z. Apoptosis induced by endoplasmic reticulum stress involved in diabetic kidney disease. *Biochemical and biophysical research communications* 370: 651-656, 2008.
4. Schmid H, Henger A, Cohen CD, Frach K, Grone HJ, Schlondorff D, and Kretzler M. Gene expression profiles of podocyte-associated molecules as diagnostic markers in acquired proteinuric diseases. *J Am Soc Nephrol* 14: 2958-2966, 2003.
5. Vandivier RW, Henson PM, and Douglas IS. Burying the dead: the impact of failed apoptotic cell removal (efferocytosis) on chronic inflammatory lung disease. *Chest* 129: 1673-1682, 2006.
6. Wu J, Zhang R, Torreggiani M, Ting A, Xiong H, Striker GE, Vlassara H, and Zheng F. Induction of diabetes in aged C57B6 mice results in severe nephropathy: an association with oxidative stress, endoplasmic reticulum stress, and inflammation. *Am J Pathol* 176: 2163-2176.

Curriculum vitae

First Name: Jonas
Last Name: Sieber
Address: Meisen
3925 Grächen (VS)
Birth Date: 14.10.1982
Nationality: CH
E-mail: jonas.sieber@unibas.ch, jsieber82@hotmail.com
Phone number: 079 732 49 21

Education:

1997 – 2002: Kollegium Spiritus Sanctus Brig VS, Typus C
2002 – 2006: Studies in Microbiology, ETH Zurich
- Microbiology; Immunology; Medical Microbiology; Cell
Biology; Gene- and Enzyme Technology
- Diploma thesis at the Institute of Experimental Immunology at
the University Hospital Zurich in the lab of Prof. Dr.
Hengartner and Prof. Dr. Zinkernagel. Title: “Expression,
refolding and characterization of the lymphocytic
choriomeningitis virus (LCMV-WE) glycoprotein 2 (GP2)”
2008 – 2011 PhD-student at the Department of Biomedicine at the
University Hospital Basel in the lab of **PD Dr. Andreas Jehle**
Faculty representative: **Prof. Dr. Ed Palmer**
Co-referee: **Prof. Dr. Marc Donath**

Working experience:

03.2007 -06.2007 Substitution teacher (grade 7/8/9), St.Niklaus (VS)
12.2006 -02.2007
and
12.2007 -04.2008 Ski instructor, Grächen (VS)

Publication List

- Unpublished:

Diploma Thesis: Jonas Sieber "Expression, Refolding and Characterization of the lymphocytic choriomeningitis virus (LCMV-WE) glycoprotein 2 (GP2)."

- Published:

Sieber, J., M. T. Lindenmeyer, et al. "Regulation of podocyte survival and endoplasmic reticulum stress by fatty acids." Am J Physiol Renal Physiol **299**(4): F821-9.

- Manuscript in preparation:

Jonas Sieber et al. "Susceptibility of Podocytes to Palmitic Acid Is Regulated by LXR-Dependent Stearoyl-Coenzyme A Desaturases 1 and 2."

- Posters

Swiss Society of Nephrology, 41st Annual Meeting, Interlaken Dec. 2009. Jonas Sieber et al. "Regulation of podocyte survival by fatty acids."

American Society of Nephrology (ASN), Kidney Week, Denver Nov. 2010. Jonas Sieber et al. "Regulation of podocyte survival and endoplasmic reticulum stress by fatty acids."

Swiss Society of Nephrology, 42nd Annual Meeting, Lugano Dec. 2010. Jonas Sieber et al. "Regulation of podocyte survival and endoplasmic reticulum stress by fatty acids."

American Society of Nephrology (ASN), Kidney Week, Philadelphia Nov. 2011. Kapil Kampe, Jonas Sieber et al. "Regulation of fatty acid oxidation profoundly affects palmitic acid induced podocyte cell death."